Functional adaptations and muscle attachment (entheseal) patterns in the hands of apes, humans, and hominins

Dissertation
der Mathematisch-Naturwissenschaftlichen Fakultät
der Eberhard Karls Universität Tübingen
zur Erlangung des Grades eines
Doktors der Naturwissenschaften
(Dr. rer. nat.)

vorgelegt von
Jana Kunze
aus Wuppertal

Tübingen
2023

Functional adaptations and muscle attachment (entheseal) patterns in the hands of apes, humans, and hominins

Dissertation
der Mathematisch-Naturwissenschaftlichen Fakultät
der Eberhard Karls Universität Tübingen
zur Erlangung des Grades eines
Doktors der Naturwissenschaften
(Dr. rer. nat.)

vorgelegt von
Jana Kunze
aus Wuppertal

Tübingen
2023

Gedruckt mit Genehmigung der Mathematisch-Naturwissenschaftlichen Fakultät der Eberhard Karls Universität Tübingen.

Tag der mündlichen Qualifikation: 19.12.2023
Dekan: Prof. Dr. Thilo Stehle
1. Berichterstatterin: Prof. Dr. Katerina Harvati
2. Berichterstatter: PD Dr. Fotios Alexandros Karakostis
3. Berichterstatter: Prof. Dr. Christopher Miller

Table of contents

Acknowledgments

These first pages are dedicated to those who helped me throughout my Ph.D. project. The list is long, and while I cannot name everyone, I am deeply grateful for everyone who has supported me in any way.

First, I want to thank my first supervisor, Prof. Katerina Harvati (Paleoanthropology, Tübingen University, Germany), for giving me the opportunity to pursue my research interest through this dissertation. Your advice and support throughout the project have been very valuable, especially in the first tumultuous years. I am deeply grateful for my second supervisor, PD Dr. Alexandros Karakostis (Paleoanthropology, Tübingen University, Germany), who has kindled my interest in activity reconstruction. Thank you for all the hours you spent teaching me VERA and geometric morphometrics and then even more to discuss the latest research. I highly value your insight and support, without which this dissertation would not have been possible.

Thanks are also due to Prof. Christopher Miller (Geoarchaeology, Tübingen University, Germany), who agreed to act as the third reviewer of this thesis. I also thank Dr. Marlen Fröhlich (Paleoanthropology, Tübingen University, Germany) for being part of my doctoral committee. Finally, I want to express my gratitude to my TAC committee members, Prof. Nico Michiels (Animal Evolutionary Ecology, Tübingen University, Germany) and Prof. Christopher Miller, for their advice.

The manuscripts in this dissertation have greatly benefited from the contribution of the co-authors Dr. Gerhard Hotz, Dr. Vangelis Tourloukis, Prof. George Koufos, Dr. Melania Ioannidou, Dr. Stefan Merker, and Prof. Marco Peresani. Thank you for the collaboration and access to study material. I am also grateful for the following people and institutions that have given me access to their fossil specimens and comparative material: ARCHH (Ethiopia) and the Max Planck Society in Germany (W.H. Kimbel, Z. Alemseged, and F. Spoor), Evolutionary Studies Institute of the University of the Witwatersrand (B. Zipfel, S. Jirah, and T. Kivell), Ditsong National Museum of Natural History, South Africa (T. Kivell and M. Tawane), National Museum of Natural History in Paris (D. Grimaud-Hervé, F. Detroit, and M. Friess), Italian Ministry of Cultural Heritage and Activities (as well as the Museo Archeologico Del Finale and V. Sparacello), Dan David Center of Human Evolution and Biohistory Research, Shmunis Family Anthropological Institute, Sackler Faculty of Medicine, Tel Aviv University (H. May and I. Hershkovitz). I also thank the

Evolutionary Studies Institute (Johannesburg, Gauteng, South Africa), the American Museum of Natural History (S. Almécija, D. Boyer, E. Delson), Smithsonian's Division of Mammals (K. Helgen) and Human Origins Program (M. Tocheri), and the Digital Morphology Museum Kupri and the associated institutions and zoos (Kobe Oji Zoo, PRI Kyoto University, Tobe Zoological Park) for making their 3D models accessible online. Many thanks are due to Loïc Costeur for access to and information on great ape hand remains from the Mammalian Collection of the Museum of Natural History in Basel.

Working with and alongside the outstanding members of the Paleoanthropology group in Tübingen has been a pleasure. My thanks go to Michael Francken and Hannes Rathmann for their help with the osteological collection and Alessio Maiello for technical support. I am grateful to Monika Doll, Karin Kießling, and Mareike Keysan (Senckenberg HEP) for their help with administrative matters. In addition, I thank Judith Beier, from whom I have learned a lot while working as her HiWi, and Melania Ioannidou, who supported me during my first teaching experience. Finally, my current and former office mates Carolin Röding, Effrosyni Roditi, and Geanina Butiseaca – I cannot thank you enough. Your advice, support, and friendship have helped me greatly throughout these years.

All of this would not have been possible without the help and support of my family and friends. Thank you to my friends at home, whom I see nowhere often enough but who have always supported me. I am also very glad to have found the Antelopes, who have always distracted and cheered me up when it was stressful. Thank you so much to Raquel, who has been the best roommate I could ask for, and Daria, who has been and still is an amazing friend through good and bad times. In addition, I owe so many thanks and more to my parents, who have always supported me, and especially my mother, who listened to my worries and complaints deep into the night. Of course, I also thank Uwe for cheering me up when I need it most. Although she is no longer with us, I must thank my grandmother, who encouraged my interest in history and archaeology early on. Last but certainly not least, I am eternally grateful for my partner, Jan. You have always been my anchor and supported me through everything. I am so lucky to have you in my life.

Abstract

The human hand, a tool of utmost importance in our everyday activities, is markedly distinct from other extant and fossil primates. The evolution of hand bone morphology, how it was used in manipulative and locomotor activities, and the emergence of human-like hand use are therefore of great interest to Paleoanthropologists. This dissertation aims to contribute to our growing knowledge about isolated and associated hand bones of hominids and hominins. It contains three case studies applying virtual methods to analyze the morphology of hand bones with a particular focus on functional morphology.

The first case study focuses on an intermediate phalanx associated with the Miocene ape *Ouranopithecus macedoniensis*. The specimen (RPl-87) was previously identified as a hand bone based on a comparative analysis of linear measurements. To reassess this anatomical allocation, a morphological investigation of the phalanx was conducted using three-dimensional geometric morphometrics, thereby allowing for a more detailed comparison of shape differences. The results contradict the previous assessment and instead suggest that RPl-87 was likely a foot bone from the second or fifth ray. The comparison with phalanges of extant primates also highlights morphological similarities with the terrestrial primates *Gorilla* and *Papio*. This study, therefore, tentatively supports a primarily terrestrial locomotion for *O. macedoniensis*, agreeing with evidence from other disciplines.

The second and third studies aim to reconstruct habitual manual activity in early hominins. Study II combines the multivariate analysis of muscle attachment site (entheseal) patterns of the first metacarpal with a multivariate analysis of overall bone shape, thereby addressing habitual activity and mechanical efficiency within the same framework. We investigated a comparative sample of later *Homo*, including *Homo sapiens* and *Homo neanderthalensis*, and different recent great ape species. The early fossil hominin sample includes *Homo naledi*, *Australopithecus sediba*, *Australopithecus afarensis*, *Australopithecus africanus*, and SK84, an early hominin from Swartkrans with disputed species attribution. According to the results, later *Homo* and great apes differ clearly in their attachment site proportions of the first dorsal *interosseus*, a muscle heavily involved in tool-related behaviors. All early hominins, except for *A. africanus*, present entheseal patterns characterized by a relatively large attachment site of this muscle, supporting human-like hand use and, potentially, tool use in these species. Importantly, *A. sediba* and *A. afarensis* combine

human-like entheseal patterns with an ape-like morphology of the first metacarpal. This study highlights that, despite their limited manual dexterity (as shown by metacarpal shape), some hominins as early as *A. afarensis* habitually used their thumb similarly to humans and potentially engaged in tool-related behaviors. Consequently, our results suggest that biomechanical adaptations for increased manual dexterity on the hand skeleton occurred long after the emergence of human-like hand use.

The third study builds upon these results and expands the analysis of entheseal patterns to more hand muscles, focusing on the *Australopithecus* sample. The analysis shows that later *Homo* and the extant great apes differ in entheseal patterns. Like in Study II, the later *Homo* group shows a proportionally large attachment site of the first dorsal *interosseus*. Additionally, individuals of this group are characterized by large attachment sites on the fifth finger. The muscles in this pattern are involved in behaviors that play important roles in everyday human-like hand use, such as power grasping, in-hand stabilization and manipulation of objects. Among the australopiths, *A. sediba* and *A. afarensis* show similar, although not identical, attachment site proportions to later *Homo*. Our results thereby support a human-like hand use in these species that heavily relies on the muscles on the margins of the hand and, notably, the fifth finger. The fifth ray of *A. afarensis,* in particular, had previously been assessed as too inefficient and limited in movement to allow for the production of Lomekwian stone tools. These contradicting results once again highlight the need to differentiate between bone morphology that is behaviorally plastic and morphology that represents biomechanical adaptations. In contrast to the other australopiths, the entheseal pattern of *A. africanus* is unlike both that of later *Homo* and the extant great apes, suggesting that it engaged in a unique range of manual activities. In summary, this study produces evidence for human-like hand use in some *Australopithecus* specimens and emphasizes the value of activity reconstruction for human-evolutionary studies.

Altogether, this dissertation uses virtual methods to investigate hand (and foot) bone morphology to address manual and locomotor behaviors in the hominid and hominin fossil records. It also adapts these methods to allow a meaningful examination of isolated bones frequently occurring in the fossil record.

Zusammenfassung

Die menschliche Hand, ein Werkzeug von größter Bedeutung in unserem Alltag, unterscheidet sich deutlich von der anderer lebender und fossiler Primaten. Die morphologische Entwicklung von Handknochen, wie die Hand für Manipulation und in der Fortbewegung genutzt wurde und wann eine menschenähnliche Benutzung der Hand zuerst aufgetreten ist, sind daher wichtige Aspekte in der Paläoanthropologie. Diese Dissertation soll zu unserem wachsenden Wissen über isolierte und zusammenhängende Handknochen von Hominiden und Hominini beisteuern. Sie enthält drei Fallstudien, die, mit einem spezifischen Fokus auf funktionelle Morphologie, virtuelle Methoden zur Analyse von Handknochenmorphologie anwenden.

Die erste Fallstudie behandelt eine mittlere Phalanx, die dem miozänen Affen *Ouranopithecus macedoniensis* zugeschrieben wird. Der Knochen (RPl-87) war zuvor basierend auf einer vergleichenden Analyse mit linearen Messungen als Handknochen identifiziert worden. Um diese anatomische Ansprache neu einzuschätzen, untersucht diese Studie die Morphologie der Phalanx anhand von dreidimensionaler geometrischer Morphometrie. Dieser Ansatz erlaubt einen detaillierteren Vergleich der Formunterschiede. Die Ergebnisse widersprechen der zuvorigen Einschätzung und deuten stattdessen darauf hin, dass RPl-87 vermutlich einen Fußknochen vom zweiten oder fünften Zeh darstellt. Der Vergleich mit Knochen von lebenden Primaten hebt außerdem Ähnlichkeiten in der Knochenform mit *Gorilla* und *Papio* hervor. Diese Studie schlägt daher vorsichtig eine größtenteils terrestrische Fortbewegung für *O. macedoniensis* vor, was mit Beweisen aus anderen Disziplinen übereinstimmt.

Die zweite und dritte Fallstudie beschäftigen sich mit der Rekonstruktion von Handnutzung von frühen Homininen. Studie II kombiniert die multivariate Analyse von Muskelansatzstellen (Enthesen) des ersten Mittelhandknochens mit einer multivariaten Analyse der Knochenform, wodurch sie sowohl gewohnheitsmäßige Aktivität, als auch mechanische Effizienz untersucht. Die Analyse wurde mit zwei Vergleichsgruppen durchgeführt – späterer *Homo*, was *Homo sapiens* und *Homo neanderthalensis* beinhaltet, und verschiedene Spezies rezenter Menschenaffen. Zu den fossilen Hominini gehören *Homo naledi*, *Australopithecus sediba*, *Australopithecus afarensis*, *Australopithecus africanus* und SK84, ein Knochen aus Swartkrans mit umstrittener Spezieszuweisung. Das Ergebnis zeigt eine klare

Differenzierung zwischen den beiden Gruppen in der proportionellen Ausprägung der Muskelansatzstelle des ersten dorsalen *interosseus*, ein Muskel der stark in Steinwerkzeug betreffende Ativitäten involviert ist. Alle frühen Hominini, mit der Ausnahme von *A. africanus*, zeigen ein Handenthesen Muster, das durch eine proportional große Ansatzstelle dieses Muskels charakterisiert ist, was auf menschenähnliche Benutzung der Hand und möglicherweise Werkzeugnutzung hindeutet. Des Weiteren zeigen *A. sediba* und *A. afarensis* dieses menschenartige Handenthesenmuster in Kombination mit einer affen-ähnlichen Morphologie des ersten Mittelhandknochens. Diese Studie zeigt auf, dass einige Hominini bereits so früh wie *A. afarensis* trotz ihrer eingeschränkten Fingerfertigkeit (dargestellt durch die Knochengestalt) ihren Daumen regelmäßig in einer ähnlichen Art und Weise wie Menschen nutzten. Dies involviert gegebenenfalls auch die Produktion und Nutzung von Steinwerkzeugen. Unser Ergebnis legt dementsprechend nahe, dass biomechanische Anpassungen am Handskelett im Bezug auf verbesserte Fingerfertigkeit vermutlich deutlich nach dem ersten Auftreten von menschenähnlicher Handnutzung aufkamen.

Die dritte Studie baut auf diesen Ergebnissen auf und erweitert die Analyse auf weitere Muskelansatzstellen der Hand während sie sich außerdem auf die drei *Australopithecus* Spezies fokussiert. Die Analyse zeigt, dass sich spätere *Homo* Individuen und rezente Menschenaffen deutlich in der proportionalen Ausprägung ihrer Muskelansatzstellen unterscheiden. Wie in Studie II zeigt auch hier die späte *Homo* Gruppe eine relative große Ansatzstelle des ersten dorsalen *interosseus.* Zusätzlich zeichnen sich Individuen dieser Gruppe durch proportional große Enthesen am kleinen Finger aus. Die Muskeln, die dieses Muster charakterisieren sind in Verhalten involviert, die eine wichtige Rolle in der tagtäglichen Handnutzung des Menschen spielen. Darunter fallen zum Beispiel der Power-Griff und die Manipulation und Stabilisierung von Objekten mit einer Hand. Von den *Australopithecus* Spezies zeigen *A. sediba* und *A. afarensis* ähnliche, allerdings nicht identische Proportionen der Muskelansatzstellen. Unsere Ergebnisse weisen demnach auf menschenähnliche Handnutzungen in diesen Spezies hin, die besonders auf den Muskeln an den Rändern der Hand und spezifisch dem kleinen Finger basiert. Insbesonders der fünfte Finger von *A. afarensis* wurde zuvor als zu ineffizient und zu eingeschränkt in der Bewegung eingeschätzt, um für die Produktion der Lomekwi Steinwerkzeuge verantwortlich zu sein. Diese widersprüchlichen Ergebnisse zeigen erneut, dass seine Differenzierung zwischen Morphologie, die von Aktivität beinflusst wird und solcher, die biomechanische

Anpassungen reflektiert, von äußerster Wichtigkeit ist. Im Gegenteil zu den anderen Australopitheziden ähnelt das Handenthesen Muster von *A. africanus* weder den späten *Homo* Individuen, noch den rezenten Menschenaffen. Dies weist darauf hin, dass *A. africanus* seine Hand vermutlich für eine einzigartige Auswahl an Aktivitäten verwendete. Zusammenfassend liefert diese Studie Hinweise auf menschenähnliche Handnutzung in einigen *Australopithecus* Individuen und betont den Wert der Aktivitätsrekonstruktion für Untersuchungen zur menschlichen Evolution.

Zusammenfassend verwendet diese Dissertation virtuelle Methoden für die Analyse der Morphologie von Hand- und Fußknochen, um manuelle Verhaltensweisen und Fortbewegung in hominiden und homininen Fossilien zu untersuchen. Des Weiteren wurden diese Methoden angepasst, um eine aussagekräftige Untersuchung von isolierten Knochen zu ermöglichen, welche unter Fossilien häufig vorkommen.

List of Abbreviations

2D – two dimemsional

3D – three-dimensional

ABP – *abductor pollicis*

ADM – *abductor digiti minimi*

ADP – *adductor pollicis*

APL – *abductor pollicis longus*

CMC - carpometacarpal

CT – computer tomography

DFA – discriminant function analysis

DI1 – first dorsal *interosseus*

ECU – *extensor carpi ulnaris*

FDM – *flexor digiti minimi*

FDS – *flexor digitorum suberficialis*

FPB – *flexor pollicis brevis*

GMM – geometric morphometrics

LCA – last common ancestor

MC – metacarpal

MCP - metacarpophalangeal

mm – millimeter

mya – million years ago

OP – *opponens pollicis*

PC	principal component
PCA	principal component analysis/analyses
PD	Procrustes distance
RPl	Ravin de la Pluie
VERA	Validated Entheses-based Reconstruction of Activity

List of Figures

Chapter 3

List of publications

This cumulative dissertation includes two accepted and one submitted manuscript in fulfillment of the requirements. Percentages of own contribution to manuscripts are listed in parentheses (scientific idea/data generation/analysis and interpretation/paper writing).

Accepted articles

Study I: *O. macedoniensis* phalanx (0/100/100/70)

Kunze, J., Karakostis, F.A., Ioannidou, M., Koufos, G., Harvati, K., 2023. Geometric morphometric analysis of the intermediate phalanx of *Ouranopithecus macedoniensis*–a pilot study.

Manuscript accepted for publication in: *Human Evolution at the CROSSROADS: Research in Greece and beyond.* Proceedings of the Closing Symposium, February 2022 Tübingen. Paleoanthropology Book Series – Contributions in Paleoanthropology III. Tübingen University Press.

Study II: Entheseal patterns of the thumb and tool use in early hominins (50/100/80/70)

Kunze, J., Karakostis, F.A., Merker, S., Peresani, M., Hotz, G., Tourloukis, V., Harvati, K., 2022. Entheseal Patterns Suggest Habitual Tool Use in Early Hominins. *PaleoAnthropology* 2022 (2), 195-210.

DOI: 10.48738/2022.iss2.61.

Submitted Manuscripts

Study III: (50/100/80/70)

Kunze, J., Harvati, K., Hotz, G., Karakostis, F.A., submitted. Human-like manual activities in *Australopithecus*.

Manuscript submitted to the *Journal of Human Evolution.*

1 Introduction

Our hands are arguably the most diverse tools we possess. We use them to manipulate objects, feel and explore our surroundings, gesture, and talk. The human hand is unique in the vast array of activities it is used in, which renders its development throughout evolution an interesting subject for anthropologists. However, reconstructing the evolutionary pathways that led to the hominin hand is not straightforward. Primitive, ape-like traits have been observed in the hands of relatively recent species, such as *Homo naledi* (Kivell et al., 2015) or *Homo floresiensis* (Tocheri et al., 2007). In contrast, one of the earliest putative hominins, *Orrorin tugenensis*, shows a derived, more human-like pollical distal phalanx (Gommery and Senut, 2006). Another complicating factor is the preservation of the fossil record. Fairly complete hand skeletons are only known from very few hominin species, whereas incomplete hand skeletons and fragmented or isolated bones are far more frequent. For some species, such as *Orrorin* and *Homo erectus*, the evidence is too sparse to draw meaningful functional conclusions (Kivell et al., 2023). Moreover, only hard tissue is preserved in the fossil record, whereas the information that soft tissue can provide about muscles, nerves, ligaments, and tendons is lost. Reconstructions of manual abilities and hand use, therefore, have to be based solely on the bones and their internal and external morphology.

This dissertation aims to investigate different facets of hominid hand morphology. Specifically, it examines how morphology can be used for the identification of isolated bones, what it can tell us about habitual behavior, and how this should be distinguished from adaptations for increased manual dexterity.

1.1 Hand use in hominid evolution

Humans are markedly distinct from other primates in their increased manual dexterity. The human hand possesses a long, robust thumb that facilitates forceful precision grips (Marzke, 2013; Kivell, 2015). The repertoire of human grips is vast, including some not shared by other species. While research has mostly focused on power and precision grips (Napier, 1956; Landsmeer, 1962; Long, II et al., 1970; Marzke et al., 1992; Marzke, 1997; Feix et al., 2016), it has been pointed out that the manipulation of objects within the fingertips of a single hand appears to be a distinctively human trait as well (Christel, 1993; Williams et al., 2012; Marzke, 2013; Kivell, 2015; Bardo et al., 2017).

Introduction

Contrary to humans, other primates use their hands not only for manipulation but also for locomotion. As our closest living relatives, great apes are most frequently compared to modern humans and earlier hominins. Most knowledge about great ape behavior comes from observations in the wild and experimental studies in captive environments, whereas little is known about biomechanics and muscle activation of specific behaviors (Bardo et al., 2017; Kivell et al., 2023). Orangutans are the most arboreal among great apes, engaging in suspensory behavior and quadrumanous climbing. On the ground, they are fist-walking (Fleagle, 2013; Schmitt et al., 2016; Dunmore et al., 2020a). During manipulation, orangutans use various grips and readjust frequently, often using the mouth or the foot. This can likely be attributed to their arboreal lifestyle in which one hand would be occupied by grasping supports (Bardo et al., 2017). In contrast, gorillas are mainly terrestrial knuckle-walkers. However, their degree of arboreality is highly dependent on species (*Gorilla gorilla* or *Gorilla beringei*), sex, ontogenetic stage, and environment, among others (Fleagle, 2013; Schmitt et al., 2016; Dunmore et al., 2020a). Differences between species can also be observed in manipulation. Experimental studies on *G. gorilla* show low inter-individual variability in grasping techniques (Bardo et al., 2017) and the most marked hand preferences among great apes (Christel, 1993). In contrast, wild mountain gorillas (*G. beringei*) appear to be more flexible, using a variety of grips during plant food processing and bimanual role differentiation (Byrne et al., 2001; Neufuss et al., 2019). Chimpanzees, our closest living relatives, are by far the most investigated species among the great apes. They are most variable in their mode of locomotion, and their environment strongly influences their behavior (Fleagle, 2013; Dunmore et al., 2020a). Chimpanzees knuckle-walk when terrestrial but climb and scramble using power and hook grips when arboreal (Schmitt et al., 2016; Neufuss et al., 2017; Dunmore et al., 2020a). Chimpanzees are also frequent tool users. Wild populations have been observed making use of different objects in their environments, using leaves for sponging, sticks for ant dipping, honey fishing or hunting small mammals, as well as throwing or dragging branches for display (Boesch and Boesch, 1990; Fleagle, 2013; Pruetz et al., 2015). Most notably, some wild chimpanzee populations, e.g., from the Taï National Park in the Republic of Côte d'Ivoire, have been reported to crack nuts using stones or clubs (Boesch and Boesch, 1990; Boesch-Achermann and Boesch, 1993; Visalberghi et al., 2015). Percussive behavior has often been referred to as a likely proxy for the first instance of tool use in hominins (Rolian and Carvalho, 2017; Thompson et al., 2019; Gürbüz and Lycett, 2021; Luncz et al., 2022). However, chimpanzees are not the only primates displaying percussive tool use.

Bearded capuchin monkeys use stones to dig, crack open seeds, nuts, and fruits, and even unintentionally produce flakes similar to those found in archaeological contexts when destroying quartzite cobbles (Proffitt et al., 2016; Haslam et al., 2017; Falótico et al., 2018). Long-tailed macaques have been observed to use larger stones to crack nuts and shellfish on an anvil while also using smaller stone tools to process mollusks (Gumert et al., 2009; Gumert and Malaivijitnond, 2012, 2013). Despite the varied behavior observed in different primate species, chimpanzee nut cracking remains the most frequent comparison for hominin tool use (Haslam et al., 2017).

Most studies on early hominin hand use focus on their capability to produce and use stone tools. The idea that systematic tool use is limited to *Homo* has been disproven as the earliest proposed evidence of stone tools in the archaeological record predates the emergence of this genus (McPherron et al., 2010; Harmand et al., 2015; Plummer et al., 2023). To date, secure and unambiguous spatiotemporal associations of early hominins with stone tools are scarce in the archaeological record. However, the absence of contextual correlation between fossils and lithic implements need not represent the absence of the behavior per se. Therefore, researchers attempt to reconstruct tool-using capabilities and behavior directly from the fossil record. To be able to recognize the corresponding features in fossils, experimental and biomechanical modeling studies have explored various characteristics of stone tool production and use. This includes investigations of the different grip types used (Marzke and Shackley, 1986), to what extent digits are loaded (Williams et al., 2012; Williams-Hatala et al., 2018; Key et al., 2019; Williams-Hatala et al., 2021), muscle activation patterns (Marzke et al., 1998; Key et al., 2020), joint angles and degrees of flexion (Faisal et al., 2010; Fedato et al., 2020), and kinematic data (Williams et al., 2010; Rolian et al., 2011; Williams et al., 2014), among others. These studies show that the thumb is heavily recruited during tool-related activities, followed by the index and little finger (Marzke et al., 1998; Rolian et al., 2011; Williams-Hatala et al., 2018; Key et al., 2019; Key et al., 2020). Accordingly, the features involved in tool making and use are mainly located on these digits. Among the most often discussed traits is the thumb length relative to the remaining digits. Together with the increased mobility in its saddle-shaped carpometacarpal (CMC) joint, a long thumb facilitates grips involving both precise and forceful thumb opposition that are crucial for controlling cores or tools. Moreover, the human thumb is relatively robust, allowing it to withstand higher loads. Among the remaining fingers, the fifth digit is the most robust in humans. Its saddle-shaped CMC joint with the hamate allows for more abduction and axial rotation, leading to increased opposability towards the thumb

(Young, 2003; Kivell, 2015; Key et al., 2019). During tool use, the fifth finger stabilizes and secures tools within the hand, whereas it was reported to adjust the platform angle and stabilize the core during hard hammer percussion (Marzke and Shackley, 1986; Marzke et al., 1998; Key et al., 2019). Several thumb muscles are heavily recruited during tool production and use, including the intrinsic *opponens pollicis*, *flexor pollicis brevis*, the first dorsal *interosseus* originating from the thumb, and the extrinsic *flexor pollicis longus*. On the ulnar portion of the hand, the *abductor digiti minimi* attaching to the fifth digit reaches high activation levels as well. Interestingly, the highly recruited muscles during tool-related behaviors appear to be mainly related to securing and controlling objects in one hand and less to conducting large, powerful movements (Marzke et al., 1998; Key et al., 2020).

The onset of tool-related behavior is important from a bio-cultural evolutionary perspective, but it is not the only activity early hominins would have used their hands for. Although specific activities are difficult to ascertain without vestiges from the archaeological record, the manual loadings of carrying (Key, 2016) and requirements for efficient throwing and clubbing (Young, 2003) have been previously investigated. Finally, it has been argued that early hominins likely used their hands for arboreal locomotion as well. The more primitive features, such as high phalangeal curvature and well-developed flexor sheath ridges, have been pointed out as evidence for habitual climbing (e.g., Stern and Susman, 1983; Ricklan, 1987; Kivell, 2015; Kivell et al., 2018; but see Chapter 1.2).

How the last common ancestor (LCA) of the *Homo*-*Pan* clade used its hands can only be hypothesized, as no fossil evidence is known to date. It has been argued that since humans and great apes use tools, parsimony would suggest that some form of tool use was present in the LCA as well (Panger et al., 2002; Richmond et al., 2016; Rolian and Carvalho, 2017; but see Haslam et al., 2009). Generally, the hand morphology of the LCA is heavily debated. Frequent suggestions involve a morphology resembling that of great apes (Tocheri et al., 2008; Rolian et al., 2010; Prang et al., 2021), whereas others claim that extant great apes are a poor model for the LCA (Lovejoy et al., 2009b; Almécija et al., 2015; White et al., 2015). Further discussions are related to the LCA's mode of locomotion – was it climbing (Prang et al., 2021), clambering (Böhme et al., 2019), or knuckle-walking (Richmond and Strait, 2000)?

Investigating the hand bones of Miocene apes may shed more light on the potential hand morphology of the LCA. Unfortunately, phylogenetic relationships among these primates are ambiguous, making it difficult to ascertain to what extent different Miocene ape taxa contributed to the African evolution of hominins (Begun et al., 2012; Kivell et al., 2023). Morphological assessments usually focus on identifying the most likely mode of locomotion using comparative approaches. Frequently highlighted traits include bone length and robusticity, phalangeal curvature, shape of the trochlear condyles and size of the flexor sheath ridges (e.g., Begun, 1994; Madar et al., 2002; Nakatsukasa et al., 2003; Moyà-Solà et al., 2004; Almécija et al., 2007; Deane and Begun, 2008; de Bonis and Koufos, 2014). Generally, the phalanges of Miocene apes are more similar to each other than to extant primates and only slightly curved (Almécija et al., 2009, 2012). The only exception is the late Miocene ape *Hispanopithecus,* which was argued to present early signs of specific adaptations to below-branch suspension (Almécija et al., 2007).

1.2 Functional morphology

Activity reconstruction on the basis of skeletal remains necessitates good knowledge and awareness of the interpretive potentials and pitfalls entailed in the functional study of different bone traits. This includes differentiating between genetically regulated adaptive traits and morphology more responsive to individual habitual activity. There are different reasons why inferring activity from adaptive traits can be misleading. First, traits can be retained without being functionally significant. This can occur in the absence of negative selection or if the trait is genetically or developmentally linked to characters under stabilizing selection (Ward et al., 1997). Secondly, the absence of a trait does not mean that the behavior was absent (Almécija et al., 2009; Schmitt et al., 2016). Finally, individual activity is very much influenced by external factors (e.g., environment) and may, therefore, not necessarily concur with functional adaptations (Fleagle, 2013; Schmitt et al., 2016).

One prime example of the latter argument was recently examined in a study by Wallace and colleagues (2020) concerning phalangeal curvature. High phalangeal curvature is found in arboreal primates and is reported to intensify with increasing arboreality, both among species and during ontogeny (Congdon, 2012). Curvature has also been shown to reduce strain on the phalanges during arboreal locomotion (Richmond, 2007; Nguyen et al., 2014). Therefore, it has been suggested that phalangeal curvature is indicative of arboreal locomotion as it develops during life in response to arboreal activity (Stern et al., 1995; Jungers et al., 1997; Jungers et al., 2002; Richmond, 2007; Congdon, 2012). Consequently, the presence of curved phalanges in early hominins would imply that they, too, engaged in a considerable amount of arboreal locomotion. Wallace and colleagues contest this theory by studying the phalanges of a chimpanzee that was raised like a human child and spent little time in trees. They found that the phalangeal curvature of this individual was indistinguishable from wild chimpanzees, concluding that genetic factors more heavily influence this trait than mechanical stress resulting from habitual activity (Wallace et al., 2020).

Generally, bone form (i.e., size and shape) is largely regulated genetically (Currey, 2012). It is undoubtedly true that mechanical loading affects bone form and structure, but not all aspects and regions of the bone respond equally to the strain induced by activity (Ruff et al., 2006). Therefore, it would be more conservative to interpret the presence of adaptive traits as increased potential efficiency in performing specific tasks instead of the presence of a behavior.

Nonetheless, there are aspects of the bone that are responsive to individual habitual activity, such as trabecular bone (Biewener et al., 1996; Scherf et al., 2013; Tsegai et al., 2013; Kivell, 2016; Scherf et al., 2016) or muscle attachment sites. Muscle attachment sites (entheses) are the interface between the hard and soft tissue of bone and muscle. As such, their function is to dissipate the strain caused by muscle activation over a larger area to prevent tissue failure (Benjamin et al., 2002). The history of research demonstrates an ambivalent attitude toward the applicability of muscle attachment site analysis for activity reconstruction. Although the approach was used frequently in bioarchaeological studies beginning in the 1980s, the etiology of entheseal changes and their suitability for activity reconstruction have been called into question by several researchers (Zumwalt, 2006; Milella et al., 2012; Schlecht, 2012; Rabey et al., 2015; Williams-Hatala et al., 2016; Wallace et al., 2017). The debate was further complicated by shortcomings of the most frequently applied methods – scoring systems – which suffer from high inter-observer error (Cashmore and Zakrzewski, 2013; Karakostis and Lorenzo, 2016; Wilczak et al., 2017), low statistical power (Noldner and Edgar, 2013), or loss of information (presence/absence systems; Cashmore and Zakrzewski, 2013; Wilczak et al., 2017). The recently developed Tübingen University “Validated Entheses-based Reconstruction of Activity” (VERA) method (developed by F. A. Karakostis; Karakostis and Lorenzo, 2016; Karakostis and Harvati, 2021; Karakostis, 2023, and references therein) addresses several of the issues that the field faced in the past decades. The method analyzes entheseal patterns in a multivariate approach instead of comparing single entheses, thereby minimizing the impact of other influential factors (Karakostis and Lorenzo, 2016; Karakostis et al., 2018). It has been previously validated in experimental studies (Karakostis et al., 2019b; Karakostis et al., 2019a; Castro et al., 2022; Karakostis and Wallace, 2023) and using a documented skeletal sample (Karakostis et al., 2017a), and was applied in a wide variety of contexts (Karakostis et al., 2018; Karakostis et al., 2020; Karakostis et al., 2021a; Bousquié et al., 2022; Karakostis and Hotz, 2022). Crucially, a minimum sample of three entheses is deemed sufficient to implement the VERA method, facilitating its application to the often-fragmented and poorly preserved fossil record (Karakostis et al., 2018; Karakostis, 2023).

1.3 Isolated bones

The scarcity of complete and articulated skeletons in the fossil record is a well-known phenomenon. It is not uncommon for researchers to be forced to exclude individuals due to bad preservation or methods having to be adapted to accommodate less complete specimens. Isolated or comingled postcranial bones with insecure or unknown species attribution are particularly common, as noted by Grine et al. (2022). This is especially true for structures such as the hand that comprise a high number of small bones. Indeed, articulated and well-preserved hand skeletons are rare in most archaeological contexts (Cashmore and Zakrzewski, 2013; de Bonis and Koufos, 2014; Tsiminikaki et al., 2019), significantly complicating the identification process.

Few studies have attempted to facilitate the identification and allocation of hand bones (Case and Heilman, 2006; Christensen, 2009; Garrido Varas and Thompson, 2011; Karakostis et al., 2017b). In commingled contexts, methods such as pair matching have been proposed to re-associate bones of the same individual (Garrido-Varas et al., 2015; Tsiminikaki et al., 2019). However, these methods can only be confidently applied if the bones are identified and sided. While this is a feasible task if bones from multiple rays are preserved, anatomically allocating isolated hand bones, particularly phalanges, has proven to be complicated (Case and Heilman, 2006; Karakostis et al., 2017b). Importantly, phalanges should be positioned before sided, as morphological indicators of anatomical side differ among rays (Case and Heilman, 2006; Christensen, 2009; Garrido Varas and Thompson, 2011). When multiple bones are preserved, ray allocation is usually based on relative lengths. The pattern for proximal and intermediate phalanges follows III>IV>II>V(>I) (Susman, 1979; Scheuer and Black, 2000; but see Garrido Varas and Thompson, 2011), whereas distal phalanges can be distinguished by length (I>III≥IV>II>V; Case and Heilman, 2006) or by robusticity (I>III>II>IV>V; Scheuer and Black, 2000). Other approaches reporting better accuracy for positioning isolated proximal phalanges are based on morphological assessments (Garrido Varas and Thompson, 2011) and multivariate morphometrics (Karakostis et al., 2017b). Nonetheless, the identification of isolated hand bones in the fossil record can still be ambiguous, particularly as bones are often damaged and might present diverging morphological characteristics when dealing with different species. Consequently, most researchers handle the identification of these bones more conservatively by assigning them to a category (i.e., proximal, intermediate, distal; e.g., Larson et al., 2009; Détroit et al., 2019) or providing multiple possible ray determinations (de Bonis and Koufos, 2014; Détroit et al., 2019; Kivell et al., 2020; Kivell et al., 2023).

Even in those cases where hand bones can be accurately identified, the fossil record rarely presents complete hand skeletons. This leaves paleoanthropologists with the task of finding a way to meaningfully analyze what is preserved. One option is to use composite skeletons, consisting of isolated bones from multiple individuals. Composite hand skeletons of *Australopithecus afarensis* (Hadar; Bush et al., 1982; Kivell, 2015), *Australopithecus africanus* (Sterkfontein; Ricklan, 1987; Richmond et al., 2016) and *Ardipithecus ramidus* (combination of left and right elements of ARA-VP-6/500; Richmond et al., 2016) are more commonly referred to, but combinations of isolated phalanges are also possible for other species and locations (e.g., *Paranthropus robustus* / early *Homo*, Swartkrans (Susman, 1988)). The downside of composite skeletons is that they do not represent a specific individual; consequently, conclusions drawn from their analysis can only yield information on the species in general. Moreover, when reconstructing habitual behavior, combining bones from different individuals might even introduce conflicting signals (e.g., cf. Study III).

Alternatively, analyses have to be adapted to focus only on single bones. In the case of the hand, this approach is prevalent for the bones of the thumb due to its great importance for human-like manipulation (Niewoehner, 2005; Almécija et al., 2010; Marchi et al., 2017; Galletta et al., 2019; Dunmore et al., 2020b; Bowland et al., 2021; Morley et al., 2022). This approach circumvents the issues introduced by combining bones from different individuals; however, focusing the analysis on only a single bone can limit the information gained. Despite their downsides, both approaches have been shown to yield important information about manual abilities and behavior in fossil hominids.

2 Research Strategy

2.1 Objectives

The overall aim of this doctoral research was to investigate the hand bone morphology of selected hominids and early hominins while focusing on different research questions. A particular emphasis was put on functional morphology and its role in activity reconstruction while also exploring the use of analyzing morphology with virtual techniques to identify isolated bones. Specifically, the three studies presented here pursue the following objectives:

(1) To contribute to the identification of an isolated phalanx from the Miocene ape *Ouranopithecus macedoniensis* through bone morphology using geometric morphometrics.
(2) To improve our understanding of hand use in early human evolution and the onset of human-like manipulation and tool use by analyzing the manual entheseal patterns of early hominins.
(3) To demonstrate the importance of differentiating between functional adaptation and habitual activity by combining the analysis of overall bone shape, used here as a proxy for biomechanical efficiency, with the investigation of muscle attachment sites, reflecting individual behavior.

2.2 Research questions

Study I: Does the isolated intermediate phalanx RPl-87, attributed to *O. macedoniensis,* indeed belong to the hand? What ray can it be assigned to?

Ouranopithecus macedoniensis is a Late Miocene ape (9.6 – 8.7 mya) found in three localities in Northern Greece (Sen et al., 2000; de Bonis and Koufos, 2001; Koufos et al., 2016; see also Ioannidou et al., 2019). The species is mainly represented by cranial and dental remains, whereas postcranial remains are only known from the type locality Ravin de la Pluie (RPl). The remains consist of two isolated phalanges, one proximal (RPl-86) and one intermediate (RPl-87). Their attribution to *O. macedoniensis* is based on the species being the only primate found at RPl (de Bonis and Koufos, 2014).

This study focuses on the better-preserved intermediate phalanx RPl-87, which was previously attributed to a paramedian digit of the hand (de Bonis and Koufos, 2014). However, due to the isolated nature of the phalanx, an allocation to the foot could not be excluded. As the phalanges are the only postcranial remains associated with this species to date, and since postcranial remains of Late Miocene hominoids are generally rare (de Bonis and Koufos, 2014), a secure identification of the phalanx is even more crucial. Therefore, the goal of this study is to contribute to the identification of the phalanx using three-dimensional (3D) geometric morphometrics. The analysis of shape in a comparative framework also allows for preliminary assessments of functional morphology.

Study II: Can we see signs of tool-related behavior in the entheseal patterns of the thumb of early hominins? How does the activity-related signal compare to overall bone shape and biomechanical efficiency?

When did systematic stone tool production and use first develop in our lineage? And who were the first tool users? These questions are heavily debated in human evolutionary studies as the evidence is inconclusive. The first potential evidence of tool production and use from the archaeological record is proposed to date to around 3.4-3.3 mya (McPherron et al., 2010; Harmand et al., 2015; alternatively, the oldest Oldowan was found at a site from ~3-2.6 mya; Plummer et al., 2023). However, the chronology and context of these finds have been criticized (Domínguez-Rodrigo and Alcalá, 2016; Archer et al., 2020). The hands of early hominins show a mixture of primitive (ape-like) and derived (human-like) traits (Marzke, 2013; Kivell, 2015; Richmond et al., 2016; and references therein). The retention of ancestral traits likely prohibited early hominins from using and producing tools as efficiently as modern humans (Domalain et al., 2017; Marchi et al., 2017; Galletta et al., 2019). However, these signs of lower manual dexterity should not be conflated with an absence of habitual tool-related behaviors. Generally, overall bone shape is largely genetically regulated due to its importance for functional and motoric aspects and, therefore, less malleable by physical activity (Parfitt et al., 2000; Currey, 2002, 2012). Consequently, when aiming to reconstruct behavior in early hominins, it is crucial to focus on aspects of the bone that are more responsive to habitual activity.

In this study, we analyze the entheseal patterns on the first metacarpals of early hominins in order to reconstruct habitual thumb use in a comparative framework, including a sample of later *Homo* and extant great apes. Additionally, we examine overall bone shape, including entheseal shape, as a proxy for adaptive functional morphology and efficiency. In combination, the two approaches aim to shed light on whether habitual tool use proceeded or was founded upon morphological adaptations that enabled increased manual dexterity.

Study III: Do australopiths show signs of human-like hand use? Is there a difference in hand use among *Australopithecus* species?

The final study presented in this thesis builds upon the framework and results of Study II. Whereas Study II focuses on the analysis of the first metacarpal, Study III extends the analysis of entheseal patterns to more bones of the hand skeleton. This approach, while excluding isolated bones and some fragmented hand skeletons used in the previous study, allows the analysis of synergies of muscles in different regions of the hand. In human-like hand use, the interaction of muscles on the margins of the hand is of particular interest (Marzke et al., 1998; Marzke, 2013; Kivell, 2015).

The human thumb differs notably from the thumbs of other primates and plays a crucial role in human-like hand use. As a result, it has also received ample attention in the analysis of early hominin hands (e.g., see Marchi et al., 2017; Galletta et al., 2019; Bowland et al., 2021; Karakostis et al., 2021b). In contrast, comparatively few studies directly address the importance of the fifth finger (Key et al., 2019). This digit and the muscles attaching to it are not only crucial during tool production and use (Marzke and Shackley, 1986; Marzke et al., 1998; Marzke, 2013; Kivell, 2015; Key et al., 2019; Fedato et al., 2020) but are also heavily involved in more general manipulative behaviors. These include, among others, throwing (Young, 2003), power grasping (Marzke et al., 1992; Goislard de Monsabert et al., 2012; Karakostis et al., 2017a), as well as stabilizing and manipulating objects within one hand (Marzke et al., 1998; Marzke, 2013; Kivell, 2015; Key et al., 2019). In addition to manipulative behaviors, early hominins, like *Australopithecus*, might have also used their hands for arboreal locomotion (Marzke, 1983; Rolian and Gordon, 2013; Kivell et al., 2018; Dunmore et al., 2020b). As discussed previously (see Chapter 1.2), treating phalangeal curvature as a reliable indicator of habitual arboreal locomotion might be misleading (Wallace et al., 2020). Alternatively, the attachment sites of the extrinsic flexor muscles on the phalanges could yield insight into the proportionate use of these muscles and, therefore, potential arboreality in early hominins.

This study investigates the entheseal patterns of *A. africanus, A. afarensis*, and *A. sediba* in a comparative framework to reconstruct their habitual hand use. By including more bones and attachment sites, it aims to identify signs of general human- or ape-like hand use in the australopiths and examine differences among the three species.

3 Materials and Methods

The three studies presented here applied virtual anthropological techniques to answer the research questions listed above. The following sections serve to introduce the respective materials and methods. As Study III used similar materials and methods to Study II, both will be discussed together. More detailed descriptions and information can be found in the appendices and references therein.

3.1 Study I (Appendix A)

RPl-87 is an intermediate phalanx associated with the Miocene ape *O. macedoniensis*. It was found *in situ* at Ravin de la Pluie, Greece, but was not associated with other skeletal remains found at the site, including another phalanx RPl-86 (de Bonis and Koufos, 2014). To produce a 3D model of the bone, RPl-87 was scanned using an Artec Space Spider (Artec3D Inc., Luxembourg), a structured light scanner with a measuring accuracy reaching 50 microns.

In order to identify the isolated phalanx, we included a comparative sample of manual and pedal intermediate phalanges from extant primates, of which ray and side were known. The material consists of phalanges from rays two to five of *Gorilla gorilla*, *Pan troglodytes*, *Pongo pygmaeus*, *Papio hamadryas,* and *Macaca arctoides*. The phalanges were downloaded as CT scans from Morpho-Source.org and are courtesy of the American Museum of Natural History Mammal Collections. As the anatomical side of RPl-87 could not be determined prior to the analysis, the sample includes both left and right phalanges.

The morphological variation among the phalanges was analyzed and visualized using landmark-based geometric morphometrics (GMM). In contrast to traditional morphometrics, wherein shape is analyzed using linear measurements – distances, ratios, or angles – GMM quantifies shape variation through 2D or 3D landmarks. The latter are defined as cartesian coordinates of fixed points placed in homologous positions on the specimens of interest (Mitteroecker and Gunz, 2009; Adams and Otárola-Castillo, 2013). The morphology of the object is preserved throughout the analysis, as geometric relationships between measurements are maintained through landmark data. Among others, this allows the visualization of shape differences among the sample (Baab et al., 2012; Adams and Otárola-Castillo, 2013). After eliminating differences in orientation, location, and scaling, the resulting Procrustes shape coordinates can be used to quantify the shape variation in the sample (Mitteroecker and Gunz, 2009; Baab et al., 2012).

Unfortunately, neither hand nor foot phalanges show structures suitable for type I landmarks, usually characterized by the intersection of multiple features and, thereby, the most homologous (Bookstein, 1991; Baab et al., 2012). Due to the scarcity of recognizable and homologous features in general, we only used type III landmarks (placed in geometrically corresponding positions) in this study. In addition to the eleven fixed landmarks, 70 surface semilandmarks, slid based on minimizing bending energy, were used to capture more of the overall bone shape. The landmark placement was repeated three times on RPl-87 to assess accuracy.

For the analysis, the phalanges were grouped based on the respective research questions. This resulted in the following procedure: 1. Hand and foot bones were grouped by ray to determine what extremity RPl-87 belonged to; 2. Depending on these results, either hand or foot bones were excluded and phalanges from all rays were analyzed together to determine the ray RPl-87 was associated with; 3. Further reducing the sample size through elimination aimed to narrow down the ray identification.

Procrustes superimposition was performed separately for each analysis, and the resulting shape coordinates were analyzed with principal component analyses (PCA) based on covariance matrices. The principal components (PC) best separating the groups of interest were plotted in PC plots. RPl-87 was removed beforehand to ensure that its morphology didn’t affect the analyses. Its principal component scores were calculated separately and projected onto the PC plots. The shape variation in the sample was depicted using thin-plate spline grids (Bookstein, 1989), warping the mean specimen to represent the shapes at the extremes of the principal components. Additionally, as our comparative sample includes bones from species of vastly different sizes, correlation analyses of the first PC and centroid size (as a proxy for bone size) were performed to investigate the effect of size on the shape variation displayed in the PC plots. Finally, to further support the classification of RPl-87, neighbor joining trees were created using Procrustes distances (PD).

3.2 Study II (Appendix B) and Study III (Appendix C)

Studies II and III examine the manual muscle attachment sites of early hominins. Both studies use a similar sample, including early hominins and a comparative sample of later *Homo* (*Homo sapiens* and *Homo neanderthalensis*) and extant great apes (*Gorilla gorilla*, *Pan troglodytes*, *Pongo pygmaeus*, *Pongo abelii*). The sample includes only adult individuals, with one exception (a *G. gorilla* individual). Since an exact biological age could not be determined for all individuals, hand-bone fusion was used as an indicator. The data was collected from 3D models of the bones either created through surface or CT scanning. For Study II, bones from the right anatomical side were prioritized, but bones from the left side were used if the right side was not sufficiently preserved. In study III, bones were preferably used from the side showing better preservation. However, bones from different anatomical sides of the same individual had to be pooled in some cases due to taphonomical damage. Analyses of variance were conducted to examine whether the anatomical side affected the outcome of our analyses. Minor damage in the area of muscle attachment was tolerated as long as it did not visibly affect the results of the analyses (i.e., created outliers; see Chapter Enthesis Identification and Delineation in Appendix B). As Study III includes more bones and muscle attachment sites, some individuals who were part of Study II had to be removed due to insufficient preservation. For a detailed account of the specimens used per study, see Tables 1-3 in Appendix B and 1-3 in Appendix C.

Study II investigates the entheseal patterns of the first metacarpal (MC) in one specimen each of *Australopithecus sediba*, *A. afarensis*, *A. africanus*, *H. naledi,* and SK84, an isolated MC associated with early *Homo* or *Paranthropus* (Susman, 1988; Trinkaus and Long, 1990). The muscles attaching to the first MC include the *opponens pollicis* (OP), the *abductor pollicis longus* (APL), and the insertion site of the first dorsal *interosseus* (DI1). Study III focuses on the entheseal patterns of the *Australopithecus* species and additionally includes the attachment sites of the *adductor pollicis* (ADP), *abductor pollicis* (ABP), and *flexor pollicis brevis* (FPB) on the first proximal phalanx; the *extensor carpi ulnaris* (ECU) on the fifth MC; the *abductor digiti minimi* (ADM) and *flexor digiti minimi* (FDM) on the fifth proximal phalanx; and the *flexor digitorum superficialis* (FDS) on the third intermediate phalanx (Fig. 1). The majority of these muscles show a similar site of attachment and function among all species of the sample. Notably, the DI1 is absent in *P. troglodytes.* In this species, the *intermetacarpales* 1-4 are not fused with the *flexores brevis profundi* 3, 5, 6 and 8 to form the dorsal *interossei*, a secondary revision to the plesiomorphic primate condition (Diogo et al., 2012). However, as they attach in the same area of the bone, it was suggested that the first *intermetacarpalis* and the DI1 have a similar function (Diogo et al., 2013; Lemelin and Diogo, 2016; Vereecke and Wunderlich, 2016). In contrast, differences in secondary muscle function between *P. troglodytes* and humans have been reported for the OP. While, in addition to flexion, its activation leads to thumb abduction in humans, it instead adducts the thumb in chimpanzees (Marzke et al., 1999).

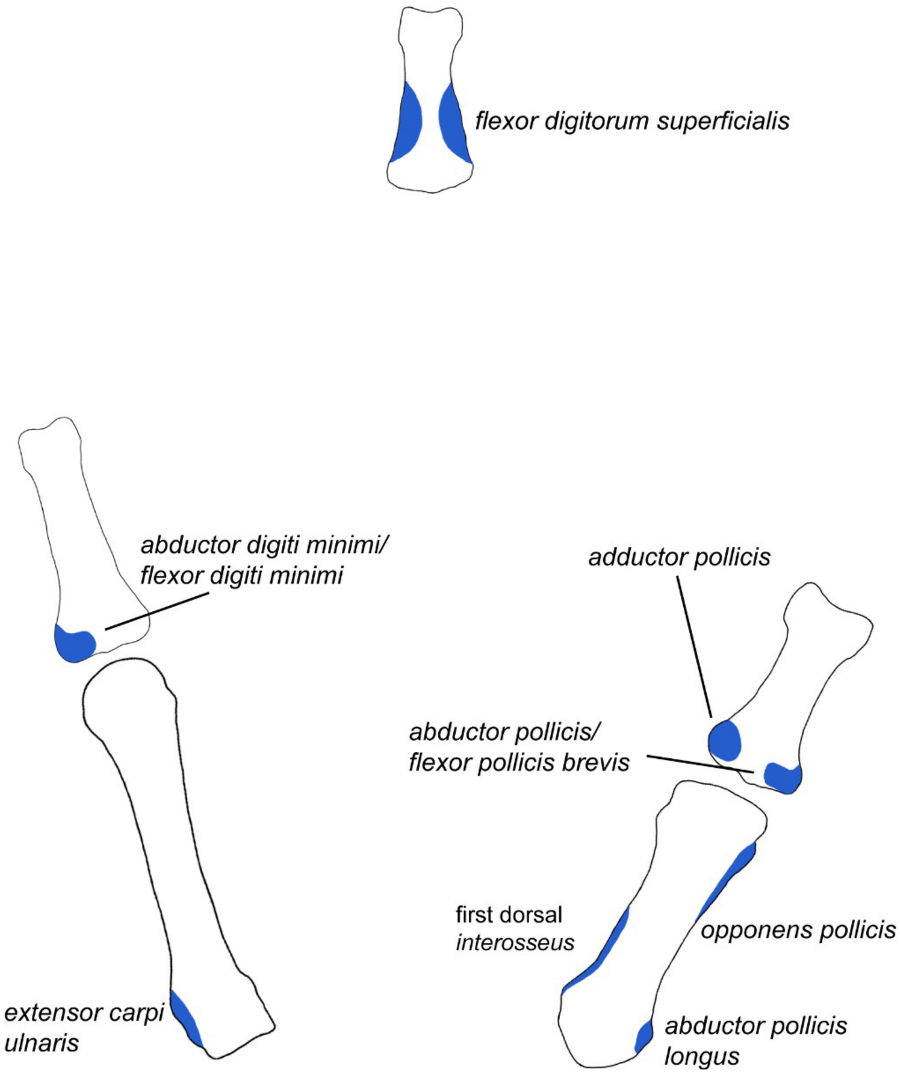

Figure 1: Schematic depiction of the entheses used in Studies II and III on a human hand skeleton. Grevenmacher individual 117 (Paleoanthropology Human Osteology Collection, University of Tübingen) was used as a reference.

In both studies, entheseal patterns were analyzed using the VERA protocol (Karakostis and Lorenzo, 2016; Karakostis and Harvati, 2021; Karakostis, 2023). 3D models of the bones were opened in MeshLab (v. 2021.07 Cignoni et al., 2008), where virtual filters were used to identify differences in elevation (both protrusion and depression), surface texture, and coloration (in the case of surface scans) in the areas of muscle attachment. Following the identification through these criteria, the entheses were delineated and cut from the surrounding bone. After final corrections to the delineations were made, aided by the use of filters, the entheseal surface area was measured in mm². Measurement accuracy was assured through precision tests in both studies. The geometric mean of all entheseal measurements was calculated for each individual to account for the influential effect of size. Subsequently, each entheseal measurement was divided by the geometric mean (Karakostis, 2023). The resulting values are referred to as entheseal proportions. Instead of the raw surface area measurement, these values reflect how large a muscle attachment site is in relation to the total entheseal surface area recorded for the individual. For Study III, an additional step was required for size adjustment due to the differences in proportionate digit length among species. Specifically, humans have a longer thumb relative to the fingers than great apes, whereas the fifth digit is longer in great apes than humans. Consequently, when both species are analyzed together, the entheseal proportions of thumb muscles will naturally be larger in humans than in great apes, while the latter will show larger proportions of muscles from ray five. This was circumvented by dividing each entheseal measurement by the overall surface area of the bone it is located on before adjusting the resulting value using the geometric mean (cf. Methods Appendix C).

The entheseal proportions were analyzed using multivariate statistics. First, the proportions were entered into PCAs based on a covariance matrix to explore variation in entheseal patterns within the sample. Groups were not assumed *a priori*, and different species were instead indicated visually in the resulting PC plots. Relevant PCs were chosen based on the scree-plot approach (Field, 2017). The early hominins were not included in the original analyses but projected onto the PC plots to not influence the outcome of the analyses. Additionally, discriminant function analyses (DFA) based on a within-groups covariance matrix were performed in order to determine the attachment site proportions that best distinguished between later *Homo* and extant great apes. For this, the comparative sample was divided into two groups (later *Homo* and extant great apes), whereas the early hominins were entered as unknown to classify them based on the variables that best separate the two groups. The entheseal proportions were used as variables and were entered stepwise. A Leave-one-out classification was deployed for cross-validation.

In addition to the analysis of entheseal patterns, Study II included a 3D GMM analysis of overall bone shape to investigate the functional morphology of the first MC. Fixed landmarks were placed in geometrically corresponding positions on the bone diaphysis, the articular surfaces, and the three muscle attachment sites. The precision of landmark placement was tested using the Centroid Radius approach (Singleton, 2002; Cramon-Taubadel et al., 2007). After Procrustes superimposition, the Procrustes shape variables were analyzed in a shape PCA without a priori group assumptions. The early hominins were not included in the analysis and were instead projected onto the PC plots based on their calculated PC scores. PCs relevant for plotting were determined using the scree-plot approach (Field, 2017).

4 Results and Discussion

The following chapter briefly discusses the main results of each study included in this cumulative thesis.

4.1 Study I: The intermediate phalanx RPl-87 of Ouranopithecus macedoniensis

The first study aimed to contribute to the identification of the isolated intermediate phalanx RPl-87 attributed to *O. macedoniensis*. A previous analysis of the bone has tentatively identified it as a hand bone, but the lack of comparative material from the same species complicates the allocation (de Bonis and Koufos, 2014). However, a definite identification of both isolated phalanges found at RPl is crucial, as they represent the only postcranial remains associated with *O. macedoniensis*. It is an important first step for continuative analyses of their functional morphology, which could yield important insight into their locomotor capabilities, adaptations, and habitual behavior.

Our analyses encompassed different steps. First, the goal was to identify whether RPl-87 belongs to the foot or the hand. For this, hand and foot bones were analyzed together in groups depending on their ray. In the analyses focusing on the second and fifth ray, RPl-87 shows a similar shape to the foot bones of the comparative sample (cf. Fig. 1 Appendix A). This is supported by the PD values, as the phalanx is closest to a *Papio* foot bone of both the second and fifth ray. In contrast, in analyses including phalanges from either rays three or four, RPl-87 diverges in shape from the comparative sample. Nonetheless, both PCA and PD place it closer in shape to foot than to hand bones. The results of these first analyses suggest that RPl-87 is closer in shape to the foot bones of our comparative sample, irrespective of the ray. Consequently, all hand bones were removed in the next step in order to determine the ray to which RPl-87 belongs. Analyzing foot bones of all rays together shows that shape variation in the sample is mainly attributed to differences among species, as there is a considerable overlap among rays (cf. Fig. 2 Appendix A). Specifically, rays two and five are concentrated on one end of the plot, whereas rays three and four are clustered on the other, indicating shape differences among these rays. RPl-87 plots in the range of shape variation of rays two and five and notably differs from rays three and four, as the previous analyses had already indicated. Unfortunately, it was not possible to further specify what ray RPl-87 belongs to. When analyzing bones from rays two and five in a separate analysis, the overlap among rays is too extensive to draw meaningful conclusions about the ray allocation of RPl-87.

The mean PDs show a similar picture – while RPl-87 is slightly closer to foot bones of the fifth ray, the difference is exiguous. Therefore, the results of our shape analysis suggest that RPl-87 belongs to a paramedian (second or fifth) digit of the foot. This partially contradicts the findings of the previous morphometric study by de Bonis and Koufos (2014), who assigned the phalanx to a paramedian digit of the hand.

Correlation analyses of centroid size and the first PC of each PCA show moderate correlations of the shape variation depicted in the PC plots and size. Although Procrustes superimposition generally corrects for size by scaling to the same centroid size (Mitteroecker et al., 2013), it can still have a significant effect on shape variation. Frequently, researchers investigate size-related shape variation during development, referred to as ontogenetic allometry. However, shape can also vary in response to different sizes among individuals of the same age group, i.e., static allometry (Mosimann, 1970; Mitteroecker et al., 2013; Klingenberg, 2016). Our comparative sample contains species that vary significantly in body size and mode of locomotion, both of which can affect (relative) bone size. As size (centroid size) and shape (PC1) are correlated in most of our analyses, it could be argued that the variation in our sample is mainly driven by size differences among species. In that case, the phalanges of the overall largest species, *Gorilla* and *Pongo*, should consistently plot together and away from the smallest species (*Macaca*). However, bones of *Gorilla* and *Pongo* are usually situated in opposite positions of the plot (PC1), whereas *Macaca* phalanges plot close to the center. Therefore, we propose that the correlation of shape and size can be explained by size differences among hand and foot bones, as well as among the different rays. Consequently, we argue that the variation represented in the PC plots is mainly driven by differences in shape, whereas the correlation with size is likely an ancillary effect.

The final goal was to assess whether RPl-87 shows shape-related affinities with the extant primate species of the comparative sample. The species separation in our analyses appears to be largely driven by functional adaptations to the mode of locomotion. As pointed out in the previous paragraph, the phalanges of *Gorilla* and *Pongo*, mainly terrestrial and arboreal species, respectively, are consistently separated in the analyses. *Gorilla* phalanges show a similar shape to *Papio* phalanges, whereas *Pan* phalanges are more similar in shape to *Pongo*. The phalanges of *Macaca* are usually situated in an intermediary position. This species separation is best depicted in the plot including the foot phalanges of all rays (cf., Figure 2 Appendix A). The shape variation in this analysis is mainly related to changes in robusticity and relative length and breadth. The species engaging in a comparatively large amount of arboreal locomotion (*Pongo*, *Macaca*, and likely most *Pan* individuals) are characterized by a proportionally long and slender bone shape, whereas the primates more adapted to terrestrial locomotion (*Gorilla* and *Papio*) show broader and relatively shorter phalanges. Interestingly, the plot also separates the great apes, characterized by a more robust bone shape, from the Old World monkeys that show a more slender bone shaft and an angled proximal articular surface. In this plot specifically, RPl-87 falls inside the range of variation of *Gorilla*. Generally, RPl-87 is more similar in shape to the terrestrial than the arboreal species and shows affinities to *Papio* and *Gorilla* throughout the analyses. This similarity could potentially indicate that *O. macedoniensis* was also a mainly terrestrial primate. However, as pointed out throughout this dissertation, bone shape is a poor indicator of habitual activity. Therefore, the morphological similarities with terrestrial primates rather indicate that the Miocene ape exhibits a phalangeal shape facilitating terrestrial locomotion.

Previous studies of the *O. macedoniensis* skeletal material have found similar affinities. The study analyzing the isolated phalanges from RPl for the first time found them to be similar in shape to *Papio* and *Macaca*, leading the authors to suggest a terrestrial mode of locomotion for the Miocene ape (de Bonis and Koufos, 2014). Additionally, a study investigating the cranial remains of *O. macedoniensis*, using a 3D GMM approach and a comparative sample of fossil hominoids, extant great apes, and humans, discovered morphological similarities between *Ouranopithecus* and *Gorilla* (Ioannidou et al., 2019). Morphological similarities can be caused by several different factors. Among these are dietary, environmental, or locomotor adaptations, as well as phylogeny (Harvati and Weaver, 2006; Ruff et al., 2006; Cramon-Taubadel et al., 2013; Silva et al., 2019). Therefore, it is crucial to consider them in combination with other forms of evidence. Investigations of the faunal remains found at RPl indicate a relatively open landscape during the late Miocene, characterized by a Mediterranean climate and savannah-like bushland (with C_3 plants; de Bonis et al., 1992; de Bonis et al., 1999; Merceron et al., 2007; Rey et al., 2013). Dental microwear (Ungar, 1996; Merceron et al., 2005) and enamel thickness (Andrews and Martin, 1991) suggest that *O. macedoniensis* was a hard object feeder with a diet including mainly terrestrial food sources – similar to *Papio* (Merceron et al., 2005). Consequently, morphological, environmental, and dietary evidence would support a mainly terrestrial mode of locomotion in *O. macedoniensis*.

In conclusion, the 3D GMM analysis of the isolated intermediate phalanx RPl-87 yielded that it was likely not a hand but a foot bone that can be assigned to a paramedian digit. Moreover, the phalanx shows morphological affinities with *Gorilla* and *Papio*, thereby lending further support to the notion that *O. macedoniensis* was presumably a terrestrial primate.

4.2 Study II: Entheseal patterns and overall shape of the first metacarpal of early hominins

Study II investigated the manual entheseal patterns of early hominins in combination with an analysis of overall MC shape. This case study was the first time the VERA method was applied to early hominins. It was used here to investigate habitual thumb use in early hominins, whereas the analysis of bone morphology, including the shape of entheses, assessed their manual dexterity. Together, these two approaches examine whether the early hominins engaged in habitual human-like tool-using behavior and whether biomechanical adaptations for increased manual dexterity are prerequisites for human-like thumb use.

The analysis of entheseal patterns clearly differentiates between later *Homo* and non-human great apes. As shown by the results of the PCA and DFA (cf., Figure 4 and Table 6 Appendix B), the two groups primarily differ in the proportions of their DI1 attachment site, which is comparatively larger in later *Homo*. Previous experimental work has pointed out the importance of this muscle for Oldowan tool production (Marzke et al., 1998) and stone tool use, irrespective of the type (Key et al., 2020). Particularly the latter is consistent with our results, which found that later *Homo* taxa associated with different lithic technologies (i.e., Neanderthals and early modern humans) exhibit broadly similar DI1 attachment site proportions, likely representing a common tendency among habitual tool-using *Homo* species to use their DI1 for stabilization during thumb opposition (Marzke et al., 1998; Tocheri et al., 2008; Kivell, 2015; Key et al., 2020). Moreover, recent modern humans show similarly large proportions, highlighting the importance of the DI1 for human-like manipulation in general. Additionally, the entheseal pattern of later *Homo* is characterized by balanced proportions of the OP and APL attachment sites, indicating similar activation levels for the two muscles. Both OP and APL perform movements crucial for thumb opposition and, therefore, human-like precision grasping (Napier, 1956; Netter et al., 2019).

The majority of the early hominins show an entheseal pattern similar to later *Homo* (DFA classification rate 95-100%). *H. naledi* and *A. sediba* present even larger DI1 entheseal proportions than modern humans and Neanderthals, whereas the entheseal pattern of SK84 falls inside the variation of early and recent modern humans. While the pattern of *A. afarensis* indicates levels of DI1 activation similar to later *Homo*, its APL attachment site is proportionally more pronounced and, therefore, more similar to the *Pongo* specimens in the sample. The entheseal pattern of *A. africanus* stands out among the early hominins. Not only does it show a proportionally small DI1 enthesis compared to later *Homo*, but it also has a relatively large OP attachment site. As a consequence, its proportions are markedly different from later *Homo* and the other early hominins in the sample and more similar to non-human great apes (DFA classification rate 70%) and *G. gorilla* specifically.

The GMM analysis of overall MC shape also clearly separates later *Homo* from non-human great apes. The best separation and most meaningful shape variation can be found when combining PC1 and PC3 (cf., Figure 3 Appendix B). The shape changes along these axes represent morphological traits with high functional relevance in regard to efficient human-like manipulation (e.g., tool use). In comparison to great apes, specimens of later *Homo* are characterized by a robust MC, usually interpreted as an adaptation to increased load (Ruff et al., 2006; Kivell, 2015), a wide and flat distal articular surface, which stabilizes the MCP joint and increases load resistance in forceful precision grips (Galletta et al., 2019), and a dorsoventrally flatter proximal articular surface, associated with higher mobility in the CMC joint (Marzke et al., 2010; Marchi et al., 2017). In addition, modern humans and Neanderthals show distally extending DI1 and laterally projecting OP attachment sites, characteristics that are thought to increase the moment arms, and therefore the efficiency, of the respective muscles (Tocheri et al., 2008; Jacofsky, 2009; Maki and Trinkaus, 2011; Karakostis et al., 2021b). Altogether, the results of our shape analysis appear to reflect adaptations to biomechanical efficiency in human-like manipulation.

Among the early hominins, the overall MC shape of SK84 reflects a human-like biomechanical adaptation. In contrast, the *Australopithecus* species show a gross bone shape more similar to great apes than later *Homo*. Interestingly, among the three specimens, *A. africanus* is the closest in shape to modern humans and Neanderthals, contrary to the analysis of entheseal patterns. Finally, *H. naledi*'s overall MC shape is more similar to later *Homo* than the non-human great apes. Still, it diverges considerably from the shape displayed by other specimens in the sample. Although this appears to be mainly related to shape variation displayed on the PC3 axis (and is likely explained by its proportionally small proximal articular surface), other studies have also concluded that *H. naledi* shows an unusual and unique shape of the thumb MC, which they hypothesize to reflect a ‘transitional state’ in hand evolution (Bowland et al., 2021).

The combination of entheseal patterns and overall MC shape, including entheseal shape, yielded varying results for the early hominins. *H. naledi* and SK 84, a specimen associated with either *Paranthropus* or early *Homo* (Susman, 1988; Trinkaus and Long, 1990), combine a human-like MC morphology with an entheseal pattern consistent with habitual human-like manipulation and tool use. As mentioned previously, *H. naledi* shows both a unique entheseal pattern and MC shape, suggesting unique hand use and mechanical abilities. While this should be investigated further in the future, for the purposes of this study, we conclude that *H. naledi* is clearly more similar to modern humans and Neanderthals than to non-human great apes in both aspects. To date, no tools have been found in Rising Star Cave, the only locality where remains of *H. naledi* were found (Langdon, 2022). In contrast, Swartkrans Member 1 (SK 84) yielded both Oldowan stone tools and bone tools. However, these tools were found in Member 1's subunit Lower Bank, whereas SK 84 originates from the younger subunit Hanging Remnant (Susman et al., 2001; d'Errico and Backwell, 2003; Kuman et al., 2018; Kuman et al., 2021).

Among the australopiths, *A. afarensis* and *A. sediba* combine a human-like entheseal pattern with a more ape-like overall shape of the first MC. Specifically, their muscle attachment sites indicate human-like manipulation consistent with habitual tool use, whereas the ape-like morphology of features with high functional relevance suggests low manual dexterity and mechanical efficiency. Consequently, if these individuals engaged in habitual human-like tool production and use, they would have done so less efficiently compared to later *Homo* or even other early hominins like SK84. Notably, while *A. afarensis* shows human-like DI1 entheseal proportions, it also has a pronounced APL attachment site which is more characteristic of ape-like manipulation. This could indicate that *A. afarensis* engaged in more simple tool use and lacked the specialized behaviors seen in the later species – including *A. sediba* – that also involved regular recruitment of the OP. A recent biomechanical study reported low efficiency of the OP in *A. afarensis* (Karakostis et al., 2021b). It should be noted, however, that this muscle appears to have ape-like efficiency in all australopiths, including *A. africanus* with a proportionally large OP attachment site. Accordingly, low muscle efficiency does not necessarily entail less frequent muscle use.

Neither *A. afarensis* nor *A. sediba* has been found in direct association with stone tools. Still, the former has been suggested as the potential producer of Lomekwian tools based on contemporaneity and proximity (Harmand et al., 2015, but see Domalain et al., 2017), whereas tool use in *A. sediba* has been inferred based on its long thumb and trabecular structure (Kivell et al., 2011; Kivell et al., 2018; Dunmore et al., 2020b). In contrast, our results do not support any form of human-like tool use in *A. africanus*. Additionally, its overall MC morphology indicates ape-like manual dexterity and lower biomechanical efficiency compared to later *Homo*. Our results contradict previous analyses of its trabecular structure, which, according to the researchers, would be consistent with forceful precision grips and similar to habitual tool users and makers (Skinner et al., 2015).

Our study presents – for the first time – the analysis of manual entheseal patterns of early hominins and points out potential evidence for (human-like) tool use as early as *A. afarensis*. However, it also clearly emphasizes the importance of discriminating between efficiency and behavior. Previous studies investigating the hand bones of early hominins have found them to be characterized by both human- and ape-like traits. The retention of ape-like morphologies is often associated with reduced ranges of movement, decreased stability, or a decreased ability to accommodate high loads compared to Neanderthals and modern humans (Marzke et al., 2010; Marchi et al., 2017; Kivell et al., 2018; Galletta et al., 2019; Kivell et al., 2023). Considering biomechanical limitations when reconstructing activity is undoubtedly crucial, but using them as arguments to rule out related behaviors is problematic. 'Primitive' or ape-like traits certainly impacted how early hominins used their hands. We argue, however, that they led to a comparatively low efficiency and manual dexterity rather than preventing early hominins from engaging in human-like manual behaviors. In summary, the combination of human-like muscle use with ape-like manual dexterity in some australopiths suggests that tool-related behavior was established before the evolution of biomechanical adaptations of the thumb, likely spurring their development. In our sample, human-like hand use in combination with increased, human-like manual dexterity is first seen in SK84, a Swartkrans hominin dating to around 2.2-1.8 mya (Pickering et al., 2011; Gibbon et al., 2014), and retained in all later species examined, including *H. naledi*.

Activity reconstruction based on skeletal remains is complex and can be ambiguous, even when focusing on behaviorally plastic morphology. Our interpretations rely mainly on previous electromyographic research that links high activation levels of the DI1 with tool use (Key et al., 2020). An alternative interpretation would be that the early hominins showing an entheseal pattern similar to later *Homo* habitually engaged in more general human-like manipulatory behaviors. These activities would have to involve a frequent activation of the DI1, rendering them markedly distinct from great ape hand use. Moreover, this study focuses only on the muscles attaching to the first MC. Although these muscles play a crucial role in tool use and human-like manipulation in general, it is important to consider other thumb muscles, as well as hypothenar muscles (see Chapters 4.3 and 5).

4.3 Study III: Human-like manual activities in Australopithecus

Expanding upon our findings in Study II, Study III investigated the manual entheseal patterns of australopiths using an increased number of muscle attachment sites. Through the addition of more thumb muscles, muscles of the fifth ray, and a strand of a finger flexor (FDS, attaching to the intermediate phalanx of digit 3), we aimed to improve our understanding of how these early hominins used their hands and find potential synergies among the muscles situated on the margins of the hand. As not all bones are consistently preserved in all individuals, the analyses in this study were carried out in two groups: the first included all individuals with a reduced suite of entheses (without the FDS), whereas the second group used all entheses but included a reduced number of individuals.

The analyses, including PCA (cf., Figures 2-4, 6, 7 Appendix C) and DFA (c.f., Figures 5 and 8, Table 7 Appendix C) for both groups, present a clear separation of the entheseal patterns characterizing later *Homo* on the one hand and non-human great apes on the other hand. When included, the proportionate size of the FDS enthesis adds to that separation, as a large attachment site of this muscle is clearly associated with non-human great apes (cf. Tables 7 and 9 Appendix C). Similar to Study II, individuals of the later *Homo* group show a proportionally large DI1 attachment site, combined here with relatively large entheses of the fifth ray (ADM-FDM and ECU). The ADM muscle abducts the fifth ray, extending the hand’s reach, while the FDM flexes it at the MCP joint (Netter et al., 2019). Together with the *opponens digiti minimi* (which could not be analyzed in the scope of this study), this muscle group, known as the hypothenar muscles, is generally responsible for moving the fifth finger and opposes it toward the thumb (Neumann, 2017). The ECU is an extrinsic muscle and plays an essential role in the extension and ulnar deviation of the wrist (Netter et al., 2019).

The DI1 is crucial for human-like hand use, as has been discussed above (see Chapter 4.2). The fifth digit and the muscles attaching to it also play a vital role in human-like manipulation, involving, among others, tool production and use (Marzke and Shackley, 1986; Marzke et al., 1998; Marzke, 2013; Kivell, 2015; Key et al., 2019; Fedato et al., 2020). The muscles analyzed here are particularly involved in stabilizing the non-dominant hand during hard hammer percussion (Marzke et al., 1998), stabilization of the wrist during knapping (Williams et al., 2010, 2014), and handling tools of larger sizes (Key et al., 2020). However, these muscles are not only relevant for tool-related behaviors. More broadly, they are involved in power grasping (Long, II et al., 1970; Marzke et al., 1992; Goislard de Monsabert et al., 2012; Karakostis et al., 2017b), in-hand manipulation and repositioning of objects (Marzke et al., 1998; Marzke, 2013; Kivell, 2015; Key et al., 2019), among which the latter is more commonly seen in humans than in great apes (Christel, 1993; Bardo et al., 2017). Considering that our sample of later *Homo* consists of individuals from different chronological and geographic contexts, which used their hands in various tasks, their entheseal pattern probably reflects general human-like hand use rather than specific tool-using behavior.

The entheseal pattern characterizing non-human great apes includes proportionally large attachment sites of thumb muscles involved in thumb ab- and adduction and, when included, the FDS as a main finger flexor. Thumb adduction plays an important role in most grips observed in non-human great apes (Christel, 1993), whereas finger flexion is employed in hook grips (Bardo et al., 2018) and arboreal locomotion (Susman and Stern, 1979). Some analyses even present a separation of the different great ape species (cf. Figure 6 Appendix C), which can presumably be explained by differences in locomotion and manipulatory behavior (cf. Discussion Appendix C). Unfortunately, our knowledge about muscle involvement and coordination in great ape locomotion and manipulation is limited compared to humans (Bardo et al., 2017, but see Bardo et al., 2018). Moreover, the behavior of some species is better documented than others. Comparatively little is known about the behavior of wild *Pongo* (Bardo et al., 2018; Abdullah et al., 2021), whereas there are detailed records on multiple wild chimpanzee populations (e.g., populations from Taï National Park, Wittig, 2018; Kibale National Park, Thompson et al., 2020; Mahale Mountains National Park, Nakamura et al., 2015). Therefore, it is challenging to reconstruct specific activities from entheseal patterns.

The entheseal patterns of the australopiths are unlike those of the non-human great apes in any of the analyses, suggesting that their habitual hand use distinctively differed from these species. The absence of a proportionally large attachment site of the extrinsic finger flexor in these hominins (cf. Figures 6 and 7 Appendix C) could imply that they did not regularly engage in arboreal locomotion.

The entheseal pattern characterizing *A. africanus* creates the most questions among the australopiths. In some analyses, it appears similar to later *Homo*, while in others, its entheseal proportions are intermediate to but clearly distinct from the comparative groups. Especially in the DFAs, the attachment site proportions of this specimen vary considerably depending on the variables of the analysis. (cf. Results and Discussion Appendix C). Therefore, we conclude that *A. africanus* likely engaged in unique manual behaviors different from later *Homo*, great apes, or the other australopiths. Previous research is inconclusive in regard to the hand use of *A. africanus*. Its trabecular structure appears to imply a human-like use of the hand (Skinner et al., 2015). In contrast, the second case study in this thesis has found the entheseal patterns of its first MC to be more consistent with ape-like manual activities. Whether this discrepancy is due to a unique range of manual activities or the composite nature of its hand skeleton can currently not be resolved, as we lack a complete hand skeleton of this species (cf. Chapter 1.3 and Discussion Appendix C).

The other two australopiths show an entheseal pattern that is more similar, although not identical, to that of later *Homo*. *A. sediba* is a clear outlier in most analyses, as it presents unusually large attachment site proportions of the fifth ray and first proximal phalanx (cf. Figures 2, 3 and 6 Appendix C). Generally, however, its pattern is clearly more human- than ape-like, as shown by the results of both PCA and DFA. Among all *Australopithecus* species, *A. sediba* is most frequently associated with human-like hand use, partially because of its long thumb and robust fifth metacarpal (Kivell et al., 2018) but also because it shows trabecular bone (Dunmore et al., 2020b) and entheseal patterns (Study II) more similar to humans. On the other hand, it was argued that the retention of ape-like traits, such as a gracile MC1 shaft (Kivell et al., 2018), an ape-like shape of the distal MC1 articular surface (Galletta et al., 2019), the lack of a saddle-shaped CMC joint in the fifth ray (Kivell et al., 2018), and ape-like torque of the OP muscle (Karakostis et al., 2021b) limited the manipulative efficiency of the individual. The results of our study support human-like hand use in *A. sediba* despite these mechanical limitations and suggest that in-hand manipulation and power grasping, relying on the stabilizing muscles on the margins of the hand, were part of *A. sediba*'s manipulatory repertoire.

A. afarensis was not included in the second group of analyses involving the FDS enthesis, as we did not have access to an intermediate phalanx of this species. Therefore, the recruitment of its finger flexor and implications for potential arboreal locomotion cannot be assessed. The attachment site proportions of *A. afarensis* also resemble those of later *Homo*, suggesting that its manual activities involved a similar, although not identical, muscle recruitment. Like the other australopith species, its hand skeleton retained some ape-like traits that arguably restrict its biomechanical efficiency (Marzke et al., 2010; Rolian and Gordon, 2013; Galletta et al., 2019; Karakostis et al., 2021b, also see Study II). Studies focusing on its fifth ray report a gracile MC shaft and the lack of a saddle-shaped CMC joint (Marzke, 1983; Marzke et al., 1998; Marzke, 2013). Moreover, tests using an anatomical model suggest limited mobility in the CMC joint, leading the researchers to infer that *A. afarensis* could likely not apply the grip force required for the production of large stone tools, such as the Lomekwi assemblage (Domalain et al., 2017). Nevertheless, our results indicate that the muscles of the fifth ray that play an important role in human-like hand use are also frequently recruited in *A. afarensis*. Consequently, even though it remains unclear whether this species produced the Lomekwian stone tools, our study clearly demonstrates that the fifth finger appears to have played a more important role in *A. afarensis'* habitual manual behavior than previously thought.

This study aimed to expand our knowledge about hand use in *Australopithecus* species by investigating a sample of muscle attachment sites on their hand skeletons. Our results highlight varying habitual manual activities among the different species while all still retain a clear distinction from the entheseal pattern characterizing ape-like hand use. Furthermore, this study supports habitual manual activities resembling human-like manipulation in *A. sediba* and *A. afarensis* despite their reportedly limited biomechanical efficiency (Marzke, 1983; Marzke et al., 2010; Rolian and Gordon, 2013; Domalain et al., 2017; Kivell et al., 2018; Galletta et al., 2019; Karakostis et al., 2021b, also see Study II). In summary, human-like hand use likely emerged in some early hominins prior to 3 mya, considerably before evolutionary adaptations are first documented in specimens around two mya (Karakostis et al., 2021b, Study II). Both Studies II and III clearly emphasize that relying only on functionally relevant morphological adaptations to reconstruct hand function and use in hominins will likely produce misleading results. A multivariate or even multidisciplinary approach is necessary to understand the evolution of the versatile human hand.

5 Concluding Remarks and Future Directions

This dissertation investigated different aspects of hand bone morphology using virtual methods. These methods were applied to bones of different hominid and hominin species to identify isolated bones, reconstruct habitual hand use from muscle attachment sites of isolated bones and associated hand skeletons, and draw functional conclusions from bone morphology.

Study I focused on the intermediate phalanx of *O. macedoniensis*, which was previously attributed to the hand (de Bonis and Koufos, 2014). However, the results of our GMM shape analysis indicate that an attribution to the second or fifth ray of the foot is more likely. Additionally, the comparison with extant primate species points out similarities in morphology with *Gorilla* and *Papio*, concordant with previous studies on the phalanges (de Bonis and Koufos, 2014) and cranial remains associated with *O. macedoniensis* (Ioannidou et al., 2019). Shared morphology with these primarily terrestrial species, as well as environmental and dietary evidence (Andrews and Martin, 1991; de Bonis et al., 1992; Ungar, 1996; de Bonis et al., 1999; Merceron et al., 2005; Merceron et al., 2007; Rey et al., 2013) suggest *O. macedoniensis* to be a primarily terrestrial species as well. However, as the postcranial remains found to date are limited to two phalanges, morphological evidence regarding locomotor modes should be taken with a grain of salt. This study has highlighted the value of GMM for anatomical allocations even when bones are isolated. In the future, the approach used here should be further refined to specifically target functionally relevant aspects such as phalangeal curvature and the shape of the flexor sheath ridges. It should also be extended to the proximal phalanx RPl-86 to reevaluate its anatomical allocation and assess potential articulation with the intermediate phalanx.

Studies II and III investigated the manual entheseal patterns of early hominins to reconstruct habitual thumb use throughout human evolution. Study II focused on the first MC, combining the analysis of muscle attachment site proportions with an analysis of overall bone shape as a proxy for mechanical efficiency. The results show that the younger specimens analyzed – *H. naledi* and SK84 – combine human-like entheseal patterns characterized by a proportionally large DI1 with a human-like MC morphology. *A. africanus* leans toward the other end of the spectrum as it shows an ape-like MC shape suggesting low mechanical efficiency in the thumb (also see Karakostis et al., 2021b) and an entheseal pattern more similar to *Gorilla*. In contrast, although *A. afarensis* and *A. sediba* also present an ape-like MC shape, their entheseal proportions are consistent with habitual human-like hand use and – potentially – tool-using behaviors.

Study III built upon these results by analyzing the attachment site proportions of an expanded suite of muscles to investigate the hand use of different *Australopithecus* species. We found that when compared to extant great apes, the entheseal pattern of later *Homo* is characterized by a proportionately DI1 – as in Study II – in combination with muscles attaching to the fifth ray. These muscles are particularly active during power grasping, in-hand manipulation, and stabilization of objects. Based on their entheseal patterns, *A. sediba* and *A. afarensis* likely used their hand in a similar, albeit not identical manner, highlighting that hand use relying on the coordination of specific muscles on the margins of the hand was likely already present in hominin species as early as *A. afarensis*. Finally, *A. africanus* presents muscle attachment site proportion unlike both later *Homo* and non-human great apes. Potentially, this could be related to the composite nature of its hand skeleton, but it could also indicate that *A. africanus* used its hands in a unique manner.

These two studies contribute to the growing information on hand use in early hominins. But importantly, they also highlight the need to distinguish between morphological traits reflecting long-term biomechanical adaptations and those more plastic to individual habitual activity. Although both our own (Study II) and previous research (e.g., Marzke, 1983; Marzke et al., 2010; Domalain et al., 2017; Marchi et al., 2017; Galletta et al., 2019; Karakostis et al., 2021b) have suggested that australopiths likely experienced decreased manual dexterity compared to modern humans, the research presented here suggests that they frequently used muscles that are highly relevant for human-like manipulation. This further promotes the use of multivariate approaches, as analyzing different aspects of hand bone or, even more generally, skeletal morphology together can yield important information that would have been overlooked when focusing on isolated traits.

To further improve our understanding of hand use in early hominins, we must learn more about the mechanics of great ape manipulation. As mentioned earlier (Chapter 4.3), our knowledge of muscle use and coordination in non-human primates is limited (Bardo et al., 2017, but see Bardo et al., 2018). On an even more fundamental level, our knowledge of specific manipulative behavior in the wild varies substantially among great ape species. Addressing this research bias and improving our understanding of hand use throughout our comparative sample will greatly benefit future investigations of hominin hand use.

Extending the analysis to other fossil hominins from different species and time periods would additionally allow a better insight into the development of hand use throughout human evolution. While only a few relatively complete hand skeletons are preserved, Study II has shown that analyses focusing on a single bone can already provide valuable information on habitual manual behaviors. Potential candidates include the remains of *Ardipithecus ramidus* (ARA-VP-6/500, Lovejoy et al., 2009a), *H. habilis* (OH7, Napier, 1962; Susman and Creel, 1979), and *H. erectus* (KNM-WT 15000, Walker and Leakey, 1993), among others. Finally, future studies should include other muscles of the hand that are highly relevant for human-like manipulation, such as the *flexor pollicis longus* and the *opponens digiti minimi*.

To conclude, this cumulative thesis contributes to a growing body of research on the evolution of the hand. The included case studies show that when they can be identified and allocated, isolated bones can contribute significantly to our understanding of the function and use of hands and feet in fossil hominids. Moreover, the case studies reconstruct early hominin behavior based on morphological structures that are reportedly responsive to habitual activity. The resulting activity patterns partially contradict previous findings and caution against using the presence or absence of evolutionary adaptations as evidence for specific individual behavior.

6 References

Abdullah, N.I., Dharmalingam, S., Md-Zain, B.M., 2021. A Behavioral Study on the Bornean Orangutan (Pongo pygmaeus) in a Semi-wild Environment at Bukit Merah Orang Utan Island, Perak. jsunr 2 (2), 22–30.

Adams, D.C., Otárola-Castillo, E., 2013. Geomorph: an R package for the collection and analysis of geometric morphometric shape data. Methods in Ecology and Evolution 4 (4), 393–399.

Almécija, S., Alba, D.M., Moyà-Solà, S., 2009. Pierolapithecus and the functional morphology of Miocene ape hand phalanges: paleobiological and evolutionary implications. J. Hum. Evol. 57 (3), 284–297.

Almécija, S., Alba, D.M., Moyà-Solà, S., 2012. The thumb of Miocene apes: new insights from Castell de Barberà (Catalonia, Spain). Am. J. Phys. Anthropol. 148 (3), 436–450.

Almécija, S., Alba, D.M., Moyà-Solà, S., Köhler, M., 2007. Orang-like manual adaptations in the fossil hominoid Hispanopithecus laietanus: first steps towards great ape suspensory behaviours. Proceedings. Biological sciences 274 (1624), 2375–2384.

Almécija, S., Moyà-Solà, S., Alba, D.M., 2010. Early Origin for Human-Like Precision Grasping: A Comparative Study of Pollical Distal Phalanges in Fossil Hominins. PLOS ONE 5 (7), e11727.

Almécija, S., Smaers, J.B., Jungers, W.L., 2015. The evolution of human and ape hand proportions. Nature Communications 6, 7717.

Andrews, P., Martin, L., 1991. Hominoid dietary evolution. Phil. Trans. R. Soc. B 334 (1270), 199-209.

Archer, W., Aldeias, V., McPherron, S.P., 2020. What is 'in situ'? A reply to Harmand et al. (2015). J. Hum. Evol. 142, 102740.

Baab, K.L., McNulty, K.P., Rohlf, F.J., 2012. The shape of human evolution: a geometric morphometrics perspective. Evolutionary anthropology 21 (4), 151–165.

Bardo, A., Cornette, R., Borel, A., Pouydebat, E., 2017. Manual function and performance in humans, gorillas, and orangutans during the same tool use task. Am. J. Phys. Anthropol. 164 (4), 821–836.

Bardo, A., Vigouroux, L., Kivell, T.L., Pouydebat, E., 2018. The impact of hand proportions on tool grip abilities in humans, great apes and fossil hominins: A biomechanical analysis using musculoskeletal simulation. J. Hum. Evol. 125, 106–121.

Begun, D.R., 1994. Relations among the great apes and humans: New interpretations based on the fossil great ape Dryopithecus. Am. J. Phys. Anthropol. 37 (S19), 11–63.

Begun, D.R., Nargolwalla, M.C., Kordos, L., 2012. European Miocene hominids and the origin of the African ape and human clade. Evolutionary anthropology 21 (1), 10–23.

Benjamin, M., Kumai, T., Milz, S., Boszczyk, B., Boszczyk, A., Ralphs, J., 2002. The skeletal attachment of tendons—tendon 'entheses'. Comparative Biochemistry and Physiology Part A: Molecular & Integrative Physiology 133 (4), 931–945.

Biewener, A.A., Fazzalari, N.L., Konieczynski, D.D., Baudinette, R.V., 1996. Adaptive changes in trabecular architecture in relation to functional strain patterns and disuse. Bone 19 (1), 1–8.

Boesch, C., Boesch, H., 1990. Tool use and tool making in wild chimpanzees. Folia primatologica; international journal of primatology 54 (1-2).

Boesch-Achermann, H., Boesch, C., 1993. Tool Use in Wild Chimpanzees: New Light From Dark Forests. Curr Dir Psychol Sci 2 (1), 18–21.

Böhme, M., Spassov, N., Fuss, J., Tröscher, A., Deane, A.S., Prieto, J., Kirscher, U., Lechner, T., Begun, D.R., 2019. A new Miocene ape and locomotion in the ancestor of great apes and humans. Nature 575 (7783), 489–493.

Bookstein, F.L., 1989. Principal warps: thin-plate splines and the decomposition of deformations. IEEE Trans. Pattern Anal. Machine Intell. 11 (6), 567–585.

Bookstein, F.L., 1991. Morphometric Tools for Landmark Data: Geometry and Biology. New York: Cambridge University Press, Cambridge (UK).

Bousquié, L., Karakostis, F.A., Crevecoeur, I., Villotte, S., 2022. Technical note: investigating activity-induced 3d hand entheseal variation in a documented South African sample. Archaeol. Anthropol. Sci. 14.

Bowland, L.A., Scott, J.E., Kivell, T.L., Patel, B.A., Tocheri, M.W., Orr, C.M., 2021. Homo naledi pollical metacarpal shaft morphology is distinctive and intermediate between that of australopiths and other members of the genus Homo. Journal of human evolution 158, 103048.

Bush, M.E., Lovejoy, C.O., Johanson, D.C., Coppens, Y., 1982. Hominid carpal, metacarpal, and phalangeal bones recovered from the Hadar formation: 1974-1977 collections. Am. J. Phys. Anthropol. 57 (4), 651–677.

Byrne, R.W., Corp, N., Byrne, J.M., 2001. Manual dexterity in the gorilla: bimanual and digit role differentiation in a natural task. Animal cognition 4 (3-4), 347–361.

Case, D.T., Heilman, J., 2006. New siding techniques for the manual phalanges: a blind test. Int. J. Osteoarchaeol. 16 (4), 338–346.

Cashmore, L.A., Zakrzewski, S.R., 2013. Assessment of Musculoskeletal Stress Marker Development in the Hand. Int. J. Osteoarchaeol. 23 (3), 334–347.

Castro, A.A., Karakostis, F.A., Copes, L.E., McClendon, H.E., Trivedi, A.P., Schwartz, N.E., Garland, T., 2022. Effects of selective breeding for voluntary exercise, chronic exercise, and their interaction on muscle attachment site morphology in house mice. J. Anat. 240 (2), 279–295.

Christel, M., 1993. Grasping techniques and hand preferences in Hominoidea, In: Preuschoft, H., Chivers, D.J. (Eds.), Hands of primates. Springer-Verlag, Wien, pp. 91–108.

References

Christensen, A.M., 2009. Techniques for siding manual phalanges. Forensic science international 193 (1-3), 84–87.

Cignoni, P., Callieri, M., Corsini, M., Dellepiane, M., Ganovelli, F., Ranzuglia, G., 2008. MeshLab: an Open-Source Mesh Processing Tool, In: Sixth Eurographics Italian Chapter conference. Eurographics Italian Chapter Conference, Salerno, Italy. July 2nd - 4th, 2008. The Eurographics Association, Aire-la-Ville, pp. 129–136.

Congdon, K.A., 2012. Interspecific and Ontogenetic Variation in Proximal Pedal Phalangeal Curvature of Great Apes (Gorilla gorilla, Pan troglodytes, and Pongo pygmaeus). Int J Primatol 33 (2), 418–427.

Cramon-Taubadel, N. von, Frazier, B.C., Lahr, M.M., 2007. The Problem of Assessing Landmark Error in Geometric Morphometrics: Theory, Methods, and Modifications. Am. J. Phys. Anthropol. 134 (1), 24–35.

Cramon-Taubadel, N. von, Stock, J.T., Pinhasi, R., 2013. Skull and limb morphology differentially track population history and environmental factors in the transition to agriculture in Europe. Proceedings. Biological sciences 280 (1767), 20131337.

Currey, J.D., 2002. Bones: Structure and Mechanics. Princeton University Press, Princeton, NJ, Oxfordshire, 436 pp.

Currey, J.D., 2012. The structure and mechanics of bone. J Mater Sci 47 (1), 41–54.

de Bonis, L., Bouvrain, G., Geraads, D., Koufos, G.D., 1992. Diversity and paleoecology of Greek late Miocene mammalian faunas. Palaeogeography, Palaeoclimatology, Palaeoecology 91 (1), 99–121.

de Bonis, L., Bouvrain, G., Koufos, G.D., 1999. Palaeoenvironments of late Miocene primate localities in Macedonia, Greece, In: Agustí, J., Rook, L., Andrews, P. (Eds.), The evolution of neogene terrestrial ecosystems in Europe. Hominoid evolution and climatic change in Europe v.1. Cambridge University Press, Cambridge, pp. 205–237.

de Bonis, L., Koufos, G.D., 2001. Phylogenetic relationships of Ouranopithecus macedoniensis (Mammalia, Primates, Hominoidea, Hominidae) of the late Miocene deposits of Central Macedonia (Greece), In: de Bonis, L., Koufos, G.D., Andrews, P.A. (Eds.), Phylogeny of the Neogene Hominoid Primates of Eurasia. Hominoid evolution and climatic change in Europe Vol. 2. Cambridge University Press, New York, NY, pp. 254–268.

de Bonis, L., Koufos, G.D., 2014. First discovery of postcranial bones of Ouranopithecus macedoniensis (Primates, Hominoidea) from the late Miocene of Macedonia (Greece). Journal of human evolution 74, 21–36.

Deane, A.S., Begun, 2008. Broken fingers: retesting locomotor hypotheses for fossil hominoids using fragmentary proximal phalanges and high-resolution polynomial curve fitting (HR-PCF). Journal of human evolution 55 (4), 691–701.

d'Errico, F., Backwell, L.R., 2003. Possible evidence of bone tool shaping by Swartkrans early hominids. Journal of Archaeological Science 30 (12), 1559–1576.

Détroit, F., Mijares, A.S., Corny, J., Daver, G., Zanolli, C., Dizon, E., Robles, E., Grün, R., Piper, P.J., 2019. A new species of Homo from the Late Pleistocene of the Philippines. Nature 568 (7751), 181–186.

Diogo, R., Potau, J.M., Pastor, J.F., Paz, F.J. de, Ferrero, E.M., Bello, G., Barbosa, M., Aziz, M.A., Burrows, A.M., Arias-Martorell, J., Wood, B.A., 2013. Photographic and Descriptive Musculoskeletal Atlas of Chimpanzees: With Notes on the Attachments, Variations, Innervation, Function and Synonomy and Weight of the Muscles. CRC Press, Boca Raton.

Diogo, R., Richmond, B.G., Wood, B.A., 2012. Evolution and homologies of primate and modern human hand and forearm muscles, with notes on thumb movements and tool use. J. Hum. Evol. 63 (1), 64–78.

Domalain, M., Bertin, A., Daver, G., 2017. Was Australopithecus afarensis able to make the Lomekwian stone tools? Towards a realistic biomechanical simulation of hand force capability in fossil hominins and new insights on the role of the fifth digit. Comptes Rendus Palevol 16 (5-6), 572–584.

Domínguez-Rodrigo, M., Alcalá, L., 2016. 3.3-Million-Year-Old Stone Tools and Butchery Traces? More Evidence Needed. PaleoAnthropol. 2016, 46–53.

Dunmore, C.J., Bardo, A., Skinner, M.M., Kivell, T.L., 2020a. Trabecular variation in the first metacarpal and manipulation in hominids. Am. J. Phys. Anthropol. 171 (2), 219–241.

Dunmore, C.J., Skinner, M.M., Bardo, A., Berger, L.R., Hublin, J.-J., Pahr, D.H., Rosas, A., Stephens, N.B., Kivell, T.L., 2020b. The position of *Australopithecus sediba* within fossil hominin hand use diversity. Nat. Ecol. Evol. 4 (7), 911–918.

Faisal, A., Stout, D., Apel, J., Bradley, B., 2010. The manipulative complexity of Lower Paleolithic stone toolmaking. PLOS ONE 5 (11), e13718.

Falótico, T., Coutinho, P.H.M., Bueno, C.Q., Rufo, H.P., Ottoni, E.B., 2018. Stone tool use by wild capuchin monkeys (Sapajus libidinosus) at Serra das Confusões National Park, Brazil. Primates; journal of primatology 59 (4), 385–394.

Fedato, A., Silva-Gago, M., Terradillos-Bernal, M., Alonso-Alcalde, R., Bruner, E., 2020. Hand grasping and finger flexion during Lower Paleolithic stone tool ergonomic exploration. Archaeol. Anthropol. Sci. 12, 254.

Feix, T., Romero, J., Schmiedmayer, H.-B., Dollar, A.M., Kragic, D., 2016. The GRASP Taxonomy of Human Grasp Types. IEEE Trans. Human-Mach. Syst. 46 (1), 66–77.

Field, A., 2017. Discovering Statistics Using IBM SPSS Statistics, 5th ed. Sage Publications, Thousand Oaks CA.

Fleagle, J.G., 2013. Apes and Humans, In: Fleagle, J.G. (Ed.), Primate adaptation and evolution, 3. ed. ed. Elsevier Acad. Press, Amsterdam, pp. 151–168.

Galletta, L., Stephens, N.B., Bardo, A., Kivell, T.L., Marchi, D., 2019. Three-dimensional geometric morphometric analysis of the first metacarpal distal articular surface in humans, great apes and fossil hominins. J. Hum. Evol. 132, 119–136.

References

Garrido Varas, C.E., Thompson, T.J.U., 2011. Metric dimensions of the proximal phalanges of the human hand and their relationship to side, position, and asymmetry. Homo : internationale Zeitschrift fur die vergleichende Forschung am Menschen 62 (2), 126–143.

Garrido-Varas, C., Rathnasinghe, R., Thompson, T., Savriama, Y., 2015. A new method to pair-match metacarpals using bilateral asymmetry and shape analysis. Journal of forensic sciences 60 (1), 118–123.

Gibbon, R.J., Pickering, T.R., Sutton, M.B., Heaton, J.L., Kuman, K., Clarke, R.J., Brain, C.K., Granger, D.E., 2014. Cosmogenic nuclide burial dating of hominin-bearing Pleistocene cave deposits at Swartkrans, South Africa. Quaternary Geochronology 24, 10–15.

Goislard de Monsabert, B., Rossi, J., Berton, E., Vigouroux, L., 2012. Quantification of hand and forearm muscle forces during a maximal power grip task. Med. Sci. Sports Exerc. 44 (10), 1906–1916.

Gommery, D., Senut, B., 2006. La phalange distale du pouce d'Orrorin tugenensis (Miocène supérieur du Kenya). Geobios 39 (3), 372–384.

Grine, F.E., Mongle, C.S., Fleagle, J.G., Hammond, A.S., 2022. The taxonomic attribution of African hominin postcrania from the Miocene through the Pleistocene: Associations and assumptions. J. Hum. Evol. 173, 103255.

Gumert, M.D., Kluck, M., Malaivijitnond, S., 2009. The physical characteristics and usage patterns of stone axe and pounding hammers used by long-tailed macaques in the Andaman Sea region of Thailand. American journal of primatology 71 (7), 594–608.

Gumert, M.D., Malaivijitnond, S., 2012. Marine prey processed with stone tools by Burmese long-tailed macaques (Macaca fascicularis aurea) in intertidal habitats. Am. J. Phys. Anthropol. 149 (3), 447–457.

Gumert, M.D., Malaivijitnond, S., 2013. Long-tailed macaques select mass of stone tools according to food type. Philosophical transactions of the Royal Society of London. Series B, Biological sciences 368 (1630), 20120413.

Gürbüz, R.B., Lycett, S.J., 2021. Did the use of bone flakes precede the use of knapped stone flakes in hominin meat processing and could this be detectable archaeologically? Journal of Anthropological Archaeology 62, 101305.

Harmand, S., Lewis, J.E., Feibel, C.S., Lepre, C.J., Prat, S., Lenoble, A., Boës, X., Quinn, R.L., Brenet, M., Arroyo, A., Taylor, N., Clément, S., Daver, G., Brugal, J.-P., Leakey, L., Mortlock, R.A., Wright, J.D., Lokorodi, S., Kirwa, C., Kent, D.V., Roche, H., 2015. 3.3-million-year-old stone tools from Lomekwi 3, West Turkana, Kenya. Nature 521 (7552), 310–315.

Harvati, K., Weaver, T.D., 2006. Human cranial anatomy and the differential preservation of population history and climate signatures. The anatomical record. Part A, Discoveries in molecular, cellular, and evolutionary biology 288 (12), 1225–1233.

Haslam, M., Hernandez-Aguilar, A., Ling, V., Carvalho, S., La Torre, I. de, DeStefano, A., Du, A., Hardy, B., Harris, J., Marchant, L., Matsuzawa, T., McGrew, W., Mercader, J., Mora, R., Petraglia, M., Roche, H., Visalberghi, E., Warren, R., 2009. Primate archaeology. Nature 460 (7253), 339–344.

Haslam, M., Hernandez-Aguilar, R.A., Proffitt, T., Arroyo, A., Falótico, T., Fragaszy, D., Gumert, M., Harris, J.W.K., Huffman, M.A., Kalan, A.K., Malaivijitnond, S., Matsuzawa, T., McGrew, W., Ottoni, E.B., Pascual-Garrido, A., Piel, A., Pruetz, J., Schuppli, C., Stewart, F., Tan, A., Visalberghi, E., Luncz, L.V., 2017. Primate archaeology evolves. Nature ecology & evolution 1 (10), 1431–1437.

Ioannidou, M., Koufos, G.D., Bonis, L. de, Harvati, K., 2019. A new three-dimensional geometric morphometrics analysis of the Ouranopithecus macedoniensis cranium (Late Miocene, Central Macedonia, Greece). Am. J. Phys. Anthropol. 170 (2), 295–307.

Jacofsky, M.C., 2009. Comparative Muscle Moment Arms of the Primate Thumb: Homo, Pan, Pongo, and Papio. Dissertation, Arizona State University.

Jungers, W.L., Godfrey, L.R., Simons, E.L., Chatrath, P.S., 1997. Phalangeal curvature and positional behavior in extinct sloth lemurs (Primates, Palaeopropithecidae). PNAS 94 (22), 11998–12001.

Jungers, W.L., Godfrey, L.R., Simons, E.L., Wunderlich, R.E., Richmond, B.G., Chatrath, P.S., 2002. Ecomorphology and Behavior of Giant Extinct Lemurs from Madagascar, In: Plavcan, J.M., Kay, R.F., Jungers, W.L., van Schaik, C.P. (Eds.), Reconstructing behavior in the primate fossil record. Springer, Boston, MA, pp. 371–411.

Karakostis, F.A., 2023. Statistical protocol for analyzing 3D muscle attachment sites based on the “Validated Entheses-based Reconstruction of Activity” (VERA) approach. Int. J. Osteoarchaeol. 33 (3), 461–474.

Karakostis, F.A., Buikstra, J.E., Prevedorou, E., Hannigan, E.M., Hotaling, J., Hotz, G., Liedl, H., Moraitis, K., Siek, T.J., Waltenberger, L., Widrick, K.J., Harvati, K., 2021a. New insights into the manual activities of individuals from the Phaleron cemetery (Archaic Athens, Greece). Journal of Archaeological Science 131, 105415.

Karakostis, F.A., Haeufle, D., Anastopoulou, I., Moraitis, K., Hotz, G., Tourloukis, V., Harvati, K., 2021b. Biomechanics of the human thumb and the evolution of dexterity. Current Biology 31 (6), 1317–1325.e8.

Karakostis, F.A., Harvati, K., 2021. New horizons in reconstructing past human behavior: Introducing the “Tübingen University Validated Entheses-based Reconstruction of Activity” method. Evol. Anthropol. 30 (3), 185–198.

Karakostis, F.A., Hotz, G., 2022. Reflections of manual labor in the hand entheses of early industrial women workers with extensively documented life histories. American Journal of Biological Anthropology, https://doi.org/10.1002/ajpa.24636.

Karakostis, F.A., Hotz, G., Scherf, H., Wahl, J., Harvati, K., 2017a. Occupational manual activity is reflected on the patterns among hand entheses. Am. J. Phys. Anthropol. 164 (1), 30–40.

Karakostis, F.A., Hotz, G., Tourloukis, V., Harvati, K., 2018. Evidence for precision grasping in Neandertal daily activities. Science Advances 4 (9), eaat2369.

Karakostis, F.A., Jeffery, N., Harvati, K., 2019a. Experimental proof that multivariate patterns among muscle attachments (entheses) can reflect repetitive muscle use. Sci. Rep. 9, 16577.

Karakostis, F.A., Lorenzo, C., 2016. Morphometric patterns among the 3D surface areas of human hand entheses. Am. J. Phys. Anthropol. 160 (4), 694–707.

Karakostis, F.A., Lorenzo, C., Moraitis, K., 2017b. Morphometric variation and ray allocation of human proximal hand phalanges. Anthropologischer Anzeiger; Bericht uber die biologisch-anthropologische Literatur 74 (4), 269–281.

Karakostis, F.A., Reyes-Centeno, H., Franken, M., Hotz, G., Rademaker, K., Harvati, K., 2020. Biocultural evidence of precise manual activities in an Early Holocene individual of the high-altitude Peruvian Andes. Am. J. Phys. Anthropol. 174 (1), 35–48.

Karakostis, F.A., Wallace, I.J., 2023. Climbing influences entheseal morphology in the humerus of mice: An experimental application of the VERA methodology. American Journal of Biological Anthropology 181 (1), 130–139.

Karakostis, F.A., Wallace, I.J., Konow, N., Harvati, K., 2019b. Experimental evidence that physical activity affects the multivariate associations among muscle attachments (entheses). The Journal of Experimental Biology 222 (23), jeb213058.

Key, A.J., Farr, I., Hunter, R., Winter, S.L., 2020. Muscle recruitment and stone tool use ergonomics across three million years of Palaeolithic technological transitions. J. Hum. Evol. 144, 102796.

Key, A.J.M., 2016. Manual Loading Distribution During Carrying Behaviors: Implications for the Evolution of the Hominin Hand. PLOS ONE 11 (10), e0163801.

Key, A.J.M., Dunmore, C.J., Marzke, M.W., 2019. The unexpected importance of the fifth digit during stone tool production. Sci. Rep. 9 (1), 16724.

Kivell, T.L., 2015. Evidence in hand: recent discoveries and the early evolution of human manual manipulation. Phil. Trans. R. Soc. B 370 (1682), 20150105.

Kivell, T.L., 2016. A review of trabecular bone functional adaptation: what have we learned from trabecular analyses in extant hominoids and what can we apply to fossils? Journal of anatomy 228 (4), 569–594.

Kivell, T.L., Baraki, N., Lockwood, V., Williams-Hatala, E.M., Wood, B.A., 2023. Form, function and evolution of the human hand. American Journal of Biological Anthropology 181 (S76), 6–57.

Kivell, T.L., Churchill, S.E., Kibii, J.M., Schmid, P., Berger, L.R., 2018. The hand of *Australopithecus sediba.* PaleoAnthropol. 2018, 282–333.

Kivell, T.L., Deane, A.S., Tocheri, M.W., Orr, C.M., Schmid, P., Hawks, J., Berger, L.R., Churchill, S.E., 2015. The hand of *Homo naledi.* Nature Communications 6, 8431.

Kivell, T.L., Kibii, J.M., Churchill, S.E., Schmid, P., Berger, L.R., 2011. *Australopithecus sediba* Hand Demonstrates Mosaic Evolution of Locomotor and Manipulative Abilities. Science 333 (6048), 1411–1417.

Kivell, T.L., Ostrofsky, K.R., Richmond, B.G., Drapeau, M.S., 2020. Metacarpals and manual phalanges, In: Zipfel, B., Richmond, B., Ward, C.V. (Eds.), Hominin postcranial remains from Sterkfontein, South Africa, 1936-1995. Human evolution series. Oxford University Press, New York, NY, pp. 106–143.

Klingenberg, C.P., 2016. Size, shape, and form: concepts of allometry in geometric morphometrics. Development genes and evolution 226 (3), 113–137.

Koufos, G.D., Kostopoulos, D.S., Vlachou, T.D., 2016. Revision of the Nikiti 1 (NKT) fauna with description of new material. Geobios 49 (1-2), 11–22.

Kuman, K., Granger, D.E., Gibbon, R.J., Pickering, T.R., Caruana, M.V., Bruxelles, L., Clarke, R.J., Heaton, J.L., Stratford, D., Brain, C.K., 2021. A new absolute date from Swartkrans Cave for the oldest occurrences of Paranthropus robustus and Oldowan stone tools in South Africa. J. Hum. Evol. 156, 103000.

Kuman, K., Sutton, M.B., Pickering, T.R., Heaton, J.L., 2018. The Oldowan industry from Swartkrans cave, South Africa, and its relevance for the African Oldowan. J. Hum. Evol. 123, 52–69.

Landsmeer, J., 1962. Power grip and precision handling. Annals of the rheumatic diseases 21, 164–170.

Langdon, J.H., 2022. Erectines of the West, In: Langdon, J.H. (Ed.), Human Evolution. Bones, Cultures, and Genes, 1st ed. 2022 ed. Springer Texts in Social Sciences. Springer International Publishing; Imprint Springer, Cham, pp. 419–460.

Larson, S.G., Jungers, W.L., Tocheri, M.W., Orr, C.M., Morwood, M.J., Sutikna, T., Awe, R.D., Djubiantono, T., 2009. Descriptions of the upper limb skeleton of Homo floresiensis. J. Hum. Evol. 57 (5), 555–570.

Lemelin, P., Diogo, R., 2016. Anatomy, Function, and Evolution of the Primate Hand Musculature, In: Kivell, T.L., Lemelin, P., Richmond, B.G., Schmitt, D. (Eds.), The Evolution of the Primate Hand. Anatomical, Developmental, Functional, and Paleontological Evidence. Developments in Primatology: Progress and Prospects. Springer, New York, pp. 155–193.

Long, C., II, Conrad, P.W., Hall, E.A., Furler, S.L., 1970. Intrinsic-Extrinsic Muscle Control of the Hand in Power Grip and Precision Handling: An Electromyographic Study. JBJS 52 (5), 853–867.

Lovejoy, C.O., Simpson, S.W., White, T.D., Asfaw, B., Suwa, G., 2009a. Careful Climbing in the Miocene: The Forelimbs of Ardipithecus ramidus and Humans Are Primitive. Science 326 (5949), 70-70e8.

Lovejoy, C.O., Suwa, G., Simpson, S.W., Matternes, J.H., White, T.D., 2009b. The great divides: Ardipithecus ramidus reveals the postcrania of our last common ancestors with African apes. Science (New York, N.Y.) 326 (5949), 100–106.

Luncz, L.V., Arroyo, A., Falótico, T., Quinn, P., Proffitt, T., 2022. A primate model for the origin of flake technology. Journal of human evolution 171, 103250.

Madar, S.I., Rose, M.D., Kelley, J., MacLatchy, L., Pilbeam, D., 2002. New Sivapithecus postcranial specimens from the Siwaliks of Pakistan. Journal of human evolution 42 (6), 705–752.

Maki, J., Trinkaus, E., 2011. Opponens pollicis mechanical effectiveness in Neandertals and early modern humans. PaleoAnthropol. 2011, 62–71.

Marchi, D., Proctor, D.J., Huston, E., Nicholas, C.L., Fischer, F., 2017. Morphological correlates of the first metacarpal proximal articular surface with manipulative capabilities in apes, humans and South African early hominins. Comptes Rendus Palevol 16 (5-6), 645–654.

Marzke, M.W., 1983. Joint functions and grips of the *Australopithecus afarensis* hand, with special reference to the region of the capitate. J. Hum. Evol. 12 (2), 197–211.

Marzke, M.W., 1997. Precision grips, hand morphology, and tools. Am. J. Phys. Anthropol. 102 (1), 91–110.

Marzke, M.W., 2013. Tool making, hand morphology and fossil hominins. Phil. Trans. R. Soc. B 368 (1630), 20120414.

Marzke, M.W., Marzke, R.F., Linscheid, R.L., Smutz, P., Steinberg, B., Reece, S., An, K.N., 1999. Chimpanzee thumb muscle cross sections, moment arms and potential torques, and comparisons with humans. Am. J. Phys. Anthropol. 110 (2), 163–178.

Marzke, M.W., Shackley, M.S., 1986. Hominid hand use in the pliocene and pleistocene: Evidence from experimental archaeology and comparative morphology. J. Hum. Evol. 15 (6), 439–460.

Marzke, M.W., Tocheri, M.W., Steinberg, B., Femiani, J.D., Reece, S.P., Linscheid, R.L., Orr, C.M., Marzke, R.F., 2010. Comparative 3D quantitative analyses of trapeziometacarpal joint surface curvatures among living catarrhines and fossil hominins. Am. J. Phys. Anthropol. 141 (1), 38–51.

Marzke, M.W., Toth, N., Schick, K., Reece, S., Steinberg, B., Hunt, K., Linscheid, R.L., An, K.-N., 1998. EMG Study of Hand Muscle Recruitment During Hard Hammer Percussion Manufacture of Oldowan Tools. Am. J. Phys. Anthropol. 105 (3), 315–332.

Marzke, M.W., Wullstein, K.L., Viegas, S.F., 1992. Evolution of the power (“squeeze”) grip and its morphological correlates in hominids. Am. J. Phys. Anthropol. 89 (3), 283–298.

McPherron, S.P., Alemseged, Z., Marean, C.W., Wynn, J.G., Reed, D., Geraads, D., Bobe, R., Béarat, H.A., 2010. Evidence for stone-tool-assisted consumption of animal tissues before 3.39 million years ago at Dikika, Ethiopia. Nature 466 (7308), 857–860.

Merceron, G., Blondel, C., de Bonis, L., Koufos, G.D., Viriot, L., 2005. A New Method of Dental Microwear Analysis: Application to Extant Primates and Ouranopithecus macedoniensis (Late Miocene of Greece). PALAIOS 20 (6), 551–561.

Merceron, G., Blondel, C., Koufos, G., Viriot, L., Bonis, L. de, 2007. Dental microwear analysis of bovids from the Vallesian (late Miocene) of Axios Valley in Greece: Reconstruction of the habitat of Ouranopithecus macedoniensis (Primates, Hominoidea). Geodiversitas 29 (3), 421–433.

Milella, M., Belcastro, M.G., Zollikofer, C.P.E., Mariotti, V., 2012. The Effect of Age, Sex, and Physical Activity on Entheseal Morphology in a Contemporary Italian Skeletal Collection. Am. J. Phys. Anthropol. 148 (3), 379–388.

Mitteroecker, P., Gunz, P., 2009. Advances in Geometric Morphometrics. Evol Biol 36 (2), 235–247.

Mitteroecker, P., Gunz, P., Windhager, S., Schaefer, K., 2013. A brief review of shape, form, and allometry in geometric morphometrics, with applications to human facial morphology. Hystrix, the Italian Journal of Mammalogy 24 (1), 59–66.

Morley, J., Bucchi, A., Lorenzo, C., Püschel, T.A., 2022. Characterizing the body morphology of the first metacarpal in the Homininae using 3D geometric morphometrics. American Journal of Biological Anthropology 177 (4), 748–759.

Mosimann, J.E., 1970. Size Allometry: Size and Shape Variables with Characterizations of the Lognormal and Generalized Gamma Distributions. Journal of the American Statistical Association 65 (330), 930–945.

Moyà-Solà, S., Köhler, M., Alba, D.M., Casanovas-Vilar, I., Galindo, J., 2004. Pierolapithecus catalaunicus, a new Middle Miocene great ape from Spain. Science (New York, N.Y.) 306 (5700), 1339–1344.

Nakamura, M., Hosaka, K., Itoh, N., Zamma, K. (Eds.), 2015. Mahale chimpanzees. Cambridge University Press, Cambridge.

Nakatsukasa, M., Kunimatsu, Y., Nakano, Y., Takano, T., Ishida, H., 2003. Comparative and functional anatomy of phalanges in Nacholapithecus kerioi, a Middle Miocene hominoid from northern Kenya. Primates; journal of primatology 44 (4), 371–412.

Napier, J.R., 1956. The Prehensile Movements of the Human Hand. The Journal of Bone and Joint Surgery. British volume 38 (4), 902–913.

Napier, J.R., 1962. Fossil Hand Bones from Olduvai Gorge. Nature 196 (4853), 409–411.

Netter, F.H., Machado, C.A.G., Hansen, J.T., Benninger, B., Brueckner, J.K., 2019. Atlas of Human Anatomy, 7th ed. Netter basic science. Elsevier, Philadelphia, PA.

Neufuss, J., Robbins, M.M., Baeumer, J., Humle, T., Kivell, T.L., 2017. Comparison of hand use and forelimb posture during vertical climbing in mountain gorillas (Gorilla beringei beringei) and chimpanzees (Pan troglodytes). Am. J. Phys. Anthropol. 164 (4), 651–664.

Neufuss, J., Robbins, M.M., Baeumer, J., Humle, T., Kivell, T.L., 2019. Manual skills for food processing by mountain gorillas (Gorilla beringei beringei) in Bwindi Impenetrable National Park, Uganda. Biological Journal of the Linnean Society 127, 543–562.

Neumann, D.A., 2017. Hand, In: Neumann, D.A. (Ed.), Kinesiology of the musculoskeletal system. Foundations for rehabilitation, 3rd ed. Elsevier, St. Louis, pp. 250–303.

Nguyen, N.H., Pahr, D.H., Gross, T., Skinner, M.M., Kivell, T.L., 2014. Micro-finite element (µFE) modeling of the siamang (Symphalangus syndactylus) third proximal phalanx: the functional role of curvature and the flexor sheath ridge. J. Hum. Evol. 67, 60–75.

References

Niewoehner, W.A., 2005. A Geometric Morphometric Analysis of Late Pleistocene Human Metacarpal 1 Base Shape, In: Slice, D.E. (Ed.), Modern Morphometrics in Physical Anthropology. Springer US, Boston, MA, pp. 285–298.

Noldner, L.K., Edgar, H.J.H., 2013. Technical Note: 3D Representation and Analysis of Enthesis Morphology. Am. J. Phys. Anthropol. 152 (3), 417–424.

Panger, M.A., Brooks, A.S., Richmond, B.G., Wood, B., 2002. Older Than the Oldowan? Rethinking the Emergence of Hominin Tool Use. Evol. Anthropol. 11 (6), 235–245.

Parfitt, A.M., Travers, R., Rauch, F., Glorieux, F.H., 2000. Structural and Cellular Changes During Bone Growth in Healthy Children. Bone 27 (4), 487–494.

Pickering, R., Kramers, J.D., Hancox, P.J., Ruiter, D.J. de, Woodhead, J.D., 2011. Contemporary flowstone development links early hominin bearing cave deposits in South Africa. Earth and Planetary Science Letters 306 (1-2), 23–32.

Plummer, T.W., Oliver, J.S., Finestone, E.M., Ditchfield, P.W., Bishop, L.C., Blumenthal, S.A., Lemorini, C., Caricola, I., Bailey, S.E., Herries, A.I.R., Parkinson, J.A., Whitfield, E., Hertel, F., Kinyanjui, R.N., Vincent, T.H., Li, Y., Louys, J., Frost, S.R., Braun, D.R., Reeves, J.S., Early, E.D.G., Onyango, B., Lamela-Lopez, R., Forrest, F.L., He, H., Lane, T.P., Frouin, M., Nomade, S., Wilson, E.P., Bartilol, S.K., Rotich, N.K., Potts, R., 2023. Expanded geographic distribution and dietary strategies of the earliest Oldowan hominins and Paranthropus. Science 379 (6632), 561–566.

Prang, T.C., Ramirez, K., Grabowski, M., Williams, S.A., 2021. Ardipithecus hand provides evidence that humans and chimpanzees evolved from an ancestor with suspensory adaptations. Science Advances 7 (9), eabf2474.

Proffitt, T., Luncz, L.V., Falótico, T., Ottoni, E.B., La Torre, I. de, Haslam, M., 2016. Wild monkeys flake stone tools. Nature 539 (7627), 85–88.

Pruetz, J.D., Bertolani, P., Ontl, K.B., Lindshield, S., Shelley, M., Wessling, E.G., 2015. New evidence on the tool-assisted hunting exhibited by chimpanzees (Pan troglodytes verus) in a savannah habitat at Fongoli, Sénégal. Royal Society open science 2 (4), 140507.

Rabey, K.N., Green, D.J., Taylor, A.B., Begun, D.R., Richmond, B.G., McFarlin, S.C., 2015. Locomotor Activity Influences Muscle Architecture and Bone Growth but Not Muscle Attachment Site Morphology. J. Hum. Evol. 78, 91–102.

Rey, K., Amiot, R., Lécuyer, C., Koufos, G.D., Martineau, F., Fourel, F., Kostopoulos, D.S., Merceron, G., 2013. Late Miocene climatic and environmental variations in northern Greece inferred from stable isotope compositions (δ18O, δ13C) of equid teeth apatite. Palaeogeography, Palaeoclimatology, Palaeoecology 388, 48–57.

Richmond, B.G., 2007. Biomechanics of phalangeal curvature. Journal of human evolution 53 (6), 678–690.

Richmond, B.G., Roach, N.T., Ostrofsky, K.R., 2016. Evolution of the Early Hominin Hand, In: Kivell, T.L., Lemelin, P., Richmond, B.G., Schmitt, D. (Eds.), The Evolution of the Primate Hand. Anatomical, Developmental, Functional, and Paleontological Evidence. Developments in Primatology: Progress and Prospects. Springer, New York, pp. 515–543.

Richmond, B.G., Strait, D.S., 2000. Evidence that humans evolved from a knuckle-walking ancestor. Nature 404 (6776), 382–385.

Ricklan, D.E., 1987. Functional anatomy of the hand of *Australopithecus africanus*. J. Hum. Evol. 16 (7-8), 643–664.

Rolian, C., Carvalho, S., 2017. Tool Use and Manufacture in the Last Common Ancestor of Pan and Homo, In: Pilbeam, D.R., Muller, M.N., Wrangham, R.W. (Eds.), Chimpanzees and Human Evolution. Harvard University Press, Cambridge, MA, pp. 602–644.

Rolian, C., Gordon, A.D., 2013. Reassessing manual proportions in Australopithecus afarensis. American journal of physical anthropology 152 (3), 393–406.

Rolian, C., Lieberman, D.E., Hallgrímsson, B., 2010. The coevolution of human hands and feet. Evolution 64 (6), 1558–1568.

Rolian, C., Lieberman, D.E., Zermeno, J.P., 2011. Hand biomechanics during simulated stone tool use. J. Hum. Evol. 61 (1), 26–41.

Ruff, C., Holt, B., Trinkaus, E., 2006. Who's Afraid of the Big Bad Wolff?: "Wolff's law" and Bone Functional Adaptation. Am. J. Phys. Anthropol. 129 (4), 484–498.

Scherf, H., Harvati, K., Hublin, J.-J., 2013. A comparison of proximal humeral cancellous bone of great apes and humans. J. Hum. Evol. 65 (1), 29–38.

Scherf, H., Wahl, J., Hublin, J.-J., Harvati, K., 2016. Patterns of activity adaptation in humeral trabecular bone in Neolithic humans and present-day people. Am. J. Phys. Anthropol. 159 (1), 106–115.

Scheuer, L., Black, S.M., 2000. The Upper Limb, In: Scheuer, L., Black, S.M. (Eds.), Developmental juvenile osteology. Academic Press, San Diego, Calif., London, pp. 272–340.

Schlecht, S.H., 2012. Understanding Entheses: Bridging the Gap Between Clinical and Anthropological Perspectives. The Anatomical Record 295, 1239–1251.

Schmitt, D., Zeininger, A., Granatosky, M.C., 2016. Patterns, Variability, and Flexibility of Hand Posture During Locomotion in Primates, In: Kivell, T.L., Lemelin, P., Richmond, B.G., Schmitt, D. (Eds.), The Evolution of the Primate Hand. Anatomical, Developmental, Functional, and Paleontological Evidence. Developments in Primatology: Progress and Prospects. Springer, New York, pp. 345–369.

Sen, S., Koufos, G.D., Kondopoulou, D., de Bonis, L., 2000. Magnetostratigraphy of the late Miocene continental deposits of the lower Axios valley, Macedonia, Greece. Geological Society of Greece, Special Publications 9, 197–206.

Silva, M.J., Eekhoff, J.D., Patel, T., Kenney-Hunt, J.P., Brodt, M.D., Steger-May, K., Scheller, E.L., Cheverud, J.M., 2019. Effects of High-Fat Diet and Body Mass on Bone Morphology and Mechanical Properties in 1100 Advanced Intercross Mice. Journal of bone and mineral research : the official journal of the American Society for Bone and Mineral Research 34 (4), 711–725.

Singleton, M., 2002. Patterns of cranial shape variation in the Papionini (Primates: Cercopithecinae). J. Hum. Evol. 42 (5), 547–578.

Skinner, M.M., Stephens, N.B., Tsegai, Z.J., Foote, A.C., Nguyen, N.H., Gross, T., Pahr, D.H., Hublin, J.-J., Kivell, T.L., 2015. Human-like hand use in *Australopithecus africanus*. Science 347 (6220), 395–399.

Stern, J.T., Jungers, W.L., Susman, R.L., 1995. Quantifying phalangeal curvature: an empirical comparison of alternative methods. American journal of physical anthropology 97 (1), 1–10.

Stern, J.T., Susman, R.L., 1983. The locomotor anatomy ofAustralopithecus afarensis. Am. J. Phys. Anthropol. 60 (3), 279–317.

Susman, R.L., 1979. Comparative and functional morphology of hominoid fingers. Am. J. Phys. Anthropol. 50 (2), 215–236.

Susman, R.L., 1988. New Postcranial Remains from Swartkrans and Their Bearing on the Functional Morphology and Behavior of *Paranthropus robustus*, In: Grine, F.E. (Ed.), Evolutionary History of the “Robust” Australopithecines. Routledge, New York, pp. 149–172.

Susman, R.L., Creel, N., 1979. Functional and morphological affinities of the subadult hand (O.H. 7) from Olduvai Gorge. Am. J. Phys. Anthropol. 51 (3), 311–332.

Susman, R.L., Ruiter, D. de, Brain, C.K., 2001. Recently identified postcranial remains of Paranthropus and early Homo from Swartkrans Cave, South Africa. J. Hum. Evol. 41 (6), 607–629.

Susman, R.L., Stern, J.T., 1979. Telemetered electromyography of flexor digitorum profundus and flexor digitorum superficialis in Pan troglodytes and implications for interpretation of the O. H. 7 hand. Am. J. Phys. Anthropol. 50 (4), 565–574.

Thompson, J.C., Carvalho, S., Marean, C.W., Alemseged, Z., 2019. Origins of the human predatory pattern: The transition to large animal exploitation by early hominins-Reply. Current Anthropology 60 (1), 1–23.

Thompson, M.E., Muller, M.N., Machanda, Z.P., Otali, E., Wrangham, R.W., 2020. The Kibale Chimpanzee Project: Over thirty years of research, conservation, and change. Biological Conservation 252, 108857.

Tocheri, M.W., Orr, C.M., Jacofsky, M.C., Marzke, M.W., 2008. The evolutionary history of the hominin hand since the last common ancestor of *Pan* and *Homo*. Journal of anatomy 212 (4), 544–562.

Tocheri, M.W., Orr, C.M., Larson, S.G., Sutikna, T., Jatmiko, Saptomo, E.W., Due, R.A., Djubiantono, T., Morwood, M.J., Jungers, W.L., 2007. The primitive wrist of Homo floresiensis and its implications for hominin evolution. Science (New York, N.Y.) 317 (5845), 1743–1745.

Trinkaus, E., Long, J.C., 1990. Species Attribution of the Swartkrans Member 1 First Metacarpals: SK84 and SKX 5020. Am. J. Phys. Anthropol. 83 (4), 419–424.

Tsegai, Z.J., Kivell, T.L., Gross, T., Nguyen, N.H., Pahr, D.H., Smaers, J.B., Skinner, M.M., 2013. Trabecular bone structure correlates with hand posture and use in hominoids. PLOS ONE 8 (11), e78781.

Tsiminikaki, K., Karell, M.A., Nathena, D., Halazonetis, D., Spanakis, K., Kranioti, E.F., 2019. Three-Dimensional Geometry of Phalanges as a Proxy for Pair-Matching: Mesh Comparison Using an ICP Algorithm. Advances in experimental medicine and biology 1205, 55–69.

Ungar, P.S., 1996. Dental microwear of European Miocene catarrhines: evidence for diets and tooth use. Journal of human evolution 31 (4), 335–366.

Vereecke, E.E., Wunderlich, R.E., 2016. Experimental Research on Hand Use and Function in Primates, In: Kivell, T.L., Lemelin, P., Richmond, B.G., Schmitt, D. (Eds.), The Evolution of the Primate Hand. Anatomical, Developmental, Functional, and Paleontological Evidence. Developments in Primatology: Progress and Prospects. Springer, New York, pp. 259–284.

Visalberghi, E., Sirianni, G., Fragaszy, D., Boesch, C., 2015. Percussive tool use by Taï Western chimpanzees and Fazenda Boa Vista bearded capuchin monkeys: a comparison. Philosophical transactions of the Royal Society of London. Series B, Biological sciences 370 (1682).

Walker, A., Leakey, R.E.F. (Eds.), 1993. The Nariokotome Homo erectus skeleton. Springer, Berlin, Heidelberg, 457 pp.

Wallace, I.J., Burgess, M.L., Patel, B.A., 2020. Phalangeal curvature in a chimpanzee raised like a human: Implications for inferring arboreality in fossil hominins. PNAS 117 (21), 11223–11225.

Wallace, I.J., Winchester, J.M., Su, A., Boyer, D.M., Konow, N., 2017. Physical Activity Alters Limb Bone Structure but Not Entheseal Morphology. J. Hum. Evol. 107, 14–18.

Ward, C.V., Begun, D.R., Rose, M.D., 1997. Function and Phylogeny in Miocene Hominoids, In: Begun, D.R., Ward, C.V., Rose, M.D. (Eds.), Function, Phylogeny, and Fossils. Miocene Hominoid Evolution and Adaptations. Advances in Primatology Ser. Springer, New York, NY, pp. 1–12.

White, T.D., Lovejoy, C.O., Asfaw, B., Carlson, J.P., Suwa, G., 2015. Neither chimpanzee nor human, Ardipithecus reveals the surprising ancestry of both. PNAS 112 (16), 4877–4884.

Wilczak, C., Mariotti, V., Pany-Kucera, D., Villotte, S., Henderson, C.Y., 2017. Training and Interobserver Reliability in Qualitative Scoring of Skeletal Samples. Journal of Archaeological Science: Reports 11, 69–79.

Williams, E.M., Gordon, A.D., Richmond, B.G., 2010. Upper limb kinematics and the role of the wrist during stone tool production. Am. J. Phys. Anthropol. 143 (1), 134–145.

Williams, E.M., Gordon, A.D., Richmond, B.G., 2012. Hand pressure distribution during Oldowan stone tool production. J. Hum. Evol. 62 (4), 520–532.

Williams, E.M., Gordon, A.D., Richmond, B.G., 2014. Biomechanical strategies for accuracy and force generation during stone tool production. J. Hum. Evol. 72, 52–63.

Williams-Hatala, E.M., Hatala, K.G., Gordon, M., Key, A., Kasper, M., Kivell, T.L., 2018. The manual pressures of stone tool behaviors and their implications for the evolution of the human hand. Journal of human evolution 119, 14–26.

References

Williams-Hatala, E.M., Hatala, K.G., Hiles, S., Rabey, K.N., 2016. Morphology of Muscle Attachment Sites in the Modern Human Hand Does Not Reflect Muscle Architecture. Sci. Rep. 6, 28353.

Williams-Hatala, E.M., Hatala, K.G., Key, A., Dunmore, C.J., Kasper, M., Gordon, M., Kivell, T.L., 2021. Kinetics of stone tool production among novice and expert tool makers. American journal of physical anthropology 174 (4), 714-727.

Wittig, R.M., 2018. 40 years of research at the Taï Chimpanzee Project. Pan Africa News 25 (2), 16–18.

Young, R.W., 2003. Evolution of the human hand: the role of throwing and clubbing. J. Anat. 202 (1), 165–174.

Zumwalt, A., 2006. The Effect of Endurance Exercise on the Morphology of Muscle Attachment Sites. The Journal of Experimental Biology 209 (3), 444–454

Appendix

Appendix A

The intermediate phalanx RPl-87 of Ouranopithecus macedoniensis

Geomteric morphometric analysis of the intermediate phalanx of Ouranopithecus macedoniensis—A pilot study

By Jana Kunze, Fotios Alexandros Karakostis, Melania Ioannidou, George D. Koufos, Katerina Harvati

Manuscript accepted for publication in:
Human Evolution at the CROSSROADS: Research in Greece and beyond.
Proceedings of the Closing Symposium, February 2022 Tübingen.
Paleoanthropology Book Series – Contributions in Paleoanthropology III.
Tübingen University Press[1].

---

[1] The following version is based on the authors formatting of the manuscript and figures. General layout and position of Tables and Figures may differ in the final published manuscript.

Appendix A

1. GEOMETRIC MORPHOMETRIC ANALYSIS OF THE INTERMEDIATE PHALANX OF *OURANOPITHECUS MACEDONIENSIS*—A PILOT STUDY

JANA KUNZE[1,*], FOTIOS ALEXANDROS KARAKOSTIS[2], MELANIA IOANNIDOU[1], GEORGE D. KOUFOS[3], KATERINA HARVATI[1,2]

[1]Paleoanthropology, Institute for Archaeological Sciences and Senckenberg Centre for Human Evolution and Paleoenvironment, Eberhard Karls University of Tübingen, Tübingen, Germany. [2]DFG Centre of Advanced Studies 'Words, Bones, Genes, Tools', Eberhard Karls University of Tübingen, Tübingen, Germany.
[3]Laboratory of Geology and Palaeontology, School of Geology, Aristotle University of Thessaloniki, Thessaloniki, Greece.

*jana.kunze@senckenberg.de

Keywords: Miocene hominoids; Ouranopithecus; virtual anthropology; phalangeal shape variation; geometric morphometrics

1.1 INTRODUCTION

Ravin de la Pluie (RPl) in the Axios valley, Greece, is one of the three localities where the material of the Late Miocene ape *Ouranopithecus macedoniensis* has been found to date (de Bonis et al., 1974; de Bonis and Melentis, 1978; Koufos and de Bonis, 2006; Koufos et al., 2016). The material from RPl is rich; it includes maxillary and mandibular remains, multiple isolated teeth, and just a few postcranial specimens, which to date represent the only postcranial remains associated with this species: two phalanges (proximal: RPl-86, intermediate: RPl-87).

A first analysis of the phalanges was conducted in 2014 (de Bonis and Koufos, 2014). In that study, de Bonis and Koufos followed a comparative approach, using multivariate analyses of linear measurements to assess morphological similarities to extant and fossil primates. De Bonis and Koufos concluded that both phalanges likely belong to the hand, but that an allocation to the foot cannot be excluded due to the lack of comparative material from the same species. However, since the phalanges are the only postcranial remains associated with this species so far, identifying them as either manual or pedal phalanges, as well as allocating them to a ray, is crucial. Having this information would allow for further, more detailed examinations, such as more accurate comparative analyses and reconstruction of locomotor behavior. Therefore, the goal of this study is to contribute to the identification of the intermediate phalanx RPl-87 through the application of three-dimensional (3D) geometric morphometrics (GM). Geometric morphometrics is a statistical analysis of form (shape and size) in which, in contrast to traditional morphometrics, geometric information of the investigated structures can be retained throughout the analysis to provide a more detailed evaluation of shape differences (Slice, 2007). By comparing the shape of the better-preserved phalanx RPl-87 with manual and pedal intermediate phalanges of extant primates, we aim to address the following research questions:

1. Does RPl-87 belong to the foot or the hand?
2. What ray can RPl-87 be assigned to?
3. Does the specimen show morphological affinities to extant primates?

1.2 MATERIALS AND METHODS

Our comparative sample consists of scans of intermediate phalanges of *Gorilla gorilla* (n=23, 4 individuals), *Pan troglodytes* (n=24, 4 individuals), *Pongo pygmaeus* (n=24, 5 individuals), *Papio hamadryas* (n=15, 2 individuals), and *Macaca arctoides* (n=7, 1 individual) from the American Museum of Natural History Mammal Collections downloaded from MorphoSource.org. Manual and pedal phalanges from the second to fifth ray were selected for the shape analysis. Generally, it was attempted to keep the number of individuals low by including hand and foot bones from the same individual. However, this was not possible in some cases due to issues with preservation or scan quality. Moreover, a second intermediate phalanx from *G. gorilla* had to be removed as it presented as an outlier throughout the statistical analyses. Since the anatomical side of RPl-87 could not be determined so far, we analyzed bones from left and right anatomical sides together.

1.2.1 SHAPE ANALYSIS

The shape analysis was conducted in R-Studio (R version 4.1.2 for Windows; R Core Team, 2021) using the geomorph package (Adams and Otárola-Castillo, 2013). Eleven fixed landmarks were placed in geometrically corresponding positions (Table 1) together with 70 surface semilandmarks. For RPl-87, the landmark placing procedure was repeated three additional times. The precision of landmark placement was calculated based on the total of four repetitions using the centroid radius approach (von Cramon-Taubadel et al., 2007).

Table 1: Landmark description of the eleven fixed landmarks.

No	Orientation*	Descritpion*
1	medial	most distal point of the medial head condyle
2	lateral	most distal point of the lateral head condyle
3	medial	most palmar point of the medial head condyle
4	lateral	most palmar point of the lateral head condyle
5	distal, dorsal up	most dorsal point of the medial half of the head
6		most dorsal point of the lateral half of the head
7	proximal, palmar up	app. midpoint of palmar border of proximal articular surface, often most palmarly projecting point
8		app. midpoint of left border of proximal articular surface, often most medially projecting point
9		app. midpoint of right border of proximal articular surface, often most laterally projecting point
10		app. midpoint of dorsal border of proximal articular surface, often most proximally projecting point
11	medial	most distal point of base curvature

*Anatomical sides were pooled in the analysis, and bones were not mirrored. Therefore, to simplify landmark description, the indication of medial and lateral in this table refer to the bone as if it were right (i.e., for a bone from the left side, medial should be replaced by lateral and vice versa).

The bones were divided into different subgroups for the analyses to address our research questions. Procrustes superimposition was performed for each group separately by rotating, centering, and scaling. The resulting Procrustes coordinates were analyzed in a principal component analysis (PCA) based on a covariance matrix. RPl-87 was not included in the original PCAs; instead, its principal component scores were calculated, and it subsequently was projected onto the PC plots. The principal components depicted in the PC plot were chosen based on what best separated the sample. To display the associated shape changes, the 'warpRefMesh' function from the package geomorph was used to create thin-plate spline grids (Bookstein, 1989). In each analysis, the specimen most similar in shape to the average sample was warped to depict the shapes at the extremes of the principal components. Additionally, a matrix including the pairwise Procrustes distances was exported from R-Studio and imported into PAST (Hammer et al., 2001), to create a neighbor joining tree.

1.3 RESULTS

1.3.1 HAND OR FOOT

The precision of landmark placement was high with a maximum error rate of 2.77%.

As our first goal was to assess whether RPl-87 belonged to the hand or the foot, the sample was divided by ray, resulting in four subgroups including both hand and foot bones.

The PC plot depicting the analysis of second intermediate phalanges (Fig. 1, top left) shows the clearest separation of hand and foot bones when PC6 (2.76% of variance) is plotted against PC1 (65.88% of variance). RPl-87 plots inside the convex hull of foot bones extending mainly towards PC1 negative, whereas the hand bones are concentrated more towards PC1 positive and PC6 positive. It should be noted that the variation on PC6 appears to be mainly driven by one Gorilla specimen. In the neighbor joining tree (Fig. 1, top right), RPl-87 is closest to some *Gorilla* and *Pan* foot bones, as well as *Papio* foot bones. This is also reflected in the Procrustes distance values (not shown), as the *Ouranopithecus* phalanx shows the least mean distance to the *Papio* species.

In the analysis of the third ray (not shown), in which the best separation was achieved through a combination of PC1 (63.24% of variance) and PC4 (4.56% of variance), the *Ouranopithecus* specimen shows a distinctively higher negative loading on PC1 than the rest of the sample, placing it outside the convex hulls of either hand or foot bones. Nonetheless, it is closer to the majority of foot bones, in particular those of *Gorilla* and *Pan*, than to hand bones, which plot more towards PC1 positive and PC4 negative. The neighbor joining tree shows RPl-87 positioned at its bottom with two *Pan* foot bones in the closest proximity. As in the PC plot, the majority of hand bones are positioned further away from the *Ouranopithecus* bone, indicating that the bone is more similar to the foot bones in the sample. The species means of Procrustes distances place RPl-87 closest to *Gorilla* and *Papio*, whereas the similarity to *Pan*, as indicated by the neighbor joining tree, is limited to the two foot bones. The shape analysis of the fourth ray (not shown) consistently showed poor separation of hand and foot bones, irrespective of the combination of principal components. Therefore, it was decided to focus on the PC axes reflecting the highest amount of variance: PC1 (62.07%) and PC2 (10.33%). As in the analysis of the third intermediate phalanx, RPl-87 plots outside the range of either hand or foot bones. On PC1, it is most similar to a *Papio* hand bone that differs from the remaining hand bones in the sample by its high negative loading on that axis. When considering both PC1 and PC2, two *Gorilla* foot bones on the margin of the foot bone convex hull are slightly closer to the *Ouranopithecus* bone. On the neighbor joining tree, the *Papio* hand bone is situated on a sister branch to RPl-87 and three *Gorilla* foot bones are located on branches in the proximity. This is also reflected in the Procrustes distance values, as RPl-87 is closest to the *Papio* and *Gorilla* species. As in the PC plot, the separation of hand and foot bones is poor in the tree due to the high amount of overlap. However, there is a higher concentration of foot bones towards the bottom of the tree and in the proximity of RPl-87, while most hand bones, particularly those of *Pan* and *Pongo*, are located further away from the fossil.

Finally, when analyzing the intermediate phalanges of the fifth ray (Fig. 1, bottom left), the best separation was achieved by plotting PC1 (63.62% of variance) and PC2 (7.69% of variance). RPl-87 plots inside the shape variation of foot bones, closest to a *Papio* and a *Gorilla* specimen. The neighbor joining tree (Fig. 1, bottom right) shows the *Ouranopithecus* specimen situated close to a *Pan* and three *Gorilla* foot bones, but also in the proximity of *Papio* bones of

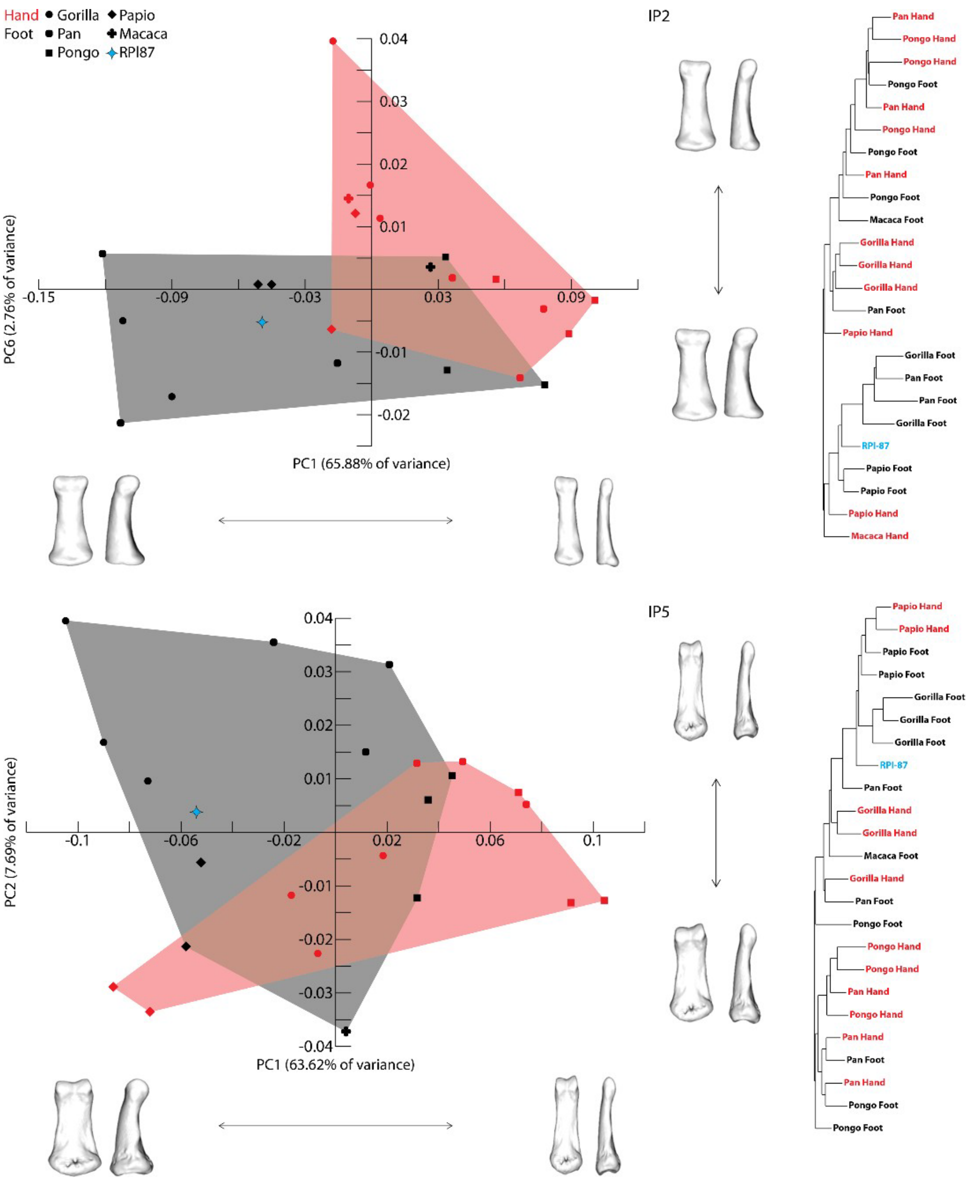

Figure 1: Top: PCA of Procrustes superimposed landmarks of the second intermediate phalanx without a priori group association. PC1 compared to PC6. Shape changes along PC1 and PC6 are illustrated below and to the right of the plot respectively. The neighbor joining tree based on the Procrustes distances is depicted on the right.
Bottom: PCA of Procrustes superimposed landmarks of the fifth intermediate phalanx without a priori group association. PC1 compared to PC2. Shape changes along PC1 and 2 are illustrated below and to the right of the plot respectively. The neighbor joining tree based on the Procrustes distances is depicted on the right. Coloration and symbology follow the legend in the top image.

both hand and foot. The latter is also reflected in the Procrustes distance values, as the mean distance is smaller from RPl-87 to *Papio* than to *Gorilla*.

Correlation analyses of PC1 and centroid size show that there is a moderate correlation (Pearson's r = 0.55-0.66, assumptions are met) between these variables. However, this correlation does not appear to be related to size differences among species, but rather to differences in size among hand and foot bones, the latter being typically larger than the former.

1.3.2 RAY ALLOCATION AND AFFINITIES TO EXTANT PRIMATES

As the previous analyses have generally placed RPl-87 closer to foot bones than to hand bones, the latter were removed from the sample. In order to determine the ray RPl-87 belongs to, the foot bones of all rays were analyzed together in the subsequent analyses.

The plot of PC1 (60.9% of variance) and PC2 (9.08% of variance) shows substantial overlap between the different rays (Fig. 2, top left). The shape changes along PC1 appear to be mostly related to length-to-width proportions, with longer and more slender bones on PC1 positive and shorter and broader bones on PC1 negative. Shape changes on PC2 can be attributed to bone robusticity, particularly at the head and base, asymmetry in distal extension of the head condyles and the degree of proximal extension of the palmar area of the base. While the overlap among rays is particularly visible around the center of PC1, some degree of separation of the different rays is apparent at the extremes of this axis. The convex hulls of the second and fifth intermediate phalanx extend towards PC1 negative, while PC1 positive shows a higher concentration of bones from the third and fourth ray. With its negative PC1 loading, RPl-87 plots inside the range of variation of both second and fifth intermediate phalanges. The neighbor joining tree also reflects the overlap among rays (Fig. 2, top right), although the branches in the proximity of RPl-87 are mainly associated with bones from the second and fifth ray, with the only exception of a *Gorilla* fourth intermediate phalanx. In terms of Procrustes distances, this *Gorilla* bone appears to be closest to the fossil specimen. Nonetheless, when calculating the mean distance of each ray, RPl-87 shows the least distance to fifth intermediate phalanges, followed by bones of the second ray.

An improved separation is achieved when the phalanges are grouped by species instead of ray (Fig. 2, bottom left). This suggests that the variation driving the principal component analysis is not related to the differences in shape among rays, but to the differences among species. With its longer and more slender foot bones, *Pongo* is located at the extreme of PC1 positive. In contrast, *Gorilla* plots towards PC1 negative, together with two *Pan* foot bones. The majority of *Pan* bones, however, are clustered around the center of PC1 and towards PC2 positive. *Papio* and *Macaca* have a similar loading on PC2 as they both fall on the negative extreme of this component, with *Papio* on PC1 negative and *Macaca* on PC1 positive. RPl-87 plots in the center of the *Gorilla* convex hull, indicating a possible similarity in shape to that species. Interestingly, in the neighbor joining tree, as well as in Procrustes distance values, the *Ouranopithecus* bone is more similar to the *Papio* foot bones. These contradictory results can be explained by that the PC plot focuses only on two axes of shape variance, whereas the Procrustes distances cover the entire shape variation in the sample.

PC1 of this analysis is again moderately correlated with centroid size (Pearson's $r = 0.52$, assumptions are met). In this case, however, this correlation appears to be driven by size differences among the rays (ray 2 and 5 compared to ray 3 and 4) instead of species-related size differences, as the two species with the overall largest phalanges (*Gorilla* and *Pongo*) are represented on both extremes of PC1.

To further localize the ray RPl-87 belongs to, an analysis was conducted including only pedal intermediate phalanges of the second and fifth ray (not shown). However, the overlap between bones of the two rays is too extensive both in the PC plot and the neighbor joining tree to draw meaningful conclusions. Procrustes distance values indicate that RPl-87 is slightly more similar to fifth intermediate phalanges than to those of the second ray, but only by a small margin (0.085 as compared to 0.087).

1.4 DISCUSSION

This pilot study was an attempt at identifying the intermediate phalanx RPl-87, one of the only two postcranial elements so far associated with *Ouranopithecus macedoniensis,* through the application of 3D geometric morphometrics. According to the results of the principal component analyses and the neighbor joining trees, the shape of RPl-87 more closely resembles the shape of foot bones in our comparative sample. It differs from most hand bones analyzed here. This would suggest that, in contrast to a previous assessment of this specimen (de Bonis and Koufos, 2014), RPl-87 can

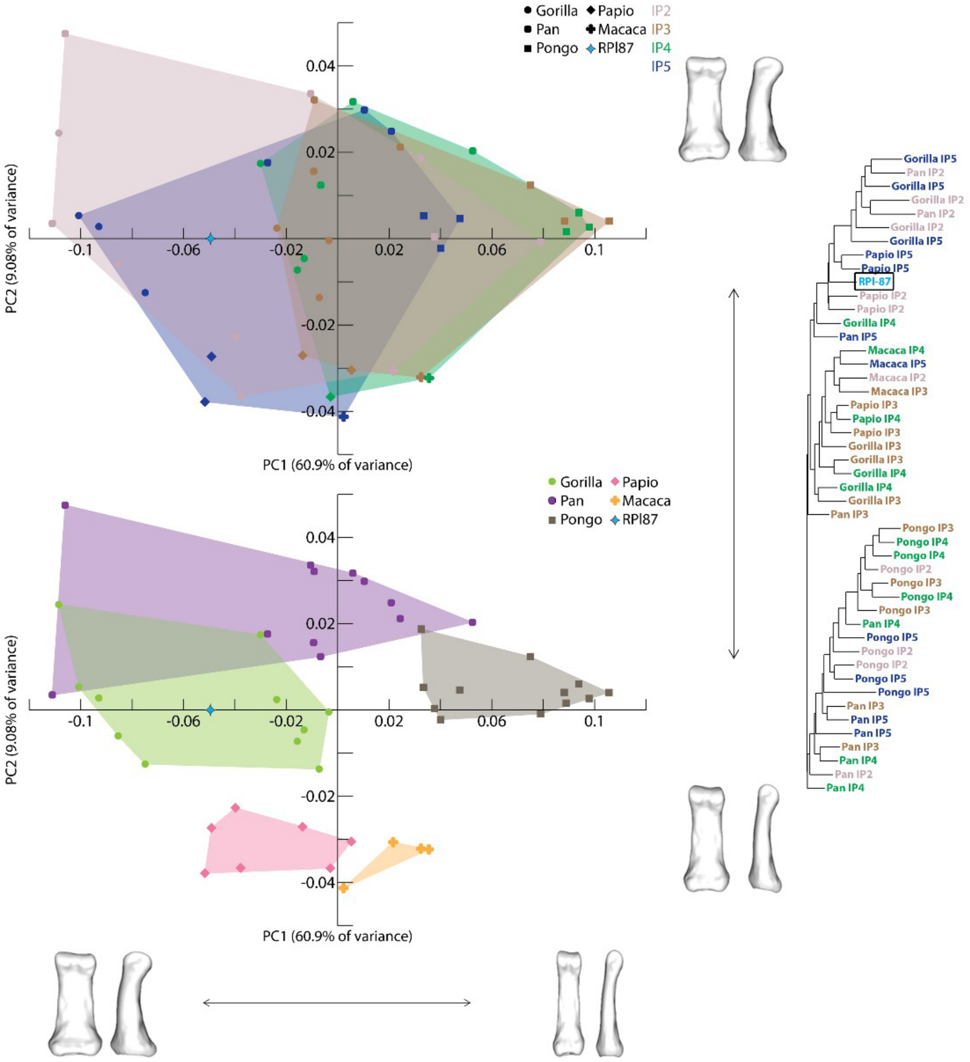

Figure 2: PCA of Procrustes superimposed landmarks of the pedal phalanges without a priori group association. PC1 compared to PC2. The upper plot depicts grouping by ray while the lower plot depicts grouping by species. Since the two plots represent the same analysis, the shape changes along PC1 and 2, illustrated below and to the right of the plots, respectively, apply for both plots. The neighbor joining tree based on the Procrustes distances is depicted on the right with coloration based on the different rays.

likely be attributed to the foot. Additionally, the fact that the fossil plots outside the shape variation of both hand and foot bones of the third and fourth ray suggests that its shape diverges notably from the bones of these rays. This is supported by our analysis including foot bones only, which focused on ray identification. Despite the overlap among rays, the PC plot indicates a similarity in shape of RPl-87 and intermediate phalanges of the second and fifth ray. These results are in accordance with those by de Bonis and Koufos (2014), who suggested that the specimen represents a paramedian digit (two and five). Unfortunately, it was not possible to further specify the ray in this pilot study, as the overlap in shape of these two rays is too great. This could possibly be due to the fact that our sample includes bones from both the right and left side. The two paramedian digits are asymmetric in their morphology, especially of the head condyles, but in the opposite direction (i.e., a more distally extending head condyle can usually be observed on the lateral side of the second and the medial side of the fifth intermediate phalanx). Therefore, for a clearer identification, it would be necessary to identify the anatomical side of RPl-87. If this is not possible without first identifying the ray, the second option is to analyze a larger sample with balanced proportions of left and right phalanges to better observe and interpret potential patterns. While our analyses have identified a moderate correlation between the respective PC1s and size, this does not appear to be associated with species-related size differences, but rather with differences in size among hands, feet, and rays. Therefore, we propose that the variance on the first PCs is mainly driven by variation in shape, whereas their correlation with size is likely an ancillary effect.

Our results additionally suggest RPl-87 to be most similar in shape to *Gorilla* and *Papio* foot bones. While reconstructing individual behavior from overall bone shape can be misleading (e.g., see Wallace et al., 2020), the fact that RPl-87 is more similar in shape to the terrestrial species than it is to *Pongo*—the most arboreal species in our sample—could suggest that *Ouranopithecus macedoniensis* was a terrestrial primate as well. A comparable conclusion has been drawn by de Bonis and Koufos (2014), as they have found similar morphological affinities in their analysis. Further support can be found in reconstructions of the paleoenvironment at Ravin de la Pluie, indicating an open and dry environment in this area (Koufos, 2006), and in the results of the microwear analysis on teeth of other fossils attributed to *O. macedoniensis* (Ungar, 1996; Merceron et al., 2005).

1.5 CONCLUSION AND OUTLOOK

The analysis of the overall bone shape of the intermediate phalanx RPl-87 has shown that the specimen can likely be attributed to the second or fifth ray of the foot. Additionally, its morphology appears to be most similar to intermediate phalanges of *Gorilla gorilla* and *Papio hamadryas*. While this study succeeded in showing the great potential of using 3D geometric morphometric analysis to identify the intermediate phalanx RPl-87, it also presented some issues that impede drawing secure conclusions. To corroborate and specify the results of this pilot study, future analyses of this bone should increase the size of the comparative sample. Not only should the number of individuals of the species analyzed here be increased, but future studies ideally should also include additional species of extant and—more crucially—fossil primates. Another important step is to apply a more detailed and specialized landmark configuration. RPl-87 shows some distinctive morphological traits such as the subtle curvature of its bone shaft and the faint development of its flexor sheath ridges. These traits could be captured with more specific landmark placement or with curve semilandmarks.

Finally, the shape analysis should be extended to the proximal phalanx RPl-86. As the two specimens represent a proximal and an intermediate phalanx, respectively, thorough analyses of not only the overall shapes of the bones, but also of their articular surfaces specifically, could shed light on whether these bones are from the same individual, the same foot or even from the same ray.

Acknowledgments

This research was supported by the ERC Consolidator Grant ERC-CoG-724703 ("CROSSROADS") awarded to K. Harvati. We are grateful to the American Museum of Natural History Mammal collection (S. Almécija, D. Boyer, E. Delson) for making the 3D models of great ape hand remains available online at MorphoSource.org (Duke University). Finally, we thank our reviewers, Abel Bosman and Eric Delson, whose comments helped improve and clarify this manuscript.

References

Adams, D.C. and Otárola-Castillo, E., 2013. Geomorph: an R package for the collection and analysis of geometric morphometric shape data. Methods in Ecology and Evolution, 4(4), pp. 393–399.

de Bonis, L. and Melentis, J., 1978. Les Primates hominoïdes du Miocène supérieur de Macédoine–Étude de la mâchoire supérieure. In Annales de Paléontologie (vertébres), 64, pp. 185–202.

de Bonis, L. and Koufos, G.D., 2014. First discovery of postcranial bones of Ouranopithecus macedoniensis (Primates, Hominoidea) from the late Miocene of Macedonia (Greece). Journal of Human Evolution, 74, pp. 21–36.

de Bonis, L., Bouvrain, G., Geraads, D. and Melentis, J. 1974. Première découverte d'un primates hominoïde dans le Miocène supérieur de Macédonie (Grèce). Comptes rendus de l'Académie des Sciences, Paris, série D, 278, pp. 3063–3066.

Bookstein, F.L., 1989. Principal Warps: Thin-Plate Splines and the Decomposition of Deformations. IEEE Transactions on Pattern Analysis and Machine Intelligence, 11(6), pp. 567-585.

Cramon-Taubadel, N. von, Frazier, B.C. and Lahr, M.M., 2007. The Problem of Assessing Landmark Error in Geometric Morphometrics: Theory, Methods, and Modifications. Am. J. Phys. Anthropol., 134(1), pp. 24–35.

Hammer, Ø., Harper, D.A.T. and Ryan, P.D., 2001. PAST: Paleontological Statistics Software Package for Education and Data Analysis. Paleontologia Electronica, 4(1), pp. 1–9.

Koufos, G.D., 2006. Palaeoecology and chronology of the Vallesian (late Miocene) in the Eastern Mediterranean region. Palaeogeography, Palaeoclimatology, Palaeoecology, 234(2-4), pp. 127–145.

Koufos, G.D. and de Bonis, L., 2006. New material of *Ouranopithecus macedoniensis* from late Miocene of Macedonia (Greece) and study of its dental attrition. Geobios, 39(2), pp. 223–243.

Koufos, G.D., de Bonis, L. and Kugiumtzis, D., 2016. New material of the hominoid *Ouranopithecus macedoniensis* from the Late Miocene of the Axios Valley (Macedonia, Greece) with some remarks on its sexual dimorphism. Folia Primatologica, 87(2), pp. 94–122.

Merceron, G., Blondel, C., de Bonis, L., Koufos, G.D. and Viriot, L., 2005. A New Method of Dental Microwear Analysis: Application to Extant Primates and *Ouranopithecus macedoniensis* (Late Miocene of Greece). Palaios, 20(6), pp. 551–561.

R Core Team, 2021. R: A language and environment for statistical computing. R Foundation for Statistical Computing, Vienna.

Slice, D.E., 2007. Geometric morphometrics. Annual Review of Anthropology, 36, pp. 261–281.

Ungar, P.S., 1996. Dental microwear of European Miocene catarrhines: evidence for diets and tooth use. Journal of Human Evolution, 31(4), pp. 335–366.

Wallace, I.J., Burgess, M.L. and Patel, B.A., 2020. Phalangeal curvature in a chimpanzee raised like a human: Implications for inferring arboreality in fossil hominins. PNAS, 117(21), pp. 11223–11225.

Appendix B

Entheseal patterns and overall shape of the first metacarpal of early hominins

Entheseal Patterns Suggest Habitual Tool Use in Early Hominins

By Jana Kunze, Fotios Alexandros Karakostis, Stefan Merker, Marco Peresani,
Gerhard Hotz, Vangelis Tourloukis, Katerina Harvati

Published (2022) in *PaleoAnthropology* 2022 (2), 195-210.
DOI: 10.48738/2022.iss2.61.

Entheseal Patterns Suggest Habitual Tool Use in Early Hominins

JANA KUNZE
Paleoanthropology, Senckenberg Centre for Human Evolution and Palaeoenvironment, Institute for Archaeological Sciences, Eberhard Karls University of Tübingen, Tübingen, GERMANY; jana.kunze@uni-tuebingen.de

FOTIOS ALEXANDROS KARAKOSTIS*
DFG Centre of Advanced Studies 'Words, Bones, Genes, Tools' Eberhard Karls University of Tübingen, Tübingen, GERMANY; fotios-alexandros.karakostis@uni-tuebingen.de

STEFAN MERKER
Department of Zoology, State Museum of Natural History Stuttgart, Stuttgart, GERMANY; stefan.merker@smns-bw.de

MARCO PERESANI
Deparment of Humanities, Section of Prehistoric and Anthropological Sciences, University of Ferrara, Ferrara; and, Institute of Environmental Geology and Geoengineering, National Research Council, Milano, ITALY; psm@unife.it

GERHARD HOTZ
Anthropological Collection, Natural History Museum of Basel, Basel; and, Integrative Prehistory and Archaeological Science, University of Basel, Basel, SWITZERLAND; Gerhard.Hotz@bs.ch

VANGELIS TOURLOUKIS
Paleoanthropology, Senckenberg Centre for Human Evolution and Palaeoenvironment, Institute for Archaeological Sciences, Eberhard Karls University of Tübingen, Tübingen, GERMANY; vangelis.tourloukis@ifu.uni-tuebingen.de

KATERINA HARVATI*
Paleoanthropology, Senckenberg Centre for Human Evolution and Palaeoenvironment, Institute for Archaeological Sciences, Eberhard Karls University of Tübingen, Tübingen; and, DFG Centre of Advanced Studies 'Words, Bones, Genes, Tools' Eberhard Karls University of Tübingen, Tübingen, GERMANY; katerina.harvati@ifu.uni-tuebingen.de

*corresponding authors: Fotios Alexandros Karakostis, *fotios-alexandros.karakostis@uni-tuebingen.de; and, Katerina Harvati, katerina.harvati@ifu.uni-tuebingen.de*

submitted: 10 October 2021; revised: 24 February 2022; accepted: 6 April 2022

ABSTRACT

Systematic tool use is a central component of the human niche. However, the timing and mode of its evolution remain poorly understood. A newly developed method for the analysis of muscle recruitment patterns (Validated Entheses-based Reconstruction of Activity - V.E.R.A.) has recently been experimentally shown to provide clear and reliable evidence of habitual activity during life from skeletal remains. It is thus ideal to investigate the emergence of tool-related behaviors in the human fossil record. Here, we investigate this question by applying V.E.R.A. to the attachment proportions of thumb (first metacarpal) muscles considered crucial for tool use, in combination with a geometric morphometric analysis of bone shape. Our sample comprises modern humans, extant great apes, Neanderthals, *Homo naledi*, three *Australopithecus* species (*A. afarensis*, *A. africanus* and *A. sediba*) and a taxonomically unassigned fossil hominin from Swartkrans, South Africa. Results show that modern humans are distinct from extant non-human great apes in the recruitment patterns of the thumb muscles examined, as expected. Importantly, all hominins except *A. africanus* exhibit human-like thumb muscle use irrespective of the overall shape of their first metacarpal. This pattern supports habitual tool-related behaviors in these early taxa—excluding *A. africanus*—despite their lack of skeletal adaptations for efficient tool use observed in the first metacarpals of later *Homo*. Our findings strongly suggest habitual tool use by early hominins, and indicate an early, mosaic establishment of this behavior among *Australopithecus* taxa, preceding the evolution of tool-related biomechanical adaptations of the hominin hand and consistent with recent archaeological discoveries.

***PaleoAnthropology* 2022:2: 195–210.** **https://doi.org/10.48738/2022.iss2.61** **ISSN 1545-0031**

INTRODUCTION

Habitual stone tool use is a fundamental element of the hominin adaptive niche and a cornerstone of human bio-cultural co-evolution. However, the time and mode of its emergence remain elusive. Since chimpanzees, our closest living relatives, are known to engage in stone hammer-and-anvil nut-cracking and plant-tool use (Haslam et al. 2009; Whiten et al. 1999), it is considered reasonable to suggest some form of tool-use in our last common ancestor (Kivell 2015; Panger et al. 2002). However, this view does not take into account several million years of independent chimpanzee evolution. To reliably assess early hominin behavior, therefore, we must turn to the direct evidence from the archaeological and fossil record.

The currently available evidence is inconclusive—the recently discovered lithic industry from Lomekwi, Kenya, dated to as early as 3.3 Ma (Harmand et al. 2015), is controversial, as both its artifactual character and its chronology have been questioned (Archer et al. 2020; Domínguez-Rodrigo and Alcalá 2016), while proposed 3.39 my-old cutmarks from Dikika, Ethiopia, (McPherron et al. 2010) may have been produced through taphonomic processes or bite marks rather than hominin activity (Domínguez-Rodrigo et al. 2012; Sahle et al. 2017). The hand anatomy of early fossil hominins has been used to infer their mechanical abilities and manual dexterity (Alba et al. 2003; Galletta et al. 2019; Green and Gordon 2008; Kivell et al. 2011; 2015; 2018; Marchi et al. 2017; Marzke 1983; Marzke et al. 2010; Ricklan 1987; Susman 1988, 1994). Current consensus of this work describes early hominins as showing a mosaic of human- and ape-like features, which may or may not be consistent with systematic tool use. However, while manual biomechanical dexterity and skeletal morphology are important indicators of evolutionary adaptation potentially related with tool-using skills, they cannot be used to directly infer the habitual performance of tool-related behaviors during life. Due to its importance for functional and motoric aspects, gross bone shape is considered to be genetically regulated, reflecting evolutionary adaptation, and thus less subject to change through physical activity during life (Currey 2002; Kivell 2016; Parfitt et al. 2000; Wallace et al. 2020). Bone shape, therefore, may inform on movements a taxon is adapted for, but may also reflect the retention of ancestral features which have little or no bearing on an individual's actual behavior in life. To overcome this problem researchers have turned to the analysis of trabecular features. Differences in trabecular bone architecture are often thought to inform on different loading regimes during life and thus to be a possible proxy for activity (Barak et al. 2011; Biewener et al. 1996; Kivell 2016; Ruff et al. 2006; Scherf et al. 2013; 2016; Stephens et al. 2018; Tsegai et al. 2013). Studies of trabecular bone in *Australopithecus sediba* and *A. africanus* suggested the possibility of frequent forceful opposition of the thumb in these taxa, possibly indicating a human-like use of the hand (Dunmore et al. 2020; Skinner et al. 2015b), despite their observed low manual biomechanical efficiency (Galletta et al. 2019; Karakostis et al. 2021b; Marchi et al. 2017). While the exact factors driving variation in trabecular features can often be difficult to assess (e.g., Almécija et al. 2015; Carlson et al. 2008; Judex and Carlson 2009; Kivell 2016; Robling 2009; Skinner et al. 2015a), such results still hint at a discrepancy between biomechanical efficiency inferred by bone functional anatomy and reconstructions of habitual behavior based on analyses of structures more responsive to mechanical loading.

Another approach to reconstructing habitual activity is the analysis of muscle recruitment patterns. As the interface of soft and hard tissue, muscle attachment sites (entheses) experience mechanical stress through muscle activation and dissipate it across larger areas, resulting in remodeling of the bone surface (Benjamin et al. 2002; Cashmore and Zakrzewski 2013; Foster et al. 2014; Schlecht 2012). The analysis of entheseal morphology has been plagued by important methodological shortcomings in the past, including a former lack of supportive experimental evidence that entheseal surfaces are affected by physical activity (Rabey et al. 2015; Wallace et al. 2017; Williams-Hatala et al. 2016; Zumwalt 2006). The Tübingen University Validated Entheses-based Reconstruction of Activity (V.E.R.A.) method, however, which focuses on muscle recruitment patterns—as revealed by the relative proportions of muscle attachment sites on bone through multivariate analysis of entheseal 3D surface areas (rather than individual entheses per se)—has overcome many of these difficulties, providing a reliable way to reconstruct habitual activity in the past (Karakostis and Lorenzo 2016). Since the development of V.E.R.A. by one of us (FAK; Karakostis and Lorenzo 2016; Karakostis and Harvati 2021 and references therein), it has been validated both in documented human samples and several independent animal experimental models, and shown to reliably discern habitual muscle coordination using multiple anatomical regions and associated groups of muscles (Castro et al. 2021; Karakostis et al. 2017; Karakostis et al. 2019a; 2019b). It can therefore shed light on habitual performance of specific body movements, and thus specific behaviors, in the past (Karakostis et al. 2017; 2018; 2020; 2021a; Karakostis and Lorenzo 2016). In a recent review dedicated to previous applications of this method, Karakostis and Harvati (2021) provided a more detailed step-by-step protocol for applying V.E.R.A., to facilitate its broader application.

Here we apply this novel method for the first time to hand bones of early hominins to help elucidate the origins of human-like tool using behavior. We investigate recruitment patterns of thumb muscles important for these behaviors across hominin species in a comparative framework to help reconstruct their habitual manual activities and shed light on their potential tool use. We focus on the first metacarpal and its three attachment sites for the muscles: *opponens pollicis* (OP), *abductor pollicis longus* (APL), and first dorsal *interosseous* (DI1) (Figure 1). These muscles, which are important for human tool use (Table 1 and Materials and Methods), are thought to share key functions across humans and apes (Diogo et al. 2013; Lemelin and Diogo 2016; Vereecke and Wunderlich 2016), enabling their comparison across taxa—the OP flexes the thumb at the carpometacarpal joint (Netter et al. 2019) and plays a central role

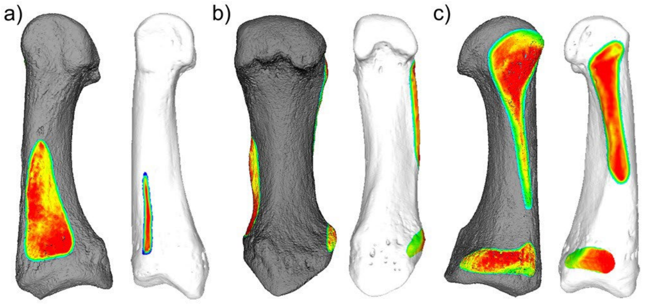

Figure 1. Depiction of the three entheses delineated on the right first metacarpal of Basel 264 (left), recent modern human, and Pan troglodytes *176229 (right) following the V.E.R.A. method developed by one of us (FAK; Karakostis and Lorenzo 2016; Karakostis and Harvati 2021 and references therein). a) medial view with the delineation of the DI1 enthesis; b) palmar view; c) lateral view with the delineations of the OP and APL entheses.*

in precision grasping, which places the thumb in an opposing position to the palm and the remaining fingers (Napier 1956). Therefore, this muscle is often associated with human-like manual dexterity (Feix et al. 2015; Karakostis et al. 2021b; Marzke 1997) and tool-use (Kivell 2015; Marzke 2013; Marzke et al. 1998). The APL is also activated during thumb opposition and precision grasping through thumb abduction at the carpometacarpal joint (Napier 1956; Netter et al. 2019). Finally, the DI1 abducts the second digit at the metacarpophalangeal joint (Netter et al. 2019), which is critical for habitual tool production (Williams-Hatala et al. 2020), and is also thought to stabilize the thumb (Marzke et al. 1998). Previous work has found that this muscle is less developed in great apes compared to modern humans (Jacofsky 2009; Tocheri et al. 2008). Importantly, electromyographic work has shown that the DI1 is consistently activated together with the *flexor pollicis longus* (FPL) during human-like stone tool use irrespective of tool type, as well as during hard hammer percussion manufacture (which involves both the dominant and the non-dominant hand), underlining the importance of this muscle for tool-related behaviors in general (Key et al. 2020; Marzke et al. 1998). Similar to the other muscles analyzed here, the FPL is generally thought to play a major role in human-like object manipulation, and particularly in tool use (Hamrick et al. 1998; Kivell 2015; Susman 1988, 1994). However, it is usually either absent or not a distinct muscle in the non-human great apes (Diogo et al. 2012). Its insertion ridge on the first distal phalanx is therefore typically not discernible in these species and, as a result, could not be included here.

In addition to the recruitment patterns of these muscles, we analyze the overall 3D shape of the first metacarpal including the shape of its entheses (see Supplementary Online Material (SOM); the terms 'overall shape' or 'overall morphology' will be used throughout the paper to refer to the shape of the bone, its head and base, as well as of the respective muscle attachment sites) to assess whether differences in muscle recruitment are independent of gross external morphology of the bone. The latter is generally assumed to reflect genetic adaptation directly associated with biomechanical efficiency (including morphological characters across the bone diaphysis and articular surfaces; see, e.g., Galletta et al. 2019; Kivell 2015; Marchi et al. 2017; Marzke 2013).

Overall, we expect that habitual human-like tool users (later *Homo*, here comprising fossil and recent *Homo sapiens* and *Homo neanderthalensis*) will differ in their overall first metacarpal shape from the non-human great apes, reflecting genetic adaptation and possibly biomechanical efficiency related to tool use in the former (e.g., Karakostis et al. 2021b). At the same time, we predict muscle recruitment patterns showing proportionately larger DI1 entheses in species with human-like tool use (recent and fossil *Homo sapiens*, *Homo neanderthalensis*), and proportionally smaller DI1 attachments in the non-human great apes. Because

TABLE 1. DETAILS ON EARLY FOSSIL HOMININ SAMPLE
(references are provided for the dating of the fossil or the respective site).

ID	Species	Date	Location*	Reference
A.L. 333w(-39)	*Australopithecus afarensis*	~3.2 mya	Hadar, ET	Walter 1994
StW 418	*Australopithecus africanus*	1.95–2.95 mya	Sterkfontein, SA	Pickering et al. 2011
UW 88-119	*Australopithecus sediba*	1.78–1.95 mya	Malapa, SA	Pickering et al. 2011
SK 84	early *Homo* / *Paranthropus robustus*†	1.8–1.9 mya	Swartkrans, SA	Pickering et al. 2011
UW 101-1321	*Homo naledi*	241–335 kya	Rising Star Cave, SA	Robbins et al. 2021

*Abbreviations following ISO 3166 country codes.
†See Susman (1988) and Trinkaus and Long (1990).

of the reported importance of the DI1 across tool-related behaviors irrespective of tool type or industry (Key et al. 2020; Marzke et al. 1998), we consider it to reflect generalized tool-related tasks. If early hominins already practiced generalized human-like tool use habitually, we expect them to also exhibit proportionally larger DI1 attachments, irrespective of human- or ape-like overall bone shape. Finally, the muscles OP and APL are also essential for human precise thumb manipulatory activities (e.g., Clarkson 2000; Marzke 1997, 2013), with recent biomechanical research demonstrating the substantial contribution of OP to the adaptive evolution of increased thumb efficiency in hominins after approximately 2 Ma (Karakostis et al. 2021b). Since more developed tool-related thumb use is thought to have emerged among later hominins (e.g., Karakostis et al. 2021b; Marzke 1997; also see Shea 2016), we would not necessarily expect early hominins to exhibit a human-like pattern in the entheses of these two pollical muscles, even if they show evidence for habitual generalized tool-use as reflected by proportionally larger DI1 attachments.

MATERIALS AND METHODS

Our sample comprises *Australopithecus*, *Homo naledi*, and SK 84 (an unassigned specimen from Swartkrans, South Africa) (see Table 1), as well as fossil and recent *Homo sapiens*, *Homo neanderthalensis*, and the three great ape genera (*Pongo pygmaeus*: n=7, *Pongo abelii*: n=2, *Gorilla gorilla*: n=7, *Pan troglodytes*: n=9) (Tables 2, 3). Our analysis focuses on the first metacarpal, as preservation of complete hand skeletons is rare in the fossil record (Kivell et al. 2011; 2018). Additionally, the first metacarpal contains three muscle attachment sites (see Figure 1), among which the OP and the DI1 are thought to play an important role during human-like tool use (Key et al. 2020; Marzke et al. 1998). Details on muscle function and location of the attachment sites can be found in Table 4.

The muscles examined here (OP, APL, DI1) share important corresponding functions across humans and the great apes (Diogo et al. 2013; Lemelin and Diogo 2016; Vereecke and Wunderlich 2016). It has been reported that OP serves as a flexor both in humans and *Pan troglodytes*, whereas it functions as an adductor rather than an abductor of the thumb in the latter species (Karakostis et al. 2021b; Marzke et al. 1999). Although the dorsal *interossei* have been reported absent in *Pan troglodytes*, in fact they present a plesiomorphic state, where the *intermetacarpales* 1 to 4 are not fused with the *flexores brevis profundi* 3, 5, 6 and 8 to form the dorsal *interossei* (Diogo et al. 2012). However, since *intermetacarpalis* 1 attaches in the same exact bone areas as DI1 (Diogo et al. 2013), it is assumed here that it has a similar function (i.e., contraction of the muscle would naturally lead to abduction of the index finger) (Lemelin and Diogo 2016; van Leeuwen et al. 2018; Vereecke and Wunderlich 2016). Most critically for our study, the attachment site of the DI1 can be identified reliably across all taxa in the form of a bone modification at the basal medial aspect of the first metacarpal, predominantly in the form of a depression in the area of muscle attachment (see Figure 1), indicating the presence of biomechanical stress associated with muscle pull.

During data collection, the right anatomical side was generally prioritized. However, the left metacarpal was used if the right side was damaged. In our analyses, all bones associated with the same species consistently plotted together irrespective of anatomical side (see Figure 4 below), indicating that any bilateral differences were not considerable compared to interspecies variation.

ENTHESIS IDENTIFICATION AND DELINEATION

Previous work has shown that multivariate analyses of the proportions among different entheses can be used to reconstruct habitual activity and are not influenced by systemic factors such as body size or genetics (Castro et al. 2021; Karakostis et al. 2017; 2018; 2019a; 2019b; 2020; Karakostis and Lorenzo 2016). We applied this new, experimentally verified method (V.E.R.A.) to the analysis of the entheseal proportions of the first metacarpal muscles OP, DI1 and APL (see Table 4). The entheses were delineated on three-dimensional surface models of the bones using tools provided by Meshlab (CNR, Rome; version 2016.12 for Windows, Cignoni et al. 2008). The identification of the entheses and subsequent delineation followed the published V.E.R.A. protocols (Karakostis and Harvati 2021; Karakostis and Lorenzo 2016; Karakostis et al. 2020). Briefly, different filters in Meshlab (e.g., the 'Discrete Curvatures', 'Equalize Vertex Color' and 'Principal Directions of Curvature' filters) were applied to the 3D models of the bones to identify differences in elevation—including both projection and depression—coloration, and surface complexity in the area of muscle attachment. Based on these criteria, the entheseal surfaces were delineated and then separated from the surrounding bone. Afterwards, the 3D surface areas of the entheses were measured in square millimeters by the tools provided by Meshlab, to be used as variables in the V.E.R.A. analysis (Karakostis and Lorenzo 2016). Our measuring protocol allowed for minimal taphonomic damage of the entheses, which is common in fossil and archaeological specimens, so as to maximize the fossil hominin samples. Minimal damage on one enthesis was exhibited by La Chapelle-aux-Saints, La Ferrassie 1, Qafzeh 9, Villabruna, and Grevenmacher 93. These specimens nonetheless plotted close to other individuals of their respective taxa, suggesting that our analysis is robust towards slight taphonomic damage. This allowed us to confidently include early fossil hominin UW 88-119 (*A. sediba*) that presents slight damage on its DI1 muscle attachment site.

PRECISION TEST

The entheses of all australopiths, *H. naledi*, and one randomly selected individual each of Neanderthals and early modern humans (La Ferrassie 1, Ohalo 2) were delineated twice by the same observer (JK), leaving at least one month between the first and the second observation. Precision was calculated by taking the mean of the two measurements and dividing it by their standard deviation. The result was

TABLE 2. DETAILS ON LATER *HOMO* SAMPLE (references are provided for the dating of the fossil or the respective site).

ID	Species	Age	Sex	Date	Location*	Reference
Abrí Pataud 1	fossil *H. sapiens*	20–29	Female	26–28 kya	France	Villotte et al. 2015
Abrí Pataud 3	fossil *H. sapiens*	adult	Female	26–28 kya	France	Villotte et al. 2015
Arene Candide 2	fossil *H. sapiens*	~25	Male	11–12 kya	Italy	Sparacello et al. 2018
Ohalo 2	fossil *H. sapiens*	~35–40	Male	ca. 19 kya	Israel	Hershkovitz et al. 1995
Qafzeh 9	fossil *H. sapiens*	15–19	Female	90–100 kya	Israel	Valladas et al. 1988
Villabruna	fossil *H. sapiens*	~25	Male	ca. 14 kya	Italy	Vercellotti et al. 2008
Amud 1	*H. neanderthalensis*	~25	Male	53±8 kya	Israel	Rink et al. 2001
La Chapelle-aux-Saints	*H. neanderthalensis*	~60–70	Male	47–56 kya	France	Raynal 1990
Kebara 2	*H. neanderthalensis*	25–30	Male	60–64 kya	Israel	Schwarcz et al. 1989
La Ferrassie 1	*H. neanderthalensis*	Adult	Male	43–45 kya	France	Guérin et al. 2015
Shanidar 4	*H. neanderthalensis*	30–45	Male	60–100 kya	Iraq	Trinkaus 1983
B 137	modern *H. sapiens*	31	Male	19th century AD	Basel, CH	Hotz and Steinke 2012
B 211	modern *H. sapiens*	21	Male	19th century AD	Basel, CH	Hotz and Steinke 2012
B 264	modern *H. sapiens*	41	Male	19th century AD	Basel, CH	Hotz and Steinke 2012
GV 12	modern *H. sapiens*	30–40	Female	13th–14th/15th century AD	Grevenmacher, LU	Trautmann 2012
GV 29	modern *H. sapiens*	30–40	Female	13th–14th/15th century AD	Grevenmacher, LU	Trautmann 2012
GV 31	modern *H. sapiens*	20–25	Female	13th–14th/15th century AD	Grevenmacher, LU	Trautmann 2012
GV 46	modern *H. sapiens*	30–40	Male	13th–14th/15th century AD	Grevenmacher, LU	Trautmann 2012
GV 72	modern *H. sapiens*	20–30	Male	13th–14th/15th century AD	Grevenmacher, LU	Trautmann 2012
GV 93	modern *H. sapiens*	20-25	Female	13th–14th/15th century AD	Grevenmacher, LU	Trautmann 2012
GV 105	modern *H. sapiens*	30–40	Female	13th–14th/15th century AD	Grevenmacher, LU	Trautmann 2012
GV 112	modern *H. sapiens*	30–40	Male	13th–14th/15th century AD	Grevenmacher, LU	Trautmann 2012)
GV 117	modern *H. sapiens*	20–25	Male	13th–14th/15th century AD	Grevenmacher, LU	Trautmann 2012
GV 121	modern *H. sapiens*	20–25	Female	13th–14th/15th century AD	Grevenmacher, LU	Trautmann 2012
GV 132	modern *H. sapiens*	40–50	Male	13th–14th/15th century AD	Grevenmacher, LU	Trautmann 2012
GV 143	modern *H. sapiens*	30–40	Male	13th–14th/15th century AD	Grevenmacher, LU	Trautmann 2012

*Abbreviations following ISO 3166 country codes.

TABLE 3. DETAILS ON GREAT APE SAMPLE.

ID*	Species	Age†	Sex	Wild-caught / Captive	Provenance‡	Location
1784	*Gorilla gorilla*	Adult	Female	Wild-caught	Gabon	State Museum of Natural History Stuttgart, Germany
6294	*Gorilla gorilla*	Adult	Male	Wild-caught	Gabon	Natural History Museum Basel, Switzerland
7464	*Gorilla gorilla*	Subadult	Male	Wild-caught	Gabon	State Museum of Natural History Stuttgart, Germany
10429	*Gorilla gorilla*	Adult	Male	NN	NN	Natural History Museum Basel, Switzerland
38230	*Gorilla gorilla*	Adult	Female	Captive	Wilhelma Zoo Stuttgart, DE	State Museum of Natural History Stuttgart, Germany
167368	*Gorilla gorilla*	NN	NN	Wild-caught	Cameroon	American Museum of Natural History, NY, New York, USA§
176225	*Gorilla gorilla*	Adult	Male	Wild-caught	Gabon	National Museum of Natural History, Washington, DC, USA
1794	*Pan troglodytes*	Adult	Male	Wild-caught	Gabon	State Museum of Natural History Stuttgart, Germany
2738	*Pan troglodytes*	Adult	NN	Wild-caught	Southern Cameroon	State Museum of Natural History Stuttgart, Germany
7597	*Pan troglodytes*	Adult	NN	NN	NN	Natural History Museum Basel, Switzerland
8869	*Pan troglodytes*	Adult	Male	Captive	Zoological garden Basel, CH	Natural History Museum Basel, Switzerland
10449	*Pan troglodytes*	Adult	Male	Wild-caught	Ivory Coast	Natural History Museum Basel, Switzerland
10824	*Pan troglodytes*	Adult	Female	Captive	Zoological garden Basel, CH	Natural History Museum Basel, Switzerland
51376	*Pan troglodytes*	NN	Female	Wild-caught	DR Congo	American Museum of Natural History, NY, New York, USA§
176229	*Pan troglodytes*	NN	Female	Wild-caught	Cameroon	National Museum of Natural History, Washington, DC, USA§
2488	*Pan troglodytes*	NN	NN	NN	NN	Duke University, Evolutionary Anthropology Department, Durham, NC, USA§
1687	*Pongo pygmaeus*	Adult	Male	Wild-caught	Borneo	State Museum of Natural History Stuttgart, Germany
2190	*Pongo pygmaeus*	Adult	Female	Wild-caught	Borneo, MY	State Museum of Natural History Stuttgart, Germany
6286	*Pongo abelii*	NN	Male	Wild-caught	Sumatra	Natural History Museum Basel, Switzerland
7457	*Pongo pygmaeus*	Adult	Male	Wild-caught	Northern Borneo	State Museum of Natural History Stuttgart, Germany
10002	*Pongo abelii*	NN	Female	Wild-caught	Northern Sumatra	Natural History Museum Basel, Switzerland

TABLE 3. DETAILS ON GREAT APE SAMPLE (continued).

ID*	Species	Age†	Sex	Wild-caught / Captive	Provenance‡	Location
10965	*Pongo pygmaeus*	NN	Female	Captive	Zoological garden Basel, CH	Natural History Museum Basel, Switzerland
142169	*Pongo pygmaeus*	Young adult	Female	Wild-caught	Borneo, ID	National Museum of Natural History, Washington, DC, USA
145302	*Pongo pygmaeus*	Adult	Female	Wild-caught	Borneo, ID	National Museum of Natural History, Washington, DC, USA
200900	*Pongo pygmaeus*	NN	Female	Wild-caught	Borneo, ID	American Museum of Natural History, NY, New York, USA§

*Museum inventory numbers.

†The bones of all individuals were fused, including specimens with unknown exact age, indicating adult or near-adult status.

‡Abbreviations following ISO 3166 country codes.

§Specimens were downloaded from MorphoSource.

then multiplied by a hundred. The resulting number depicts the percentage of error for each enthesis. Precision was generally high among all entheses and individuals, as error rates were consistently below 5% (ranging from 0.7% to 4.61%), in broad agreement with the error tests previously reported for V.E.R.A. in its first publication (Karakostis and Lorenzo, 2016).

STATISTICAL ANALYSES

Principal Components Analysis

The surface area measurement of each enthesis was size-adjusted by dividing it by the geometric mean (e.g., Elewa 2010; Lycett et al. 2006), calculated using all three entheseal measurements of each individual. This standardization process, which constitutes part of the V.E.R.A. protocols (e.g., Karakostis et al. 2017), is shown to adequately control for the effects of bone dimensions and body size on the multivariate proportions among muscle attachment sites (Karakostis et al. 2017; 2019a; 2021a; Karakostis and Harvati 2021). The resulting values represent the proportions of the entheses among each other for each individual (SOM Table 1). These values are irrespective of total bone size (whose variability might be affected by other potential systemic factors not associated with overall entheseal size variation), as they represent the proportion of each enthesis compared to the individual's geometric mean of the entheseal surfaces on the first metacarpal. They signify whether the measurement of the enthesis is larger (value >1) or smaller (value <1) than the geometric mean of all three entheses. These size-adjusted entheseal measurements were analyzed in a Principal Components Analysis (PCA) based on a correlation matrix using PAST 3.25 (Hammer et al. 2001). This analysis does not assume *a priori* assignment of specimens to groups and is used to find the main axis of variance among the individuals. The absence of outliers was confirmed using the z-score approach (Field 2017). Relevant principal components (PCs) were selected for plotting following the scree-plot approach (Field 2017). Since the early fossil hominins were not included in the original PCA, their PC scores were calculated in R (RStudio Inc., Boston; R version 3.6.2 for Windows, R Core Team 2021)

TABLE 4. CHARACTERISTICS OF MUSCLES AND ATTACHMENT SITES (bold) USED IN THIS ANALYSIS*.

Muscle	Origin	Insertion	Muscle function
Opponens pollicis	Trapezium bone	**Radial diaphysis of MC1**	Abducts, rotates, and flexes the thumb
Abductor pollicis longus	Radius, ulna, scaphoid, trapezium, transverse carpal ligament	**Base of MC1**	Abducts the thumb at the carpometacarpal joint, abducts the wrist radially
First dorsal *interosseous*	**Diaphyses of MC1** and MC2	Base of PP2	Abducts the 2nd digit

*After Netter et al. (2019).

TABLE 5. EIGENVALUES AND FACTOR LOADINGS OF PC1–3 OF THE ANALYSIS OF ENTHESEAL PROPORTIONS.

Principal component	Eigenvalue	% of variance	Factor loadings		
			OP	APL	DI1
PC1	1.86	62.06%	0.71	0.62	-0.99
PC2	1.1	36.52%	-0.7	0.78	-0.01
PC3	0.04	1.42%	0.11	0.1	0.14

using the 'predict' function and then projected onto the PC plot. PC loadings are reported in Table 5.

Discriminant Function Analysis

We conducted a discriminant function analysis (DFA) using the IBM SPSS software package v.25 (IBM Corp. 2017) to assess whether differences in entheseal proportions serve to reliably differentiate between tool-users and non-tool-users. The sample was divided into two groups: The first encompassed the tool-users *Homo neanderthalensis* and *Homo sapiens*, designated as 'Later *Homo*', and the second included all great apes. Additionally, the fossil hominins were entered with unknown group membership to predict their classification with 'Later Homo' or great apes. The assumptions of the DFA were met (Field 2017). Since the Box's M test was non-significant, indicating homogeneity of covariance matrices (Field 2017), the within-groups covariance matrix was used for developing the discriminant functions. The variables were entered stepwise and the robustness of the classification was validated through Leave-one-out classification (SOM Tables 2 and 3). The analysis was performed using the size-adjusted measurements of all three entheses as variables. However, the stepwise procedure only retained the adjusted DI1 measurement in the analysis, as an analysis based only on this variable provides the best separation of the two groups. It should be highlighted that this variable represents the DI1 entheseal surface areas adjusted using the geometric mean, which is a measure of the DI1's proportion compared to the other entheses in each individual (i.e., their geometric mean; e.g., Elewa 2010; Lycett et al. 2006). Details on DFA statistics, including percentages of correct original and cross-validated group classification, are reported in the Supplementary Online Material (see SOM Tables 2 and 3).

OVERALL 1ST METACARPAL 3D SHAPE ANALYSIS

The analysis of overall bone shape was conducted using geometric morphometrics. A brief description of the procedure will be provided here, while details on the statistical analysis and the precision test can be found in the Supplementary Online Material.

In cases where the right first metacarpal was not sufficiently preserved, the left side was mirrored for the geometric morphometric shape analysis. Due to preservation issues, the Amud 1 Neanderthal and one *Pan* specimen had to be removed for this analysis.

The .ply files of the metacarpal surface models and of the entheses were imported into RStudio. The landmarks for the muscle attachment sites were not placed on the 3D models of the metacarpal, but on the separately imported models of the entheses, to minimize potential sources of error. Consequently, centering the models prior to digitization had to be disabled, so that the 3D model of the overall bone and the models of the corresponding entheses were still in the same coordinate system. As a result, the landmarks could later be combined for the analysis, despite being placed on separate models. Before landmarks were digitized, the entheses were placed in their correct anatomical position. For this, Meshlab was opened in a second window. Here, the 3D models of the entheses were placed on top of the models of their corresponding bone. Using this as a reference, the orientation of the entheses could be adjusted to properly match their position on the bone. For the landmark digitization in RStudio, the package geomorph (Adams and Otárola-Castillo 2013) was used to place fixed landmarks on the bone and entheseal surfaces, registered in geometrically corresponding positions. Six landmarks were placed on each enthesis, 9 landmarks were used to capture the shape of the bone, 3 landmarks were placed on the proximal, and 7 on the distal articular surface. Detailed landmark descriptions and illustrations are reported in SOM Table 4 and Figure 2.

RESULTS

Results of the overall shape analysis are reported in the Supplementary Online Material (SOM text). As expected, recent and fossil *H. sapiens* and *H. neanderthalensis* are well-differentiated from non-human great apes on PC1 of the PCA, showing minimal overlap with *Pan* and no overlap with *Gorilla* or *Pongo* (Figure 3, SOM Figure 1). All australopiths in our sample plot with the non-human great apes and away from later *Homo*. In contrast, *H. naledi* and SK 84 fall with later *Homo*.

The results of the muscle recruitment pattern analysis (Methods; see Table 5 and SOM Table 1) are depicted in Figure 4. The variation on PC1 (62.02% of variance) indicates differences in the proportionate size of the DI1 enthesis (loading negatively; see Table 5). In close agreement with our predictions, this axis clearly separates great apes

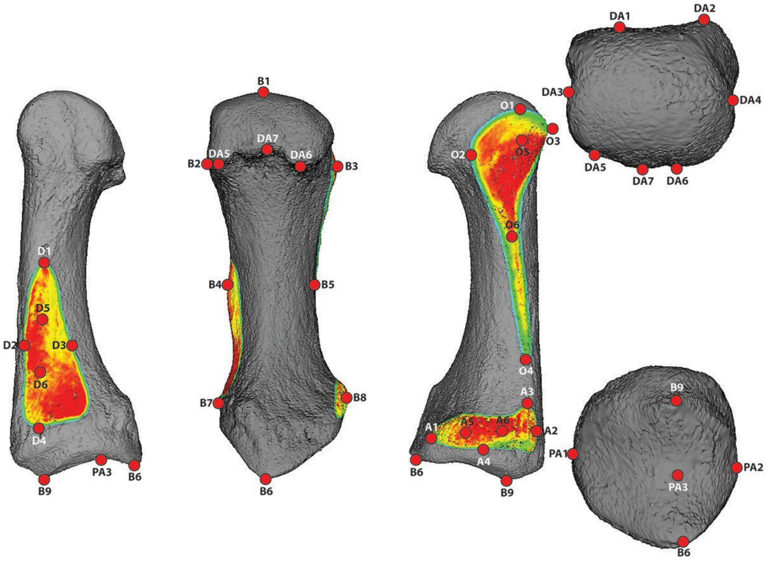

Figure 2. Location of the fixed landmarks depicted on the first metacarpal of a recent H. sapiens *from Basel (B 264). Landmark descriptions are reported in SOM Table 4.*

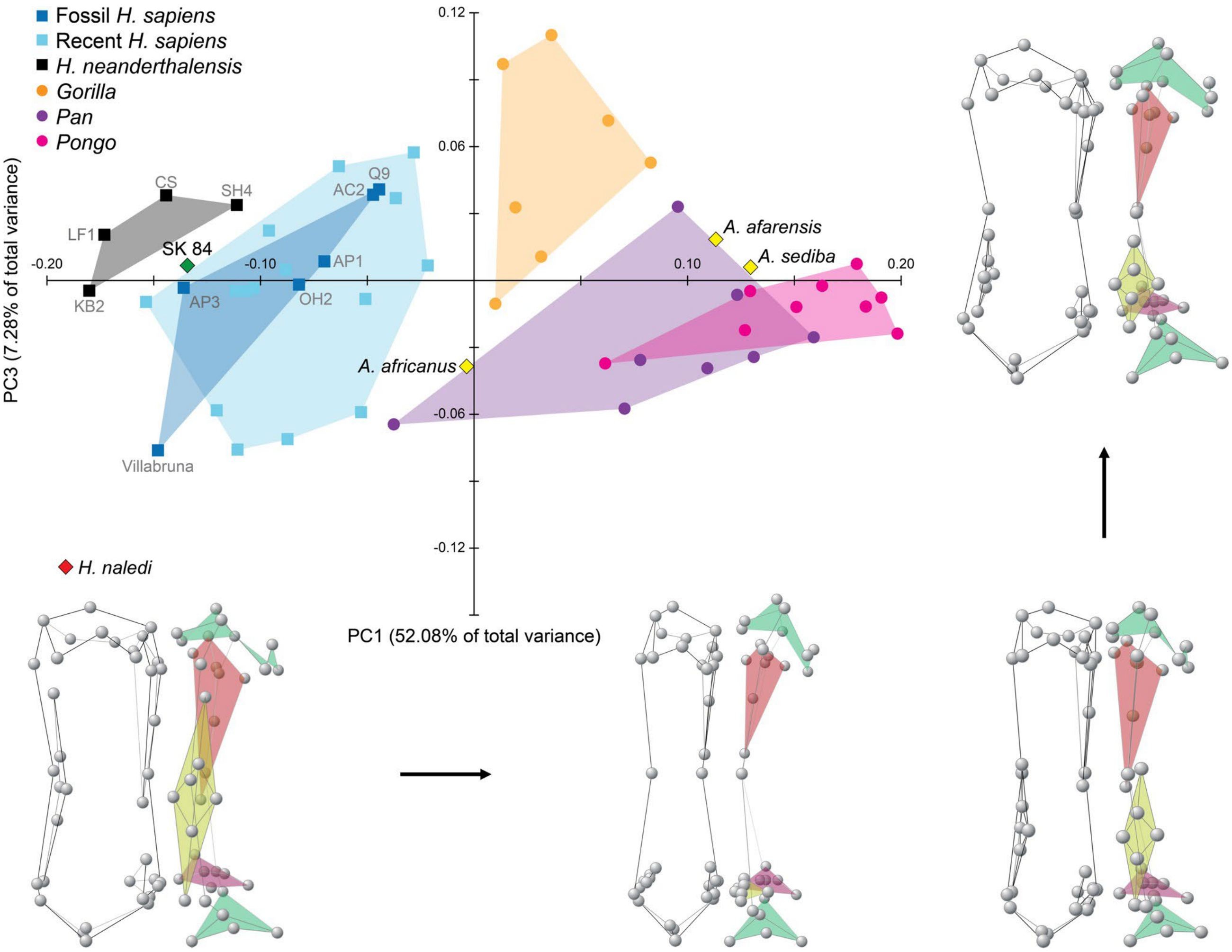

Figure 3. PCA of Procrustes-superimposed landmarks of the first metacarpal without a priori *group association, PC1 compared to PC3. Shape changes along PC1 and PC3 are illustrated below and to the right of the plot, respectively. OP: red; DI1: yellow; APL: purple; articular surfaces: green. Abbreviations: OH: Ohalo; AP: Abrí Pataud; AC: Arene Candide; Q: Qafzeh; KB: Kebara; CS: Chapelle-aux-Saints; LF: La Ferrassie; SH: Shanidar.*

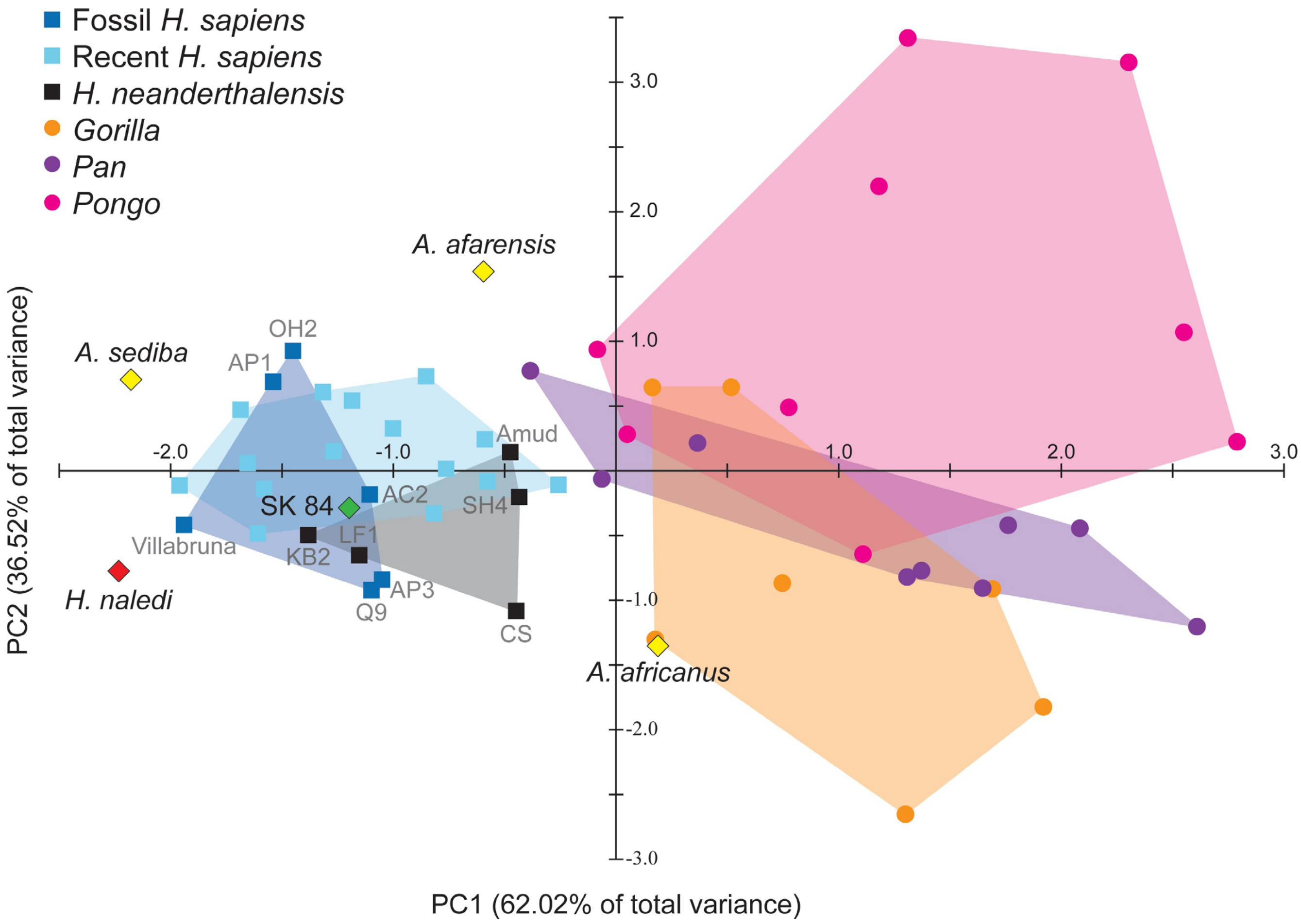

Figure 4. PCA on size-adjusted entheseal measurements without a priori *group association, PC1 compared to PC2. Abbreviations: OH: Ohalo; AP: Abrí Pataud; AC: Arene Candide; Q: Qafzeh; KB: Kebara; CS: Chapelle-aux-Saints; LF: La Ferrassie; SH: Shanidar.*

(more positive scores, indicating proportionally smaller DI1 attachments) from later *Homo* (more negative scores, reflecting proportionally larger DI1 entheses), with minimal overlap with *Pan* (one specimen) and no overlap with *Gorilla* or *Pongo*. All earlier fossil hominins except *A. africanus* show negative PC1 scores and plot close to later *Homo* when projected into the PC plot, indicating human-like DI1 proportions. *H. naledi* plots towards the negative extreme of PC1, indicating an unusually proportionally large DI1 enthesis. The only individual with similarly large DI1 proportions is *A. sediba*, plotting between early *H. sapiens* and *H. naledi*. *A. africanus* is the only hominin that clusters with the great apes, falling within the PC1 ranges of all great ape genera, indicating a proportionally smaller DI1 attachment for this taxon.

PC2 (36.52% of variance), on the other hand, differentiates specimens with a proportionally larger OP enthesis (loading negatively; see Table 5) from those with a proportionally larger APL attachment site (loading positively; see Table 5). On this axis, later *Homo* cluster tightly around 0, with scores mainly between -1 and 1, indicating a relative balance in the proportions of their OP and APL attachments, in line with the importance of both these muscles for precise thumb movements fundamental to specialized tool use. The great apes, on the other hand, show great variation and widely contrasting patterns in the relative proportions of these two entheses. While *Pan* is similar to *Homo* in its PC2 scores (clustering mainly between -1 and 1), *Pongo* plots on the positive side of PC2 with proportionally larger APL and smaller OP entheses compared to all other samples; and *Gorilla* on the negative side, showing the inverse pattern. Among earlier hominins projected into the plot, *H. naledi*, SK 84, and *A. sediba* overlap with later *Homo*, also clustering tightly around 0 in their PC2 scores. In contrast, *A. afarensis* shows a more positive PC2 value than all other hominins, similar only to *Pongo*, and *A. africanus* a more negative score, overlapping with *Gorilla*.

The discriminant function analysis (DFA) classified later *Homo* vs. the great ape genera with an accuracy of 100% and 96% respectively (see SOM Tables 2 and 3). Early hominins were treated as unknown. *A. africanus* was the only hominin classified with the great apes (posterior probability 70%, Table 6). All other hominins, including *A. afarensis*, *A. sediba*, *H. naledi*, and SK 84 were classified with later *Homo*.

TABLE 6. PREDICTED GROUP/POSTERIOR PROBABILITY VALUES OF THE DISCRIMINANT FUNCTION ANALYSIS*.

	Entheseal proportions
A. afarensis	Later *Homo* / 0.95
A. africanus	great apes / 0.70
A. sediba	Later *Homo* / 1
H. naledi	Later *Homo* / 1
SK 84	Later *Homo* / 0.99

*Later *Homo* comprises *H. sapiens* and *H. neanderthalensis.*

DISCUSSION

As expected, later *Homo* differs from the non-human great apes in the overall shape of the first metacarpal. Consistent with findings from previous studies of this bone (e.g., Karakostis et al. 2021b; Kivell et al. 2018; Marzke 2013; Susman 1988), all australopiths exhibited multiple ape-like features suggesting low biomechanical efficiency, while *H. naledi* and SK 84 were more similar to later *Homo* (see Figure 3, SOM Figure 1).

In terms of the recruitment pattern of the DI1, we predicted that the relative proportions of this muscle's enthesis would differentiate between later *Homo* and the other great apes, in part due to its importance for generalized human-like tool-related behaviors. The critical role of the DI1 was recently highlighted by experimental electromyographic work (Key et al. 2020), which reported high levels of activation of this muscle during the use of all stone tool types. On this basis, we consider that a contraction of the DI1, strongly pressing tools between the abducted index finger and the thumb's distal pad, without necessarily fully opposing or abducting the thumb (and therefore without involving systematic co-recruitment of OP and APL, respectively), as a shared component in human tool-use, which can be used to assess the origins of this behavior in the fossil record. Consistent with our prediction, we found a strong differentiation between later *Homo* and the non-human great apes, with proportionally larger DI1 muscle attachments in the former. Furthermore, all fossil hominins investigated except *A. africanus* showed DI1 proportions similar to those of later *Homo*, indicating that these taxa likely exhibited habitual tool-related behavior (see Figure 4, see Table 6).

Among australopiths, *A. sediba* and the earlier *A. afarensis* present human-like DI1 relative proportions consistent with habitual tool-use, despite both showing a clearly ape-like overall shape of the first metacarpal. *A. afarensis* has been proposed as one of the most likely potential makers of the Lomekwian due to its spatiotemporal range (Harmand et al. 2015). Although our study cannot confirm an association between this taxon and Lomekwian lithics, our results are consistent with this hypothesis. Our findings also support tool-related behaviors in *A. sediba*, previously proposed on the basis of its trabecular bone structure and its unusually long thumb (Dunmore et al. 2020; Kivell et al. 2011; 2018). While tools have not been recovered in association with this species, they have been found at nearby contemporaneous sites (Backwell and d'Errico 2001; d'Errico and Backwell 2003; Kuman and Clarke 2000; Susman 1988). Previous analyses have found that both these australopith taxa are characterized by low thumb opposition efficiency (Karakostis et al. 2021b)—as also indicated by their overall bone morphology (see Figure 3, SOM Figure 1). Therefore, while these individuals recruited the DI1 more frequently than non-human great apes, this should not be taken to suggest a human-like level of thumb dexterity. On the contrary, our findings indicate that these early hominins were likely habitual tool users *even though* their hand anatomy lacked several key adaptations for efficient tool manipulation seen in later *Homo* (e.g., see Karakostis et al. 2021b; Kivell et al. 2018). Unlike all other hominins included here, *A. africanus* was similar to the great apes in both overall first metacarpal shape and its entheseal patterns. Its proportionally small DI1 attachment indicates a less frequent use of this muscle. *A. africanus* was also the only hominin classified with the non-human great apes in our discriminant analysis (see Table 6). Our results therefore do not support habitual human-like tool use in *A. africanus*, *contra* previous interpretations of trabecular bone distribution in this specimen (Almécija et al. 2015; Skinner et al. 2015a, 2015b).

The Swartkrans specimen SK 84 was similar to later *Homo* in both overall shape and muscle recruitment patterns. Its entheseal proportions indicate frequent recruitment of the DI1, consistent with habitual tool use. This specimen is dated to ca. 2.0–1.8 Ma and is attributed to either early *Homo* or *Paranthropus* (Susman 1988; Trinkaus and Long 1990). It was found in association with bone tools (Backwell and d'Errico 2001; d'Errico and Backwell 2003), and its morphology and thumb opposition efficiency, as well as overall first metacarpal shape, point to increased manual dexterity relative to earlier hominins (Karakostis et al. 2021b; Skinner et al. 2015b; Susman 1988; Tocheri et al. 2008; Trinkaus and Long 1990). *H. naledi* was characterized by the proportionally highest observed activation levels of DI1. While this taxon has not been found in association with lithic artifacts (Kivell et al. 2015), its human-like overall first metacarpal shape (see Figure 3, SOM Figure 1), and the derived morphology of its thumb and wrist (Kivell et al. 2015) also support considerable thumb opposition and tool-using efficiency (Galletta et al. 2019; Karakostis et al. 2021b).

Finally, later *Homo* consistently presented similar relative proportions between the entheses of the other two muscles investigated here, OP and APL (reflected in the PC2 axis; see Figure 4). We interpret these findings as suggesting a similarly frequent recruitment of the OP and APL, possibly due to the important role of both muscles in precision grips. Such a relatively balanced relationship between the OP and APL entheses was also found in most hominins investigated, with the exception of the earlier *Australopithecus* specimens—*A. afarensis* was similar to *Pongo* in its relatively greater proportion of the APL, while *A. africanus* clustered with *Gorilla* in showing a relatively greater proportion of the OP. While our results do not support habitual tool use for *A. africanus*, the comparatively lower biomechanical efficiency of the muscle OP in *A. afarensis* (Karakostis et al. 2021b) makes it likely that this muscle's contribution was less important than that of DI1—whose function is proposed to be essential for all types of human-like tool use (Key et al. 2020)—for any tool-related activities of this taxon. Therefore, the combination of human-like DI1 proportions with ape-like OP / APL proportions in *A. afarensis* suggests simple tool use, without more specialized, precision-based behaviors observed in later species. In the case of *A. sediba*, both entheseal patterns (i.e., relative DI1 size and OP / APL proportions) are strikingly human-like (see Figure 4), despite the overall ape-like shape of its first metacarpal (see Figure 3, SOM Figure 1) and its relatively low biomechanical efficiency for thumb opposition (Karakostis et al. 2021b). Compared to the earlier *A. afarensis*, this finding is consistent with a more human-like and specialized pattern of tool using behavior in this taxon, preceding the evolution of heightened manual biomechanical efficiency observed in later *Homo* (see Kivell et al. 2011; Kivell et al. 2018). In contrast to *Homo* and most hominins, the great ape taxa were characterized by widely diverging patterns in their relative OP / APL proportions. At present it is unclear whether these proportional differences can be attributed to different locomotor or manipulative behaviors in these taxa, and this should be investigated further in the future.

Our proposed interpretation that some of the observed entheseal patterns in our study likely reflect habitual tool use largely relies on previous EMG experiments (e.g., Key et al. 2020; Marzke et al. 1998), which highlighted the importance of the DI1 muscle for stone tool-related activities in humans. Nonetheless, an alternative interpretation of our results would be that these entheseal proportions in early hominins may reflect the habitual performance of more generalized human-like hand use, for diverse types of object manipulation (which may or may not include stone tool-use in particular). This possibility cannot be dismissed, especially considering that these early hominin fossils were not found in association with stone tools. The hypothesis of tool use in these early taxa can be further tested by investigating additional attachment sites and other aspects of bone morphology. For example, while the thumb plays an important role in human-like tool use, recent studies have shown the relevance of the second and fifth digit for this behavior, which should be further assessed (Key et al. 2019; Williams-Hatala et al. 2020). Furthermore, here we only investigated the thumb metacarpal, excluding muscles that attach to the phalanges of this ray, such as the FPL. Like the DI1, the FPL is frequently activated during human-like tool use (Key et al. 2020), rendering the investigation of the interaction between these two muscles an intriguing objective. Future studies should therefore expand the analysis to additional bones of the thumb as well as to the remaining hand elements, to further assess how the pattern revealed in this study may interact with the entheseal proportions of other muscles that closely coordinate for human-like tool use.

CONCLUSION

Our analysis of thumb muscle attachment patterns supports an early emergence of habitual simple tool use, long before the evolution of early *Homo*, consistent with recent archaeological hypotheses. However, not all early hominins showed this pattern, underscoring the mosaic nature of the emergence of these behaviors, perhaps in a manner similar to cultural differences observed today between different chimpanzee societies (Whiten et al. 1999). Furthermore, the combination of ape-like manual dexterity (Karakostis et al. 2021b) with the human-like muscle use observed here in australopiths suggests that habitual tool use was established before the evolution of biomechanical adaptations of the human thumb, likely acting as selective pressure spurring their development, and highlighting the role of manual behavior as a leading factor in human bio-cultural evolution (Karakostis et al. 2021b). Future investigation of the hand musculature in these taxa will help further illuminate their behavior.

ACKNOWLEDGEMENTS

Aspects of this research were supported by the European Research Council (ERC CoG no. 724703) and the German Research Foundation (DFG FOR 2237). We are grateful to the following institutions and researchers for granting us access to fossil specimens and/or data: ARCHH (Ethiopia) and the Max Planck Society in Germany (W.H. Kimbel, Z. Alemseged, and F. Spoor), Evolutionary Studies Institute of the University of the Witwatersrand (B. Zipfel, S. Jirah, and T. Kivell), Ditsong National Museum of Natural History, South Africa (T. Kivell and M. Tawane), National Museum of Natural History in Paris (D. Grimaud-Hervé, F. Detroit, and M. Friess), and the Italian Ministry of Cultural Heritage and Activities (as well as the Museo Archeologico Del Finale and V. Sparacello). The 3D models of hand bone fossils from Israel are courtesy of the Dan David Center of Human Evolution and Biohistory Research, Shmunis Family Anthropological Institute, and Sackler Faculty of

Medicine, Tel Aviv University (H. May and I. Hershkovitz). We are grateful to Armando Falcucci, who produced the 3D models for the Villabruna metacarpal. For access to the 3D models of *Homo naledi*'s hand bones, we would like to thank the Evolutionary Studies Institute (Johannesburg, Gauteng, South Africa) for making the 3D models available online at Morphosource.org. We are grateful to the Smithsonian's Division of Mammals (K. Helgen), and Human Origins Program (M. Tocheri), as well as the American Museum of Natural History, for making the 3D models of great ape hand remains available online at Morphosource.org (Duke University). Finally, many thanks are due to Loïc Costeur for providing us with access to and information on great ape hand remains from the Mammalian Collection of the Museum of Natural History in Basel.

REFERENCES

Adams, D.C., Otárola-Castillo, E., 2013. Geomorph: an R package for the collection and analysis of geometric morphometric shape data. *Methods in Ecology and Evolution* 4(4), 393–399.

Alba, D.M., Moyà-Solà, S., Köhler, M., 2003. Morphological affinities of the *Australopithecus afarensis* hand on the basis of manual proportions and relative thumb length. *J. Hum. Evol.* 44(2), 225–254.

Almécija, S., Wallace, I.J., Judex, S., Alba, D.M., Moyà-Solà, S., 2015. Human evolution. Comment on "Human-like hand use in *Australopithecus africanus*". *Science* 348(6239), 1101.

Archer, W., Aldeias, V., McPherron, S.P., 2020. What is 'in situ'? A reply to Harmand et al. (2015). *J. Hum. Evol.* 142, 102740.

Backwell, L.R., d'Errico, F., 2001. Evidence of termite foraging by Swartkrans early hominids. *PNAS* 98 (4), 1358–1363.

Barak, M.M., Lieberman, D.E., Hublin, J.-J., 2011. A Wolff in sheep's clothing: trabecular bone adaptation in response to changes in joint loading orientation. *Bone* 49(6), 1141–1151.

Benjamin, M., Kumai, T., Milz, S., Boszczyk, B., Boszczyk, A., Ralphs, J., 2002. The skeletal attachment of tendons—tendon 'entheses'. *Comp. Biochem. Physiol., Part A: Mol. Integr. Physiol.* 133(4), 931–945.

Biewener, A.A., Fazzalari, N.L., Konieczynski, D.D., Baudinette, R.V., 1996. Adaptive changes in trabecular architecture in relation to functional strain patterns and disuse. *Bone* 19(1), 1–8.

Carlson, K.J., Lublinsky, S., Judex, S., 2008. Do different locomotor modes during growth modulate trabecular architecture in the murine hind limb? *'Integr. Comp. Biol.* 48(3), 385–393.

Cashmore, L.A., Zakrzewski, S.R., 2013. Assessment of musculoskeletal stress marker development in the hand. *Int. J. Osteoarchaeol.* 23(3), 334–347.

Castro, A.A., Karakostis, F.A., Copes, L.E., McClendon, H.E., Trivedi, A.P., Schwartz, N.E., Garland, T., 2021. Effects of selective breeding for voluntary exercise, chronic exercise, and their interaction on muscle attachment site morphology in house mice. *J. Anat.* 240(2), 279–295.

Cignoni, P., Callieri, M., Corsini, M., Dellepiane, M., Ganovelli, F., Ranzuglia, G., 2008. MeshLab: an ppen-source mesh processing tool, In: *Sixth Eurographics Italian Chapter Conference*. Eurographics Italian Chapter Conference, Salerno, Italy. July 2nd - 4th, 2008. The Eurographics Association, Aire-la-Ville, pp. 129–136.

Clarkson, H.M., 2000. *Musculoskeletal Assessment: Joint Range of Motion and Manual Muscle Strength*, 2nd ed. Lippincott Williams & Wilkins, Baltimore, Philadelphia.

Currey, J.D., 2002. *Bones: Structure and Mechanics*. Princeton University Press, Princeton, NJ, Oxfordshire.

d'Errico, F., Backwell, L.R., 2003. Possible evidence of bone tool shaping by Swartkrans early hominids. *J. Archaeol. Sci.* 30(12), 1559–1576.

Diogo, R., Potau, J.M., Pastor, J.F., Paz, F.J. de, Ferrero, E.M., Bello, G., Barbosa, M., Aziz, M.A., Burrows, A.M., Arias-Martorell, J., Wood, B.A., 2013. *Photographic and Descriptive Musculoskeletal Atlas of Chimpanzees: With Notes on the Attachments, Variations, Innervation, Function and Synonomy and Weight of the Muscles*. CRC Press, Boca Raton.

Diogo, R., Richmond, B.G., Wood, B.A., 2012. Evolution and homologies of primate and modern human hand and forearm muscles, with notes on thumb movements and tool use. *J. Hum. Evol.* 63(1), 64–78.

Domínguez-Rodrigo, M., Alcalá, L., 2016. 3.3-million-year-old stone tools and butchery traces? More evidence needed. *PaleoAnthropol.* 2016, 46–53.

Domínguez-Rodrigo, M., Pickering, T.R., Bunn, H.T., 2012. Experimental study of cut marks made with rocks unmodified by human flaking and its bearing on claims of ~3.4-million-year-old butchery evidence from Dikika, Ethiopia. *J. Archaeol. Sci.*39(2), 205–214.

Dunmore, C.J., Skinner, M.M., Bardo, A., Berger, L.R., Hublin, J.-J., Pahr, D.H., Rosas, A., Stephens, N.B., Kivell, T.L., 2020. The position of *Australopithecus sediba* within fossil hominin hand use diversity. *Nat. Ecol. Evol.* 4 (7), 911–918.

Elewa, A.M.T., 2010. *Morphometrics for Nonmorphometricians*. Lecture Notes in Earth Sciences 124. Springer, Berlin, London.

Feix, T., Kivell, T.L., Pouydebat, E., Dollar, A.M., 2015. Estimating thumb-index finger precision grip and manipulation potential in extant and fossil primates. *J. R. Soc. Interface* 12(106), 20150176.

Field, A., 2017. *Discovering Statistics Using IBM SPSS Statistics*, 5th ed. Sage Publications, Thousand Oaks CA.

Foster, A., Buckley, H., Tayles, N., 2014. Using enthesis robusticity to infer activity in the past: a review. *J. Archaeol. Method. Theory* 21(3), 511–533.

Galletta, L., Stephens, N.B., Bardo, A., Kivell, T.L., Marchi, D., 2019. Three-dimensional geometric morphometric analysis of the first metacarpal distal articular surface in humans, great apes and fossil hominins. *J. Hum. Evol.* 132, 119–136.

Green, D.J., Gordon, A.D., 2008. Metacarpal proportions in *Australopithecus africanus*. *J. Hum. Evol.* 54(5), 705–719.

Guérin, G., Frouin, M., Talamo, S., Aldeias, V., Bruxelles, L., Chiotti, L., Dibble, H.L., Goldberg, P., Hublin, J.-J., Jain, M., Lahaye, C., Madelaine, S., Maureille, B., McPherron, S.J., Mercier, N., Murray, A.S., Sandgathe, D., Steele, T.E., Thomsen, K.J., Turq, A., 2015. A multi-method luminescence dating of the Palaeolithic sequence of La Ferrassie based on new excavations adjacent to the La Ferrassie 1 and 2 skeletons. *J. Archaeol. Sci.* 58, 147–166.

Hammer, Ø., Harper, D.A.T., Ryan, P.D., 2001. PAST: Paleontological Statistics Software Package for Education and Data Analysis. *Paleontologia Electronica* 4(1), article 4.

Hamrick, M.W., Churchill, S.E., Schmitt, D., Hylander, W.L., 1998. EMG of the human flexor pollicis longus muscle: implications for the evolution of hominid tool use. *J. Hum. Evol.* 34(2), 123–136.

Harmand, S., Lewis, J.E., Feibel, C.S., Lepre, C.J., Prat, S., Lenoble, A., Boës, X., Quinn, R.L., Brenet, M., Arroyo, A., Taylor, N., Clément, S., Daver, G., Brugal, J.-P., Leakey, L., Mortlock, R.A., Wright, J.D., Lokorodi, S., Kirwa, C., Kent, D.V., Roche, H., 2015. 3.3-million-year-old stone tools from Lomekwi 3, West Turkana, Kenya. *Nature* 521(7552), 310–315.

Haslam, M., Hernandez-Aguilar, A., Ling, V., Carvalho, S., La Torre, I. de, DeStefano, A., Du, A., Hardy, B., Harris, J., Marchant, L., Matsuzawa, T., McGrew, W., Mercader, J., Mora, R., Petraglia, M., Roche, H., Visalberghi, E., Warren, R., 2009. Primate archaeology. *Nature* 460(7253), 339–344.

Hershkovitz, I., Speirs, M.S., Frayer, D.W., Nadel, D., Wish-Baratz, S., Arensburg, B., 1995. Ohalo II H2: a 19,000-year-old skeleton from a water-logged site at the Sea of Galilee, Israel. *Am. J. Phys. Anthropol.* 96(3), 215–234.

Hotz, G., Steinke, H., 2012. Knochen, Skelette, Krankengeschichten. Spitalfriedhof und Spitalarchiv – zwei sich ergänzenden Quellen. *Basler Zeitschrift für Geschichte und Altertumskunde* 112, 105–138.

IBM Corp., 2017. *IBM SPSS Statistics for Windows*. IBM Corp., Armonk, NY.

Jacofsky, M.C., 2009. *Comparative Muscle Moment Arms of the Primate Thumb:* Homo, Pan, Pongo, *and* Papio. Ph.D. Dissertation, Arizona State University.

Judex, S., Carlson, K.J., 2009. Is bone's response to mechanical signals dominated by gravitational loading? *Med. Sci. Sports Exerc.* 41(11), 2037–2043.

Karakostis, F.A., Buikstra, J.E., Prevedorou, E., Hannigan, E.M., Hotaling, J., Hotz, G., Liedl, H., Moraitis, K., Siek, T.J., Waltenberger, L., Widrick, K.J., Harvati, K., 2021a. New insights into the manual activities of individuals from the Phaleron cemetery (Archaic Athens, Greece). *J. Archaeol. Sci.* 131, 105415.

Karakostis, F.A., Haeufle, D., Anastopoulou, I., Moraitis, K., Hotz, G., Tourloukis, V., Harvati, K., 2021b. Biomechanics of the human thumb and the evolution of dexterity. *Cur. Biol.* 31(6), 1317–1325.e8.

Karakostis, F.A., Harvati, K., 2021. New horizons in reconstructing past human behavior: introducing the "Tübingen University Validated Entheses-based Reconstruction of Activity" method. *Evol. Anthropol.* 30(3), 185-198.

Karakostis, F.A., Hotz, G., Scherf, H., Wahl, J., Harvati, K., 2017. Occupational manual activity is reflected on the patterns among hand entheses. *Am. J. Phys. Anthropol.* 164(1), 30–40.

Karakostis, F.A., Hotz, G., Tourloukis, V., Harvati, K., 2018. Evidence for precision grasping in Neandertal daily activities. *Sci. Adv.* 4(9), eaat2369.

Karakostis, F.A., Jeffery, N., Harvati, K., 2019a. Experimental proof that multivariate patterns among muscle attachments (entheses) can reflect repetitive muscle use. *Sci. Rep.* 9, 16577.

Karakostis, F.A., Lorenzo, C., 2016. Morphometric patterns among the 3D surface areas of human hand entheses. *Am. J. Phys. Anthropol.* 160(4), 694–707.

Karakostis, F.A., Reyes-Centeno, H., Franken, M., Hotz, G., Rademaker, K., Harvati, K., 2020. Biocultural evidence of precise manual activities in an Early Holocene individual of the high-altitude Peruvian Andes. *Am. J. Phys. Anthropol.* 174(1), 35–48.

Karakostis, F.A., Wallace, I.J., Konow, N., Harvati, K., 2019b. Experimental evidence that physical activity affects the multivariate associations among muscle attachments (entheses). *J. Exp. Biol.* 222(23), jeb213058.

Key, A.J.M., Dunmore, C.J., Marzke, M.W., 2019. The unexpected importance of the fifth digit during stone tool production. *Sci. Rep.* 9(1), 16724.

Key, A.J.M., Farr, I., Hunter, R., Winter, S.L., 2020. Muscle recruitment and stone tool use ergonomics across three million years of Palaeolithic technological transitions. *J. Hum. Evol.* 144, 102796.

Kivell, T.L., 2015. Evidence in hand: recent discoveries and the early evolution of human manual manipulation. *Phil. Trans. R. Soc. B* 370(1682), 20150105.

Kivell, T.L., 2016. A review of trabecular bone functional adaptation: what have we learned from trabecular analyses in extant hominoids and what can we apply to fossils? *J. Anat.* 228(4), 569–594.

Kivell, T.L., Churchill, S.E., Kibii, J.M., Schmid, P., Berger, L.R., 2018. The hand of *Australopithecus sediba*. *PaleoAnthropol.* 2018, 282–333.

Kivell, T.L., Deane, A.S., Tocheri, M.W., Orr, C.M., Schmid, P., Hawks, J., Berger, L.R., Churchill, S.E., 2015. The hand of *Homo naledi*. *Nat. Commun.* 6, 8431.

Kivell, T.L., Kibii, J.M., Churchill, S.E., Schmid, P., Berger, L.R., 2011. *Australopithecus sediba* hand demonstrates mosaic evolution of locomotor and manipulative abilities. *Science* 333(6048), 1411–1417.

Kuman, K., Clarke, R.J., 2000. Stratigraphy, artefact industries and hominid associations for Sterkfontein, Member 5. *J. Hum. Evol.* 38(6), 827–847.

Lemelin, P., Diogo, R., 2016. Anatomy, function, and evolution of the primate hand musculature, In: Kivell, T.L., Lemelin, P., Richmond, B.G., Schmitt, D. (Eds.), *The Evolution of the Primate Hand. Anatomical, Developmental,* *Functional, and Paleontological Evidence*. Developments in Primatology: Progress and Prospects. Springer, New York, pp. 155–193.

Lycett, S.J., Cramon-Taubadel, N. von, Foley, R.A., 2006. A crossbeam co-ordinate caliper for the morphometric analysis of lithic nuclei: a description, test and empirical examples of application. *J. Archaeol. Sci.* 33(6), 847–861.

Marchi, D., Proctor, D.J., Huston, E., Nicholas, C.L., Fischer, F., 2017. Morphological correlates of the first metacarpal proximal articular surface with manipulative capabilities in apes, humans and South African early hominins. *C. R. Palevol* 16(5-6), 645–654.

Marzke, M.W., 1983. Joint functions and grips of the *Australopithecus afarensis* hand, with special reference to the region of the capitate. *J. Hum. Evol.* 12(2), 197–211.

Marzke, M.W., 1997. Precision grips, hand morphology, and tools. *Am. J. Phys. Anthropol.* 102(1), 91–110.

Marzke, M.W., 2013. Tool making, hand morphology and fossil hominins. *Phil. Trans. R. Soc. B* 368(1630), 20120414.

Marzke, M.W., Marzke, R.F., Linscheid, R.L., Smutz, P., Steinberg, B., Reece, S., An, K.N., 1999. Chimpanzee thumb muscle cross sections, moment arms and potential torques, and comparisons with humans. *Am. J. Phys. Anthropol.* 110(2), 163–178.

Marzke, M.W., Tocheri, M.W., Steinberg, B., Femiani, J.D., Reece, S.P., Linscheid, R.L., Orr, C.M., Marzke, R.F., 2010. Comparative 3D quantitative analyses of trapeziometacarpal joint surface curvatures among living catarrhines and fossil hominins. *Am. J. Phys. Anthropol.* 141(1), 38–51.

Marzke, M.W., Toth, N., Schick, K., Reece, S., Steinberg, B., Hunt, K., Linscheid, R.L., An, K.-N., 1998. EMG study of hand muscle recruitment during hard hammer percussion manufacture of Oldowan tools. *Am. J. Phys. Anthropol.* 105(3), 315–332.

McPherron, S.P., Alemseged, Z., Marean, C.W., Wynn, J.G., Reed, D., Geraads, D., Bobe, R., Béarat, H.A., 2010. Evidence for stone-tool-assisted consumption of animal tissues before 3.39 million years ago at Dikika, Ethiopia. *Nature* 466(7308), 857–860.

Napier, J.R., 1956. The prehensile movements of the human hand. *J. Bone Jt. Surg.* 38(4), 902–913.

Netter, F.H., 2019. *Atlas of Human Anatomy*, 7th ed. Netter Basic Science. Elsevier, Philadelphia.

Panger, M.A., Brooks, A.S., Richmond, B.G., Wood, B., 2002. Older than the Oldowan? Rethinking the emergence of hominin tool use. *Evol. Anthropol.* 11(6), 235–245.

Parfitt, A.M., Travers, R., Rauch, F., Glorieux, F.H., 2000. Structural and cellular changes during bone growth in healthy children. *Bone* 27(4), 487–494.

Pickering, R., Kramers, J.D., Hancox, P.J., Ruiter, D.J. de, Woodhead, J.D., 2011. Contemporary flowstone development links early hominin bearing cave deposits in South Africa. *Earth and Planetary Science Letters* 306(1–2), 23–32.

R Core Team, 2021. *R: A Language and Environment for Statistical Computing*. R Foundation for Statistical Computing, Vienna.

Rabey, K.N., Green, D.J., Taylor, A.B., Begun, D.R., Richmond, B.G., McFarlin, S.C., 2015. Locomotor activity influences muscle architecture and bone growth but not muscle attachment site morphology. *J. Hum. Evol.* 78, 91–102.

Raynal, J.P., 1990. Essai de datation directe, In: Raynal, J.P., Pautrat, Y. (Eds.), *La Chapelle-aux-Saints et la Préhistoire en Corrèze*. l' Association pour la Recherche Archéologique en Limousin, Limoges, pp. 43–46.

Ricklan, D.E., 1987. Functional anatomy of the hand of *Australopithecus africanus*. *J. Hum. Evol.* 16(7–8), 643–664.

Rink, W.J., Schwarcz, H.P., Lee, H.K., Rees-Jones, J., Rabinovich, R., Hovers, E., 2001. Electron spin resonance (ESR) and thermal ionization mass spectrometric (TIMS) $^{230\text{Th}}/^{234}$U dating of teeth in Middle Paleolithic layers at Amud Cave, Israel. *Geoarchaeol.* 16(6), 701–717.

Robbins, J.L., Dirks, P.H., Roberts, E.M., Kramers, J.D., Makhubela, T.V., Hilbert-Wolf, H.L., Elliott, M., Wiersma, J.P., Placzek, C., Evans, M., Berger, L., 2021. Providing context to the *Homo naledi* fossils: Constraints from flowstones on the age of sediment deposits in Rising Star Cave, South Africa. *Chemical Geology* 567, 120108.

Robling, A.G., 2009. Is bone's response to mechanical signals dominated by muscle forces? *Med. Sci. Sports Exerc.* 41(11), 2044–2049.

Ruff, C., Holt, B., Trinkaus, E., 2006. Who's afraid of the big bad Wolff?: "Wolff's law" and bone functional adaptation. *Am. J. Phys. Anthropol.* 129(4), 484–498.

Sahle, Y., El Zaatari, S., White, T.D., 2017. Hominid butchers and biting crocodiles in the African Plio-Pleistocene. *PNAS* 114(50), 13164–13169.

Scherf, H., Harvati, K., Hublin, J.-J., 2013. A comparison of proximal humeral cancellous bone of great apes and humans. *J. Hum. Evol.* 65(1), 29–38.

Scherf, H., Wahl, J., Hublin, J.-J., Harvati, K., 2016. Patterns of activity adaptation in humeral trabecular bone in Neolithic humans and present-day people. *Am. J. Phys. Anthropol.* 159(1), 106–115.

Schlecht, S.H., 2012. Understanding entheses: bridging the gap between clinical and anthropological perspectives. *Anat. Rec.* 295, 1239–1251.

Schwarcz, H.P., Buhay, W.M., Grün, R., Valladas, H., Tchernov, E., Bar-Yosef, O., Vandermeersch, B., 1989. ESR dating of the Neanderthal site, Kebara Cave, Israel. *J. Archaeol. Sci.* 16(6), 653–659.

Shea, J.J., 2016. *Stone Tools in Human Evolution: Behavioral Differences among Technological Primates*. Cambridge University Press, Cambridge, MA.

Skinner, M.M., Stephens, N.B., Tsegai, Z.J., Foote, A.C., Nguyen, N.H., Gross, T., Pahr, D.H., Hublin, J.-J., Kivell, T.L., 2015a. Human evolution. Response to Comment on "Human-like hand use in *Australopithecus africanus.*" *Science* 348(6239), 1101.

Skinner, M.M., Stephens, N.B., Tsegai, Z.J., Foote, A.C., Nguyen, N.H., Gross, T., Pahr, D.H., Hublin, J.-J., Kivell, T.L., 2015b. Human-like hand use in *Australopithe-*

cus africanus. *Science* 347(6220), 395–399.

Sparacello, V.S., Rossi, S., Pettitt, P., Roberts, C., Riel-Salvatore, J., Formicola, V., 2018. New insights on Final Epigravettian funerary behavior at Arene Candide Cave (Western Liguria, Italy). *J. Anthropol. Sci.* 96, 161–184.

Stephens, N.B., Kivell, T.L., Pahr, D.H., Hublin, J.-J., Skinner, M.M., 2018. Trabecular bone patterning across the human hand. *J. Hum. Evol.* 123, 1–23.

Susman, R.L., 1988. Hand of *Paranthropus robustus* from Member 1, Swartkrans: fossil evidence for tool behavior. *Science* 240(4853), 781–784.

Susman, R.L., 1988. New postcranial remains from Swartkrans and their bearing on the functional morphology and behavior of *Paranthropus robustus*. In: Grine, F.E. (Ed.), *Evolutionary History of the "Robust" Australopithecines*. Routledge, New York, pp. 149–172.

Susman, R.L., 1994. Fossil evidence for early hominid tool use. *Science* 265(5178), 1570–1573.

Tocheri, M.W., Orr, C.M., Jacofsky, M.C., Marzke, M.W., 2008. The evolutionary history of the hominin hand since the last common ancestor of *Pan* and *Homo*. *J. Anat.* 212(4), 544–562.

Trautmann, B., 2012. *Luxembourg in the Middle Ages - An Anthropological Study of the Living Conditions of the Rural Society of Grevenmacher*. Ph.D. Dissertation. Eberhard Karls Universität Tübingen.

Trinkaus, E., 1983. *The Shanidar Neandertals*. Academic Press, New York.

Trinkaus, E., Long, J.C., 1990. Species attribution of the Swartkrans Member 1 first metacarpals: SK84 and SKX 5020. *Am. J. Phys. Anthropol.* 83(4), 419–424.

Tsegai, Z.J., Kivell, T.L., Gross, T., Nguyen, N.H., Pahr, D.H., Smaers, J.B., Skinner, M.M., 2013. Trabecular bone structure correlates with hand posture and use in hominoids. *PLoS One* 8(11), e78781.

Valladas, H., Reyss, J.L., Joron, J.L., Valladas, G., Bar Yosef, O., Vandermeersch, B., 1988. Thermoluminescence dating of Mousterian 'Proto-Cro-Magnon' remains from Israel and the origin of modern man. *Nature* 331, 614–616.

van Leeuwen, T., Vanhoof, M.J.M., Kerkhof, F.D., Stevens, J.M.G., Vereecke, E.E., 2018. Insights into the musculature of the bonobo hand. *J. Anat.* 233(3), 328-340.

Vercellotti, G., Alciati, G., Richards, M.P., Formicola, V., 2008. The Late Upper Paleolithic skeleton Villabruna 1 (Italy): a source of data on biology and behavior of a 14,000 year-old hunter. *J. Anthropol. Sci.* 86, 143–163.

Vereecke, E.E., Wunderlich, R.E., 2016. Experimental research on hand use and function in primates. In: Kivell, T.L., Lemelin, P., Richmond, B.G., Schmitt, D. (Eds.), *The Evolution of the Primate Hand. Anatomical, Developmental, Functional, and Paleontological Evidence*. Developments in Primatology: Progress and Prospects. Springer, New York, pp. 259–284.

Villotte, S., Chiotti, L., Nespoulet, R., Henry-Gambier, D., 2015. Étude anthropologique des vestiges humains récemment découverts issus de la couche 2 de l'abri Pataud (Les Eyzies-de-Tayac-Sireuil, Dordogne, France). *Bull. Mem. Soc. Anthropol. Paris* 27(3–4), 158–188.

Wallace, I.J., Burgess, M.L., Patel, B.A., 2020. Phalangeal curvature in a chimpanzee raised like a human: implications for inferring arboreality in fossil hominins. *PNAS* 117(21), 11223–11225.

Wallace, I.J., Winchester, J.M., Su, A., Boyer, D.M., Konow, N., 2017. Physical activity alters limb bone structure but not entheseal morphology. *J. Hum. Evol.* 107, 14–18.

Walter, R.C., 1994. Age of Lucy and the First Family: single-crystal ^{40}Ar/^{39}Ar dating of the Denen Dora and lower Kada Hadar members of the Hadar Formation, Ethiopia. *Geol.* 22(1), 6–10.

Whiten, A., Goodall, J., McGrew, W.C., Nishida, T., Reynolds, V., Sugiyama, Y., Tutin, C.E.G., Wrangham, R.W., Boesch, C., 1999. Cultures in chimpanzees. *Nature* 399(6737), 682–685.

Williams-Hatala, E.M., Hatala, K.G., Hiles, S., Rabey, K.N., 2016. Morphology of muscle attachment sites in the modern human hand does not reflect muscle architecture. *Sci. Rep.* 6, 28353.

Williams-Hatala, E.M., Hatala, K.G., Key, A., Dunmore, C.J., Kasper, M., Gordon, M., Kivell, T.L., 2020. Kinetics of stone tool production among novice and expert tool makers. *Am. J. Phys. Anthropol.* 174, 714–727.

Zumwalt, A., 2006. The effect of endurance exercise on the morphology of muscle attachment sites. *J. Exp. Biol.* 209(3), 444–454.

Supplement 1: Entheseal Patterns Suggest Habitual Tool Use in Early Hominins

JANA KUNZE
Paleoanthropology, Senckenberg Centre for Human Evolution and Palaeoenvironment, Institute for Archaeological Sciences, Eberhard Karls University of Tübingen, Tübingen, GERMANY; jana.kunze@uni-tuebingen.de

FOTIOS ALEXANDROS KARAKOSTIS*
DFG Centre of Advanced Studies 'Words, Bones, Genes, Tools' Eberhard Karls University of Tübingen, Tübingen, GERMANY; fotios-alexandros.karakostis@uni-tuebingen.de

STEFAN MERKER
Department of Zoology, State Museum of Natural History Stuttgart, Stuttgart, GERMANY; stefan.merker@smns-bw.de

MARCO PERESANI
Deparment of Humanities, Section of Prehistoric and Anthropological Sciences, University of Ferrara, Ferrara; and, Institute of Environmental Geology and Geoengineering, National Research Council, Milano, ITALY; psm@unife.it

GERHARD HOTZ
Anthropological Collection, Natural History Museum of Basel, Basel; and, Integrative Prehistory and Archaeological Science, University of Basel, Basel, SWITZERLAND; Gerhard.Hotz@bs.ch

VANGELIS TOURLOUKIS
Paleoanthropology, Senckenberg Centre for Human Evolution and Palaeoenvironment, Institute for Archaeological Sciences, Eberhard Karls University of Tübingen, Tübingen, GERMANY; vangelis.tourloukis@ifu.uni-tuebingen.de

KATERINA HARVATI*
Paleoanthropology, Senckenberg Centre for Human Evolution and Palaeoenvironment, Institute for Archaeological Sciences, Eberhard Karls University of Tübingen, Tübingen; and, DFG Centre of Advanced Studies 'Words, Bones, Genes, Tools' Eberhard Karls University of Tübingen, Tübingen, GERMANY; katerina.harvati@ifu.uni-tuebingen.de

SUPPLEMENT 1

OVERALL 1ST METACARPAL SHAPE

We combined the analysis of entheseal patterns with a 3D geometric morphometric analysis of standard functional morphology in the overall bone shape, including the first metacarpal's diaphysis, articular surfaces, and three muscle attachment sites (e.g., Karakostis et al. 2018). In contrast to entheseal proportions, which focus on proportionate size (i.e., surface area) and are analyzed to reconstruct habitual activity (Castro et al. 2021; Karakostis et al. 2017; Karakostis et al. 2019a; 2019b; Karakostis and Harvati 2021), entheseal shape has been associated with muscle force-producing efficiency. For example, in previous biomechanical modeling research (Karakostis et al. 2020; 2021), a more relatively projecting OP attachment site has shown to significantly increase joint moment arms for flexion, and thus the force-producing efficiency, of the attaching muscle.

METHODS

Statistical analysis

To analyze all aspects of overall metacarpal shape together, the 37 landmarks were combined in one .nts file per individual and then imported into RStudio (RStudio Inc., Boston; R version 3.6.2 for Windows, R Core Team 2021). There, the landmark coordinates were Procrustes superimposed by rotation, centering, and scaling. The resulting Procrustes coordinates of the comparative sample were then analyzed in a shape Principal Component Analysis, an analysis with no *a priori* group assumptions. The scree-plot approach was used to determine the number of relevant PCs for plotting and further analysis (Field 2017). Subsequently, the PC scores of the early fossil hominins were calculated in R using the 'predict' function and then projected onto the PC plot. The absence of outliers was visually confirmed.

Precision test

All landmarks of six individuals were digitized a second time by the same observer (JK) a month after the first digitization (see precision test in the main article). The error between repetitions was analyzed using the Centroid Radius approach. This method measures the Euclidian distance between the landmark repetitions and their centroid, which is calculated based on the provided landmark configurations (Cramon-Taubadel et al. 2007; Singleton 2002). Thereby, the deviation between repetitions can be calculated for each landmark separately. The digitization error was consistently below 5% for all landmarks with a maximum error of 3.4% and a mean error of 0.32%.

RESULTS AND DISCUSSION

The results of the morphological analysis of shape involving functional morphological characters are illustrated in Figure 3 and SOM Figure 1. In the former, PC1 is plotted against PC2, while the latter includes PC3 on the y-axis. Here, we mainly focus on the PC plot including PC3 (see Figure 3), as the shape variation depicted on this axis is more relevant for the purposes of this study. Additionally, this Principal Component shows better separation of taxa than PC2. The shape differences represented along PC1 (52.08% of variance, SOM Table 5) comprise morphological characters (captured by our landmark configurations; Methods, see Figure 2, SOM Table 4) widely interpreted as indicators of efficiency—metacarpal robusticity (Ruff et al. 2006); width and curvature of the distal articular surface (Galletta et al. 2019); dorsoventral curvature of the proximal articular surface (Marchi et al. 2017; Marzke et al. 2010); the degree of distal extension of the DI1 enthesis (Jacofsky 2009; Tocheri et al. 2008); proximal extension and lateral projection of the OP attachment site (Karakostis et al. 2020; 2021; Maki and Trinkaus 2011). PC3 (7.28 % of total variance), on the other hand, reflects changes in metacarpal robusticity, elongation of the DI1 enthesis, shape of the APL attachment site, OP lateral projection, dorsopalmar length of the proximal articular surface, and medial extension of the distal articular surface and head asymmetry. Finally, the shape variation on PC2 (14.65% of variance) is mainly driven by the proximal extension of the OP enthesis, but also reflects orientation of the DI1 (palmar-dorsal) and APL entheses (proximal-distal) and dorsoventral curvature of the proximal articular surface (see SOM Figure 1).

PC1 shows a clear separation between *H. sapiens* / *H. neanderthalensis* and the great apes, with only slight overlapping between later *Homo* and *Pan* (one specimen, likely driven by a distally extending DI1 enthesis), while PC3 separates *Gorilla* from *Pan* and *Pongo*. On PC2 on the other hand, there is an extensive overlap among all groups. The early fossil hominins (projected onto the PC plot) are more widely dispersed than in the analysis of entheseal proportions. While SK 84 plots with *H. sapiens* / *H. neanderthalensis* with a positive PC1 score, all *Australopithecus* specimens, including *A. sediba*, are characterized by more negative scores, plotting away from later hominins and at the margins of the *Pan* convex hull. Although *H. naledi* overlaps with the other *Homo* samples on PC1, it shows an extreme negative PC3 score, thus occupying a unique position on the plot. This can at least partially be explained by its unusually small proximal articular surface.

The shape analysis revealed patterns of variation that directly reflect morphological characters widely associated with manual mechanical capacity. Compared to great apes, modern humans and Neanderthals showed a robust thumb metacarpal, usually seen as an adaptation to increased load on this bone (Kivell 2015; Ruff et al. 2006); a wide and flat distal articular surface, associated with increased stability of the metacarpophalangeal joint to increase the load resistance of the thumb during forceful precision grips (Galletta et al. 2019); and a dorsoventrally flatter proximal articular surface that provides higher mobility of the trapeziometacarpal joint (Marchi et al. 2017; Marzke et al. 2010) (see shape changes in Figure 2 and SOM Figure 1). Due to their functional importance, these characteristics are commonly associated with efficient human-like tool production and use. Importantly, our analysis shows these highly functional features co-occurring with distinct, functionally relevant, entheseal shapes, including a distally extending DI1 and a laterally projecting OP enthesis, in both Neanderthals and modern humans. A histological study on DI1 (Jacofsky 2009) and recent modelling work on OP (Karakostis et al. 2021) have linked these characteristics with a larger joint moment arm, and therefore greater efficiency for the attaching muscles (Karakostis et al. 2018; 2020; 2021; Maki and Trinkaus 2011; Tocheri et al. 2008). We therefore interpret the results of our combined shape analysis as reflecting adaptations to biomechanical efficiency. In contrast to the entheseal proportion analysis, earlier hominins did not all share these biomechanically important features with later *Homo*, indicating that only some of the taxa examined here had evolved these biomechanical adaptations. Despite their human-like entheseal proportions, both *A. afarensis* and *A. sediba* present an overall bone morphology similar to *Pan* and *Pongo* and therefore likely experienced low manual dexterity compared to later *Homo*. Although *A. africanus* appears to differ in morphology from the other two australopiths, it also shows an overall bone shape more similar to that of great apes. In contrast, the overall morphology of SK 84 clearly reflects a human-like biomechanical adaptation, and the bone and entheseal shape of *H. naledi* is the most distinct from that of great apes in the entire sample.

REFERENCES

Castro, A.A., Karakostis, F.A., Copes, L.E., McClendon, H.E., Trivedi, A.P., Schwartz, N.E., Garland, T., 2021. Effects of selective breeding for voluntary exercise, chronic exercise, and their interaction on muscle attachment site morphology in house mice. *J. Anat.* 240(2), 279–295.

Cramon-Taubadel, N. von, Frazier, B.C., Lahr, M.M., 2007. The problem of assessing landmark error in geometric morphometrics: theory, methods, and modifications. *Am. J. Phys. Anthropol.* 134(1), 24–35.

Field, A., 2017. *Discovering Statistics Using IBM SPSS Sta-*

tistics, 5th ed. Sage Publications, Thousand Oaks, CA.

Galletta, L., Stephens, N.B., Bardo, A., Kivell, T.L., Marchi, D., 2019. Three-dimensional geometric morphometric analysis of the first metacarpal distal articular surface in humans, great apes and fossil hominins. *J. Hum. Evol.* 132, 119–136.

Jacofsky, M.C., 2009. *Comparative Muscle Moment Arms of the Primate Thumb: Homo, Pan, Pongo, and Papio*. Ph.D. Dissertation, Arizona State University.

Karakostis, F.A., Haeufle, D., Anastopoulou, I., Moraitis, K., Hotz, G., Tourloukis, V., Harvati, K., 2021. Biomechanics of the human thumb and the evolution of dexterity. *Curr. Biol.* 31(6), 1317–1325.e8.

Karakostis, F.A., Harvati, K., 2021. New horizons in reconstructing past human behavior: introducing the "Tübingen University Validated Entheses-based Reconstruction of Activity" method. *Evol. Anthropol.* 30(3), 185–198.

Karakostis, F.A., Hotz, G., Scherf, H., Wahl, J., Harvati, K., 2017. Occupational manual activity is reflected on the patterns among hand entheses. *Am. J. Phys. Anthropol.* 164(1), 30–40.

Karakostis, F.A., Hotz, G., Scherf, H., Wahl, J., Harvati, K., 2018. A repeatable geometric morphometric approach to the analysis of hand entheseal three-dimensinal form. *Am. J. Phys. Anthropol.* 166(1), 246–260.

Karakostis, F.A., Jeffery, N., Harvati, K., 2019a. Experimental proof that multivariate patterns among muscle attachments (entheses) can reflect repetitive muscle use. *Sci. Rep.* 9, 16577.

Karakostis, F.A., Reyes-Centeno, H., Franken, M., Hotz, G., Rademaker, K., Harvati, K., 2020. Biocultural evidence of precise manual activities in an Early Holocene individual of the high-altitude Peruvian Andes. *Am. J. Phys. Anthropol.* 174(1), 35–48.

Karakostis, F.A., Wallace, I.J., Konow, N., Harvati, K., 2019b. Experimental evidence that physical activity affects the multivariate associations among muscle attachments (entheses). *J. Exp. Biol.* 222(23), jeb213058.

Kivell, T.L., 2015. Evidence in hand: recent discoveries and the early evolution of human manual manipulation. *Phil. Trans. R. Soc. B* 370(1682), 20150105.

Maki, J., Trinkaus, E., 2011. Opponens pollicis mechanical effectiveness in Neandertals and early modern humans. *PaleoAnthropol.* 2011, 62–71.

Marchi, D., Proctor, D.J., Huston, E., Nicholas, C.L., Fischer, F., 2017. Morphological correlates of the first metacarpal proximal articular surface with manipulative capabilities in apes, humans and South African early hominins. *C. R. Palevol* 16(5–6), 645–654.

Marzke, M.W., Tocheri, M.W., Steinberg, B., Femiani, J.D., Reece, S.P., Linscheid, R.L., Orr, C.M., Marzke, R.F., 2010. Comparative 3D quantitative analyses of trapeziometacarpal joint surface curvatures among living catarrhines and fossil hominins. *Am. J. Phys. Anthropol.* 141(1), 38–51.

R Core Team, 2021. *R: A Language and Environment for Statistical Computing*. R Foundation for Statistical Computing, Vienna.

Ruff, C., Holt, B., Trinkaus, E., 2006. Who's afraid of the big bad Wolff?: "Wolff's law" and bone functional adaptation. *Am. J. Phys. Anthropol.* 129(4), 484–498.

Singleton, M., 2002. Patterns of cranial shape variation in the Papionini (Primates: Cercopithecinae). *J. Hum. Evol.* 42(5), 547–578.

Tocheri, M.W., Orr, C.M., Jacofsky, M.C., Marzke, M.W., 2008. The evolutionary history of the hominin hand since the last common ancestor of *Pan* and *Homo*. *J. Anat.* 212(4), 544–562.

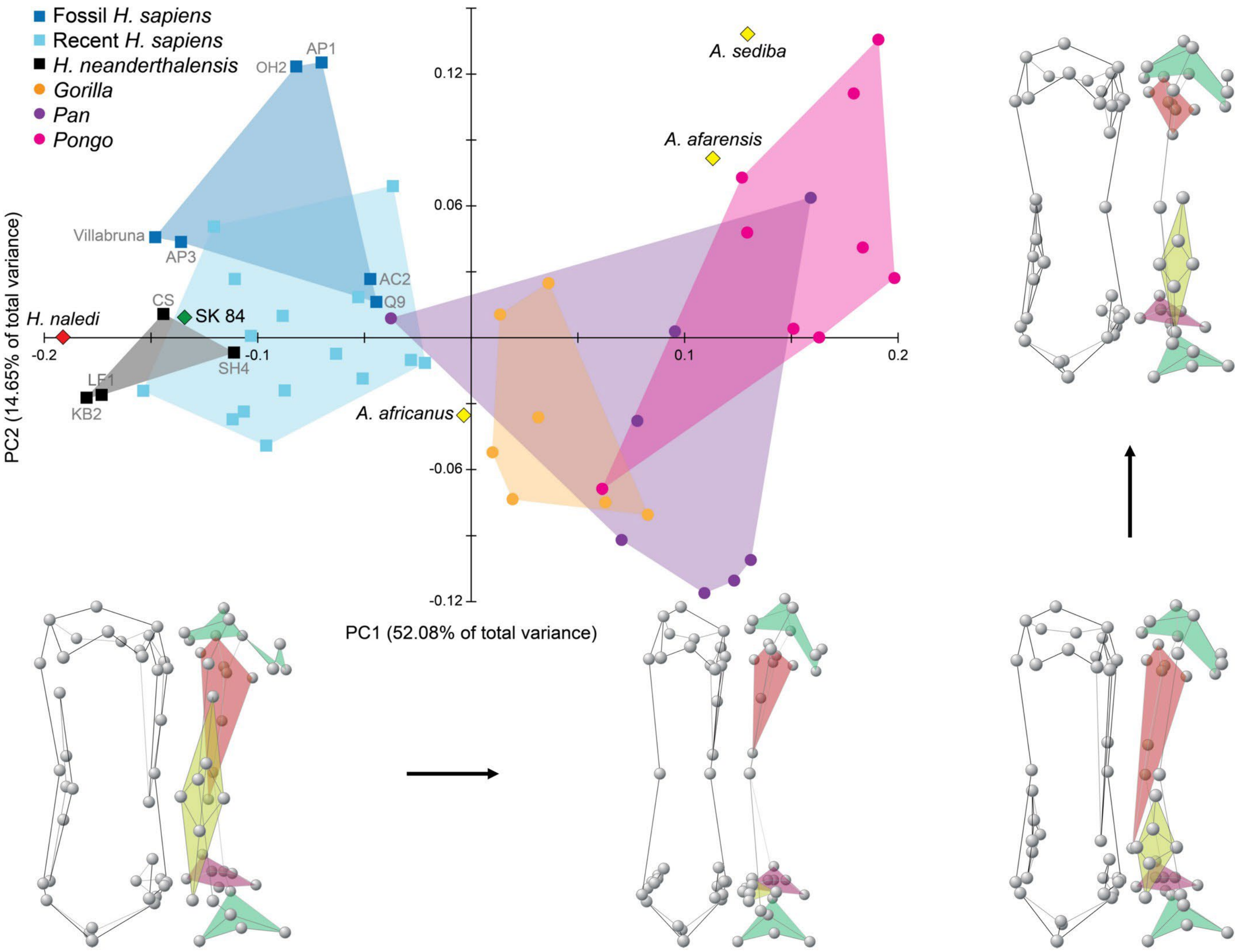

SOM Figure 1. PCA of Procrustes-superimposed landmarks of the first metacarpal without a priori *group association, PC1 compared to PC2. Shape changes along PC1 and PC2 are illustrated below and to the right of the plot, respectively. OP: red; DI1: yellow; APL: purple; articular surfaces: green. Abbreviations: OH: Ohalo; AP: Abrí Pataud; AC: Arene Candide; Q: Qafzeh; KB: Kebara; CS: Chapelle-aux-Saints; LF: La Ferrassie; SH: Shanidar.*

SOM TABLE 1. DESCRIPTIVE STATISTICS FOR THE SIZE-ADJUSTED ENTHESEAL SURFACE AREA MEASUREMENTS.

		OP	APL	DI1
Modern *H. sapiens* (n=15)	Mean	1.227	0.618	1.346
	SD	0.149	0.074	0.173
Fossil *H. sapiens* (n=6)	Mean	1.292	0.564	1.442
	SD	0.304	0.130	0.117
***H. neanderthalensis* (n=5)**	Mean	1.508	0.546	1.242
	SD	0.184	0.090	0.156
***Gorilla* (n=7)**	Mean	2.100	0.657	0.789
	SD	0.608	0.163	0.154
***Pan* (n=9)**	Mean	1.988	0.771	0.706
	SD	0.499	0.070	0.226
***Pongo* (n=9)**	Mean	1.503	1.104	0.690
	SD	0.484	0.334	0.216

SOM TABLE 2. STATISTICS OF THE DISCRIMINANT FUNCTION ANALYSIS.

DFA	Later *Homo**	Great apes*	Group centroid†
Entheseal patterns	100/100	96/96	1.66/-1.73

*% of original / cross-validated grouped cases correctly classified. Later *Homo* includes *H. sapiens* and *H. neanderthalensis.*

†*H. sapiens* and *H. neanderthalensis* / great apes.

SOM TABLE 3. CANONICAL DISCRIMINANT FUNCTION COEFFICIENT OF THE DISCRIMINANT FUNCTION ANALYSIS.

	Entheseal patterns
DI1	5.43
Constant	-5.67

SOM TABLE 4. LANDMARK DESCRIPTION FOR THE SHAPE ANALYSIS.

Landmark	Structure	Orientation	Landmark description
O1	OP	Lateral view	Most distal point of the enthesis
O2			Most palmar point in the area of the head (not the ridge)
O3			Most dorsal point in the area of the head (not ridge)
O4			Most proximal point of the enthesis
O5			App. Midpoint between points O2 and 3
O6			Midpoint along a virtual line that halves the OP ridge
A1	APL	Lateral view	Most palmar point on the proximo-palmar end of the enthesis
A2			Most dorsal point
A3			Most distal point
A4			Point on proximal border with app. equal distance to most palmar and most dorsal point of enthesis
A5&A6			Two equidistant points between A1 and 2, but projected onto most laterally elevated ridge
D1	DI1	Medial view	Most distal point on enthesis
D2			Midpoint on vertical line from landmark D1 to proximal end of enthesis, projected onto dorsal border
D3			Corresponding point on palmar border
D4			Most proximal point on enthesis
D5&D6			Two equidistant points placed between D1 and 4
B1	Overall bone	Dorsal view	Most distal point of the head
B2			Most projecting point of medial epicondyle of the head
B3			Most projecting point of lateral epicondyle/OP attachment of the head
B4		Palmar view	Medial midpoint of the shaft
B5			Lateral midpoint of the shaft
B6			Most proximally projecting point of the base
B7			Most medially projecting point of base
B8			Most laterally projecting point of base/APL
B9		Dorsal view	Most proximally projecting point of the base
PA1	Proximal articular surface	Proximal view	App. midpoint of medial border of articular surface, often where it's curved most distally
PA2			App. midpoint of lateral border of articular surface, often where it's curved most distally
PA3		Medial view	Most distal point of base curvature
DA1	Distal articular surface	Distal view	Most dorsal point on medial half of art. surface
DA2			Most dorsal point on lateral half of art. surface
DA3			Approximate midpoint of medial border
DA4			Approximate midpoint of lateral border
DA5		Disto-palmar view	Most proximal point on palmar-radial condyle
DA6			Most proximal point on palmar-ulnar condyle
DA7			Point between DA5 and 6, most distally (or most palmarly) protruding point on middle of palmar articular ridge

SOM TABLE 5. EIGENVALUES OF PC1–3 OF THE SHAPE PRINCIPAL COMPONENT ANALYSIS.

Principal component	Eigenvalues	% of variance
PC1	0.013	52.08
PC2	0.004	14.65
PC3	0.002	7.28

Appendix C

Human-like manual activities in *Australopithecus*

Human-like manual activities in Australopithecus

By Jana Kunze, Katerina Harvati, Gerhard Hotz, Fotios Alexandros Karakostis

Authors version of the manuscript representing the first submission to the Journal of Human Evolution[2].

---

[2] This thesis includes the originally submitted version of the manuscript and is anonymized according to the requirements of the journal. The final version may deviate from the manuscript included in this thesis.

Human-like manual activities in *Australopithecus*

Jana Kunze[a,*], Katerina Harvati[a,b], Gerhard Hotz[c,d], Fotios Alexandros Karakostis[b]

[a]Paleoanthropology, Senckenberg Centre for Human Evolution and Palaeoenvironment, Institute for Archaeological Sciences, Eberhard Karls University of Tübingen, Tübingen, Germany.

[b]DFG Centre of Advanced Studies 'Words, Bones, Genes, Tools', Eberhard Karls University of Tübingen, Tübingen, Germany.

[c]Anthropological Collection, Natural History Museum Basel, Basel, Switzerland.

[d]Integrative Prehistory and Archaeological Science, University of Basel, Basel, Switzerland.

Abstract

The human hand is unique among the primate order, rendering its evolution a topic of great interest in paleoanthropology. As the hand can be involved in a vast array of activities, how it was used by early hominins can yield crucial information on the factors driving biocultural evolution. Most previous research on early hominin hands has focused on overall bone shape. However, while such approaches can inform on mechanical abilities and the evolved efficiency of manipulation, they cannot be used as a definite proxy for individual habitual (lifetime) activity. For this purpose, it is crucial to examine bone structures more responsive to lifelong biomechanical loading, such as muscle attachment sites or internal bone architecture. In this study, we investigate the manual entheseal patterns of *Australopithecus afarensis*, *Australopithecus africanus,* and *Australopithecus sediba* through the application of the Validated Entheses-based Reconstruction of Activity(V.E.R.A.) method. Using a comparative sample of later *Homo* and three great ape genera, we analyze the muscle attachment site proportions on the thumb, fifth ray, and third intermediate phalanx to gain insight into the habitual hand use of *Australopithecus*. Our results highlight the importance of certain muscles of the first and fifth digits for human-like hand use. In humans, these muscles are required for variable in-hand manipulation (including power grasping), reaching high activation levels during stone tool production. *A. sediba* and *A. afarensis* show muscle activation patterns that indicate a similar suite of habitual manual activities as in later *Homo*. In contrast, *A. africanus* displays entheseal proportions intermediate between humans and great apes, suggesting a more unique use of the hand. Overall, these findings provide new substantial evidence that certain species predating the genus *Homo* were already habitually engaging in human-like manipulation even if their manual dexterity was likely not as high as in later *Homo*.

Keywords

Australopithecus, early hominins, hand use, entheses.

1. Introduction

Hominin hand use is frequently addressed in human evolutionary studies. Investigating how hand use developed throughout the human lineage can provide insight into when and how hominins ceased to use their hand for arboreal locomotion, the emergence of human-like grasping techniques, or the onset of systematic tool production and use. As the fossil record is sparse and the information to be gained from fossils is limited, early hominin hand use is deduced from comparisons with their closest living relatives.

The modern human hand is dexterous and used for manipulation only. Its morphology and function are widely investigated in clinical and evolutionary contexts (Taylor and Schwarz, 1955; Jones and Lederman, 2006; Feix et al., 2016; Baksa et al., 2018). Humans are capable of various manipulatory tasks and different grasping techniques, among which power and precision grips have received particular attention in the literature (Napier, 1956; Landsmeer, 1962; Long, II et al., 1970; Marzke et al., 1992; Maier and Hepp-Reymond, 1995; Marzke, 1997; Feix et al., 2016). In contrast, the hand of non-human primates is used for both locomotion (Susman and Stern, 1979; Matarazzo, 2008; Schmitt et al., 2016; Neufuss et al., 2017; Larson, 2018; Thompson, 2020; Leijnse et al., 2021) and manipulation (Christel, 1993; Byrne et al., 2001; Corp and Byrne, 2002; Marzke et al., 2015; Fragaszy and Crast, 2016; Bardo et al., 2017; Neufuss et al., 2019). Their manipulatory capabilities are limited compared to humans, which can be partially attributed to differences in their functional morphology (Kivell, 2016b; Orr, 2016) and muscular configuration (Lemelin and Diogo, 2016). In contrast to humans, little is known about muscle activities and coordination during primate manipulation (Bardo et al., 2017). The extent to which the primate hand is used for manipulatory tasks and the complexity of the applied techniques vary not only among primate species (e.g., see Christel, 1993; Bardo et al., 2017) but also among different populations. For example, some western chimpanzee populations, such as the Taï chimpanzees, habitually engage in pounding activities to crack nuts (Boesch-Achermann and Boesch, 1993; Visalberghi et al., 2015). Similar behavior has been observed in long-tailed macaques (Gumert and Malaivijitnond, 2013) and bearded capuchin monkeys (Falótico et al., 2018; also see Harmand and Arroyo, 2023 for an extensive review on pounding behaviors in primates).

Our knowledge about hand use in hominins is more limited. The lack of soft-tissue preservation complicates the reconstruction of manual abilities and activities. Despite this limitation, it is crucial to gain information on the capability and dexterity of hominin hands and the tasks they habitually performed. Apart from a general insight into an individual's habitual manual activities, investigating hand use in early hominins sheds light on important questions regarding bio-cultural evolution. Research on early hominin hand bones often focuses on their capability to produce and use stone tools. Early evidence of tool production and use from the archaeological record is scarce and inconclusive (Domínguez-Rodrigo et al., 2012; Harmand et al., 2015; Domínguez-Rodrigo and Alcalá, 2016; Archer et al., 2020) and does not necessarily entail information on who made or used the tools. Therefore, analyzing the manual activity patterns of hominins dating around the first archaeological evidence of tool-related behavior, like members of the genus *Australopithecus*, can help elucidate the emergence of systematic tool use.

Previous research on australopith hand use frequently focused on the hand skeleton's overall morphology (Marzke, 1983; Marzke and Shackley, 1986; Ricklan, 1987; Richmond et al., 2016; Kivell et al., 2018), including the examination of manual proportions (Alba et al., 2003; Green and Gordon, 2008; Almécija and Alba, 2014) and overall bone shape analyses (Almécija et al., 2010; Marzke et al., 2010; Marchi et al., 2017; Galletta et al., 2019; Bowland et al., 2021; Kunze et al., 2022; Morley et al., 2022; Bardo et al., 2023). Other approaches include the analysis of trabecular structures (Skinner et al., 2015; Dunmore et al., 2020b) and biomechanical muscle modeling (Domalain et al., 2017; Karakostis et al., 2021b). While overall bone morphology can yield information on mechanical limitations or efficiency, it is genetically regulated and therefore less responsive to mechanical loading (Parfitt et al., 2000; Currey, 2002; Kivell, 2016a; Wallace et al., 2020). Methods like the analysis of trabecular structures (Biewener et al., 1996; Ruffet al., 2006; Scherf et al., 2013; Tsegai et al., 2013; Kivell, 2016a; Scherf et al., 2016; Stephens et al., 2018) or entheseal patterns (Karakostis and Lorenzo, 2016; Karakostis et al., 2017; Karakostis et al., 2019b; Karakostis et al., 2019a; Castro et al., 2022) are more suitable for reconstructing the habitual activity of an individual.

Muscle attachment sites, or entheses, have been used for activity reconstruction since the 1980s (Jurmain et al., 2012; Wilczak et al., 2017). The approach is based on the assessment of changes in entheseal morphology caused by mechanical loading (Hawkey and Merbs, 1995; Benjamin et al., 2002; Schlecht, 2012). Over the years, the reliability of this approach has been heatedly debated. Researchers have questioned the influence of intrinsic and extrinsic factors (age, sex, body height, nutrition, etc.) on attachment site morphology (e.g., see Rauch, 2005; Milella et al., 2012; Schlecht, 2012; Foster et al., 2014; Turcotte et al., 2022) and emphasized shortcomings of scoring systems, a method commonly used to analyze entheseal change (Cashmore and Zakrzewski, 2013; Noldner and Edgar, 2013; Karakostis and Lorenzo, 2016; Wilczak et al., 2017). The most frequently raised criticism revolves around experimental studies reporting the lack of a correlation between entheseal change and habitual activity (Zumwalt, 2006; Rabey et al., 2015; Williams-Hatala et al., 2016; Wallace et al., 2017; Turcotte et al., 2020). However, these studies seem to present certain methodological limitations (see Karakostis and Lorenzo, 2016; Karakostis et al., 2018; Karakostis and Harvati, 2021 for a more detailed discussion), while recent years have also seen an increase in supportive experimental evidence (Deymier-Black et al., 2015; Deymier et al., 2019; Karakostis et al., 2019b; Karakostis et al., 2019a; Schlecht et al., 2019; Castro et al., 2022; Turcotte et al., 2022; Karakostis and Wallace, 2023).

The Validated Entheses based Reconstruction of Activity method (or V.E.R.A.; Karakostis and Lorenzo, 2016; Karakostis and Harvati, 2021; Karakostis, 2023 and references therein), uses a multivariate approach to investigate the proportions among entheses and thereby identify patterns of habitual muscle activation. The method has been validated in experimental studies (Karakostis et al., 2019b; Karakostis et al., 2019a; Castro et al., 2022; Karakostis and Wallace, 2023) and using an extensively documented human skeletal sample (Karakostis et al., 2017; Karakostis and Hotz, 2022). Focusing on entheseal proportions within individuals instead of comparing single entheses among individuals can account for influential factors affecting interindividual variety (Karakostis and Lorenzo, 2016; Karakostis et al., 2018). V.E.R.A. has been previously applied to different populations of modern humans (Karakostis and Lorenzo, 2016; Karakostis et al., 2017; Karakostis et al., 2020; Karakostis et al., 2021a; Bousquié et al., 2022; Karakostis and Hotz, 2022), Neanderthals (Karakostis et al., 2018) and early fossil hominins (Kunze et al., 2022). The first application of this method to the manual behaviors of early hominins investigated entheseal patterns on the first metacarpal. The authors found that later *Homo* and non-human great apes differed in proportions of the first dorsal *interosseus* (DI1) attachment site, with the former presenting proportionally larger entheses than the latter. Electromyographic research has shown that this muscle is frequently activated during tool production and use (Marzke et al., 1998; Key et al., 2020). A proportionally large DI1 enthesis was also observed in most early hominins, including *Australopithecus sediba* and *Australopithecus afarensis*, but not in *Australopithecus africanus*, who presented an entheseal pattern more similar to gorillas (Kunze et al., 2022). Kunze et al. proposed that despite their more primitive bone shape and comparatively low manual dexterity, *A. sediba* and *A. afarensis* habitually engaged in human-like hand use, potentially including human-like tool production and use.

Although the muscles attaching to the first metacarpal, specifically the *opponens pollicis* and first dorsal *interosseus*, play important roles in manipulation (Marzke, 1997; Marzke et al., 1998; Feix et al., 2015; Karakostis et al., 2021b), they cover only a small range of potential hand movements. Therefore, in this study, we aim to investigate habitual hand use in *A. sediba*, *A. afarensis,* and *A. africanus* by extending the analysis of entheseal patterns to more entheses of the hand skeleton. In a comparative framework, including later *Homo* and great apes, we examine attachment sites on the metacarpals and proximal phalanges of the first and fifth ray and the third intermediate phalanx. Previous work has highlighted the importance of the fifth ray for human-like manipulation, including tool production and use and power grasping (Marzke et al., 1998; Karakostis et al., 2017; Key et al., 2019; but see Syeda et al., 2023).

We expect later *Homo* and non-human primates to be distinct in their entheseal patterns. Based on a previous study (Kunze et al., 2022), we expect later *Homo* to show proportionally large DI1 attachment sites, as well as relatively large entheses of the fifth ray. The fifth finger is vital for stabilization, in-hand manipulation and power grasping and is reportedly involved in tool production and use (Long, II et al., 1970; Marzke and Shackley, 1986; Marzke et al., 1998; Marzke, 2013; Key et al., 2019; Key et al., 2020). In contrast, great apes will likely present proportionally larger entheses of the flexor muscle on the third intermediate phalanx due to the vital role finger flexion plays in arboreal locomotion (Susman and Stern, 1979; Syeda et al., 2023). Additionally, we expect them to display relatively larger attachment sites of the muscles related to thumb adduction, as great apes are known to adduct their thumb frequently during manipulation (Christel, 1993; Dunmore et al., 2020a; Bardo et al., 2023). Finally, if the previous results on the attachment sites of the first metacarpal are representative of the entire hand skeleton, we would assume that *A. sediba* and *A. afarensis* show entheseal patterns similar to later *Homo*, while *A. africanus* would have more great ape-like proportions.

2. Materials and methods

2.1 Materials

We used a comparative sample consisting of later *Homo* (Table 1), including recent (n = 11) and fossil *Homo sapiens* (Arene Candide 2, Ohalo 2, Qafzeh 9) and *Homo neanderthalensis* (Kebara 2, La Ferrassie 1, Shanidar 4), as well as *Gorilla gorilla* (n = 7), *Pan troglodytes* (n = 8), *Pongo abelii* (n = 1) and *Pongo pygmaeus* (n = 3) (Table 2). Our early hominin specimens (Table 3) include *Australopithecus sediba* (Malapa Hominin 2), *Australopithecus afarensis* (AL 333/333w locality) and *Australopithecus africanus* (Sterkfontein Member 4). The sample of recent *H. sapiens* includes individuals from the 19th-century collection "Basel-Spitalfriedhof" from Basel, Switzerland (n = 3) and the medieval collection from Grevenmacher, Luxemburg (n = 8). The non-human great ape sample stems from several localities (see Table 2) and contains wild-caught and captive animals.

Appendix C

The attachment sites investigated in this study (Figure 1) are mainly located on the bones of the thumb and the fifth ray. The only exception is the *flexor digitorum superficialis* (FDS) attachment on the third intermediate phalanx, used here to infer habitual arboreal activities. The attachment site on the third ray was chosen because this digit is actively used in arboreal behaviors (Samuel et al., 2018). In the case of *A. africanus*, we used the only intermediate phalanx preserved from Sterkfontein Member 4, likely of the second, third, or fourth ray (Kivell et al., 2020). Of the first and fifth ray, we analyzed the attachment sites of the following muscles: On the first metacarpal: *opponens pollicis* (OP), *abductor pollicis longus* (APL), first dorsal *interosseus* (DI1); first proximal phalanx: *abductor pollicis* (ABP), *flexor pollicis brevis* (FPB), *adductor pollicis* (ADP); fifth metacarpal: *extensor carpi ulnaris* (ECU); fifth proximal phalanx: *abductor digiti minimi* (ADM), *flexor digiti minimi* (FDM). The majority of these muscles share corresponding attachments and functions among all investigated species. The DI1 is an exception as it is absent in *P. troglodytes*. Instead, this species presents a plesiomorphic state in which the *intermetacarpales* 1-4 are not fused with the *flexores brevis profundi* 3, 5, 6 and 8 to form the dorsal interossei (Diogo et al., 2012). Nonetheless, since the first *intermetacarpalis* attaches in a similar area as the DI1 (Diogo et al., 2013), it is suggested to hold a similar function (Lemelin and Diogo, 2016; Vereecke and Wunderlich, 2016; van Leeuwen et al., 2018). Further differences in muscle function are reported for the OP, as it functions as an adductor in chimpanzees but as an abductor in humans (Marzke et al., 1999). Finally, the ABP and FPB muscles, as well as the ADM and FDM muscles, attach in a similar area of their respective bone so that their attachment sites

Table 1. Details on later Homo sample. References are provided for the dating of the fossil or the respective site.

ID	**Species**	**Age**	**Sex**	**Date**	**Location**	**Institution**[a]	**References**
Arene Candide 2	fossil *H. sapiens*	~25	Male	11–12 kya	Italy	Museo Archeologico Del Finale, IT	Sparacello et al. 2018
Ohalo 2	fossil *H. sapiens*	~35-40	Male	ca. 19 ka	Israel	Tel Aviv University, IL	Hershkovitz et al. 1995
Qafzeh 9	fossil *H. sapiens*	15-19	Female	90–100 kya	Israel	Tel Aviv University, IL	Valladas et al. 1988
Kebara 2	*H. neanderthalensis*	25-30	Male	60–64 kya	Israel	Tel Aviv University, IL	Schwarcz et al. 1989
La Ferrassie 1	*H. neanderthalensis*	Adult	Male	~43–45 kya	France	National Museum of Natural History in Paris, FR	Guérin et al. 2015
Shanidar 4	*H. neanderthalensis*	30-45	Male	60-100 kya	Iraq	Tel Aviv University, IS	Trinkaus 1983
B 137	modern *H. sapiens*	31	Male	19th century AD	Basel, Switzerland	Natural History Museum of Basel, CH	Hotz & Steinke 2012
B 211	modern *H. sapiens*	21	Male	19th century AD	Basel, Switzerland	Natural History Museum of Basel, CH	Hotz & Steinke 2012
B 264	modern *H. sapiens*	41	Male	19th century AD	Basel, Switzerland	Natural History Museum of Basel, CH	Hotz & Steinke 2012
GV 5	modern *H. sapiens*	35-45	Male	13th-14th/15th century AD	Grevenmacher, Luxembourg	University of Tübingen, DE	Trautmann 2012

Table 1. cont.

GV 12	modern *H. sapiens*	30-40	Female	13th-14th/15th century AD	Grevenmacher, Luxembourg	University of Tübingen, DE	Trautmann 2012
GV 93	modern *H. sapiens*	20-25	Female	13th-14th/15th century AD	Grevenmacher, Luxembourg	University of Tübingen, DE	Trautmann 2012
GV 105	modern *H. sapiens*	30-40	Female	13th-14th/15th century AD	Grevenmacher, Luxembourg	University of Tübingen, DE	Trautmann 2012
GV 112	modern *H. sapiens*	30-40	Male	13th-14th/15th century AD	Grevenmacher, Luxembourg	University of Tübingen, DE	Trautmann 2012
GV 117	modern *H. sapiens*	20-25	Male	13th-14th/15th century AD	Grevenmacher, Luxembourg	University of Tübingen, DE	Trautmann 2012
GV 121	modern *H. sapiens*	20-25	Female	13th-14th/15th century AD	Grevenmacher, Luxembourg	University of Tübingen, DE	Trautmann 2012
GV 132	modern *H. sapiens*	40-50	Male	13th-14th/15th century AD	Grevenmacher, Luxembourg	University of Tübingen, DE	Trautmann 2012

[a] Abbreviations following ISO 3166 country codes.

Table 2. Details on great ape sample.

ID[a]	Species	Age[b]	Sex	wild-caught/ captive	Provenance[c]	Institution[c]
1784	*Gorilla gorilla*	Adult	Female	wild-caught	Gabon	State Museum of Natural History Stuttgart, DE
6294	*Gorilla gorilla*	Adult	Male	wild-caught	Gabon	Natural History Museum Basel, CH
7464	*Gorilla gorilla*	Subadult	Male	wild-caught	Gabon	State Museum of Natural History Stuttgart, DE
38230	*Gorilla gorilla*	Adult	Female	captive	Wilhelma Zoo Stuttgart, DE	State Museum of Natural History Stuttgart, DE
1353	*Gorilla gorilla*	Adult	Male	captive	Fukuoka City Zoo, JP	Kobe Oji Zoo, Kobe, JP[d]
167340	*Gorilla gorilla*	Adult	female	wild-caught	Cameroon	American Museum of Natural History, New York, New York, US[e]
235603	*Gorilla gorilla*	Adult	male	captive	Bronz Zoo, US	American Museum of Natural History, New York, New York, US[e]
1794	*Pan troglodytes*	Adult	Male	wild-caught	Gabon	State Museum of Natural History Stuttgart, DE
2738	*Pan troglodytes*	Adult	NN	wild-caught	Southern Cameroon	State Museum of Natural History Stuttgart, DE
10824	*Pan troglodytes*	Adult	Female	captive	Zoological garden Basel, CH	Natural History Museum Basel, CH
51376	*Pan troglodytes*	NN	Female	wild-caught	DR Congo	American Museum of Natural History, New York, New York, US[e]
587	*Pan troglodytes*	Adult	Female	captive	Kamine Zoo, JP	PRI Kyoto University, Inuyama, JP[d]
498	*Pan troglodytes*	Adult	Female	captive	Tennoji Zoo, JP	Tobe Zoological Park, Tobe, JP[d]

Table 2. cont.

51205	*Pan troglodytes*	Adult	NN	wild-caught	Zaire	American Museum of Natural History, New York, New York, US[e]
89355	*Pan troglodytes*	Adult	Male	wild-caught	Ivory Coast	American Museum of Natural History, New York, New York, US[e]
1687	*Pongo pygmaeus*	Adult	Male	wild-caught	Borneo	State Museum of Natural History Stuttgart, DE
2190	*Pongo pygmaeus*	Adult	Female	wild-caught	Borneo, MY	State Museum of Natural History Stuttgart, DE
6286	*Pongo abelii*	NN	Male	wild-caught	Sumatra	Natural History Museum Basel, CH
7457	*Pongo pygmaeus*	Adult	Male	wild-caught	Northern Borneo	State Museum of Natural History Stuttgart, DE

[a] Museum inventory numbers.

[b] The bones of all individuals were fused, including specimens with unknown exact age, indicating adult or near-adult status.

[c] Abbreviations following ISO 3166 country codes.

[d] Specimens were downloaded from DMM Kupri.

[e] Specimens were downloaded from MorphoSource.

Table 3. Details on Australopithecus sample (references are provided for the dating of the respective site).

Species	**IDs**	**Date**	**Location**	**Institution**	**References**
A. afarensis	A.L. 333w-39, A.L. 333-62, -69, -89	~3.2mya	Hadar, Ethiopia	ARCHH (Ethiopia) and the Max Planck Society in Germany	Walter 1994
A. africanus	StW 28, -63, -418, -331, -575	3.4–3.7 mya	Sterkfontein, South Africa	University of the Witwatersrand, South Africa	Granger et al. 2022
A. sediba	U.W. 88-118, -119, -121, -160, -161	1.78–1.95 mya	Malapa, South Africa	University of the Witwatersrand, South Africa	Pickering et al. 2011

are often indistinguishable (Karakostis and Lorenzo, 2016). Therefore, we will consider the surface area of the two entheses as one combined attachment site and address them as ABP-FPB and ADM-FDM throughout the study. More information on muscle origin, insertion, and function can be found in Table 4.

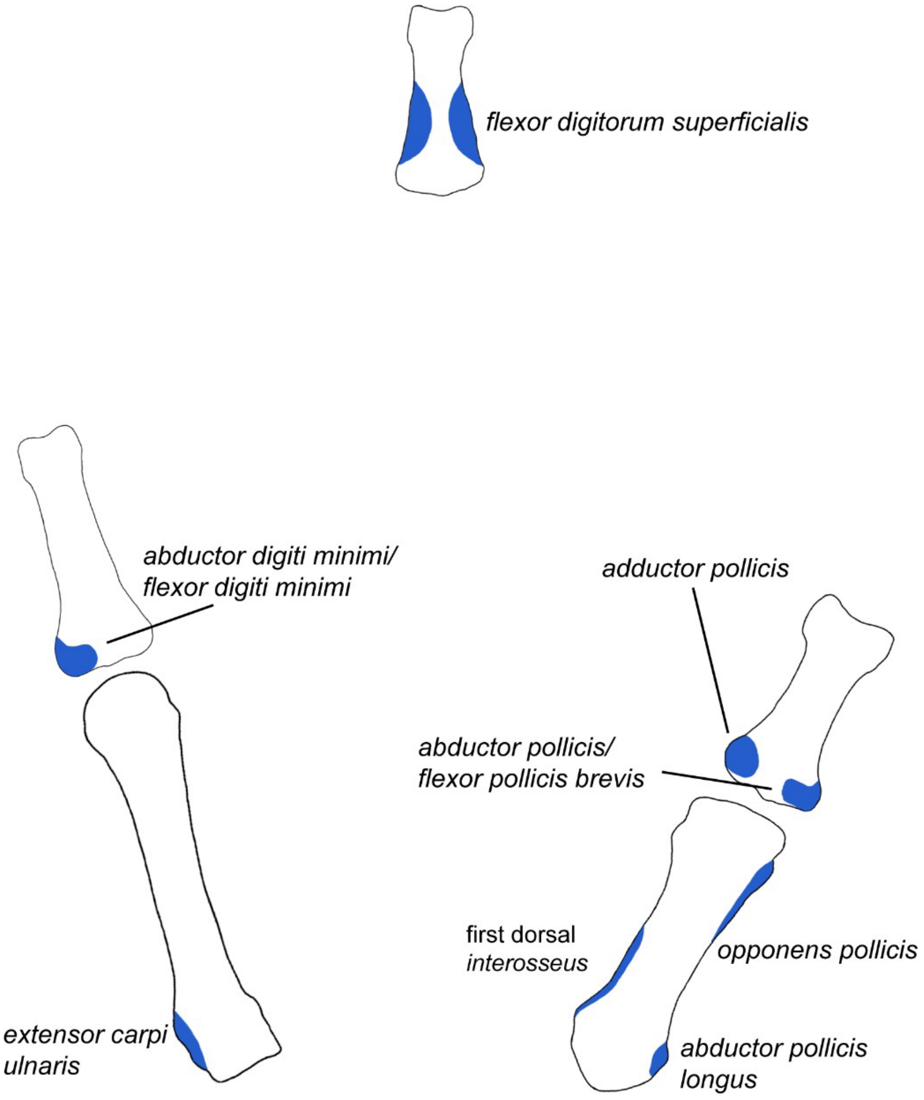

Figure 1. Schematic depiction of the entheses used in the analysis on a human hand skeleton. Grevenmacher individual 117 (Paleoanthropology Human Osteology Collection, University of Tübingen) was used as a reference.

Appendix C

Table 4. Characteristics of muscles and attachment sites used in the analysis.

Muscle	**Origin**	**Insertion**	**Muscle function**[a]
Opponens pollicis	Trapezium bone	Radial diaphysis of MC1	Abducts, rotates, and flexes the thumb
Abductor pollicis longus	Radius, ulna, scaphoid, trapezium, transverse carpal ligament	Base of MC1	Abducts and rotates the MC1 medially
First dorsal *interosseus*	MC1 and MC2 diaphyses	Base of PP2	Abducts the 2nd digit
Abductor pollicis brevis	Scaphoid, trapezium, flexor retinaculum	Base of PP1 (radial)	Abducts the thumb
Flexor pollicis brevis	Capitate, trapezium, flexor retinaculum	Base of PP1 (radial)	Flexes the thumb
Adductor pollicis	Palmar surface and base of MC3, base of MC2, capitate	Base of PP1 (ulnar)	Adducts the thumb at the CMC joint, flexes at the MCP joint
Extensor carpi ulnaris	Humerus, ulna	Base of MC5	Extends and adducts the hand
Abductor digiti minimi	Pisiform	Base of PP5 (ulnar) and dorsal digital expansion of 5th digit	Flexes and abducts 5th digit at MCP joint, extends at PIP and DIP joints
Flexor digiti minimi brevis	Hook of hamate, flexor retinaculum	Base of PP5 (ulnar)	Flexes the 5th digit
Flexor digitorum superficialis	Humerus, ulna, radius	sides of intermediate phalanges of 2nd to 5th digits	weak elbow flexion, flexes the wrist, MCP and PIP joints

[a] CMC: carpometacarpal; MCP: metacarpalphalangeal; PIP: proximal interphalangeal; DIP: distal interphalangeal.

During data collection, bones from the right anatomical side were generally prioritized as this side appeared to be better preserved in our sample, although including bones from the same anatomical side was given higher priority. However, the preservation of mainly the fossil specimens required pooling anatomical sides for some individuals in order to analyze all relevant attachment sites. While this did not seem to affect the analyses (i.e., anatomical sides did not create any visual patterns in the plots), we additionally tested whether anatomical side had an effect on PC scores through analyses of variance (ANOVA or Kruskal-Wallis tests if assumptions were violated).

2.2 Methods

Enthesis identification and delineation

Delineations of the muscle attachment sites were performed on three-dimensional (3D) surface models of the bones. The process followed the V.E.R.A. method (Karakostis and Lorenzo, 2016; Karakostis et al., 2020; Karakostis and Harvati, 2021; Karakostis, 2023; and references therein). The procedure will be briefly outlined here, while a more detailed description of the method can be found elsewhere (Karakostis et al., 2020; Karakostis and Harvati, 2021; Karakostis, 2023). The entheses were identified and delineated in meshlab v. 2021.07 (Cignoni et al., 2008) using filters provided by the program (e.g., 'Discrete Curvature', 'Equalize Vertex Colors', 'Principal Directions of Curvature'). These filters are used to identify differences in elevation – including depression and projection –, coloration (in cases where color information was available in the 3D model), and surface complexity. After identification, the area of muscle attachment was delineated and then separated from the remaining bone. Delineations were subsequently improved using the 'Principal Directions of Curvature' filter. Lastly, the 3D surface area measurements were taken in square millimeters using the 'Compute Geometric Measures' function.

The attachment site of the FDS on the third intermediate phalanx should be mentioned here specifically, as it attaches in two separate regions of the bone. The muscle belly of the FDS separates into four tendons prior to inserting into the intermediate phalanges of rays two to five. Shortly before these tendons attach to the bone, they further separate into two strands each, connecting medially and laterally on the palmar surface of the intermediate phalanges (Netter, 2017). On the bone, these attachment sites typically manifest as elevated ridges on each side of the bone, often accompanied by an adjacent, distinct depression or elevation. For this study, we will analyze the combined surface area of both attachment areas, as we are interested in the more general use of the muscle and its main contribution to finger flexion, irrespective of whether the lateral or medial side of the attachment is more pronounced. Consequently, after the two attachment sites were delineated separately, their surface area measurements were added and treated as one attachment site.

Given that the surface area measurements of entheses are affected by bone size and other systemic factors (e.g., Rauch, 2005; Milella et al., 2012; Foster et al., 2014), we adjusted the measurements before analyzing them further. For this, we used a combined adjustment through total bone surface area and the geometric mean (see below). Non-human primates and humans have different finger-to-thumb ratios – the thumb is proportionally larger in humans, whereas non-human primates generally have longer fingers. Differences in bone size affect entheseal size as larger bones will naturally show bigger entheses. Consequently, if not corrected for, entheses located on the fifth ray will naturally be proportionally larger in non-human great apes compared to humans, as these species have a proportionately larger fifth ray. Similarly, entheses of the first ray would naturally show higher proportions in humans, simply due to the fact that they have a proportionally larger thumb than great apes. To account for these differences in manual proportions, we first divided each entheseal measurement by the total bone surface area of the bone it is located on (following Karakostis and Lorenzo, 2016). Subsequently, the resulting values were additionally adjusted using the geometric mean, which is a common step of the V.E.R.A. protocols (e.g., Karakostis et al., 2017; see Karakostis, 2023). Its application can be used to control for the effects of bone and body size, as well as other extrinsic and intrinsic factors affecting inter-individual variation in entheseal surface area (Karakostis et al., 2017; Karakostis et al., 2019a; Karakostis et al., 2021a; Karakostis and Harvati, 2021). It is used to calculate the proportions of the entheses among each other, indicating whether an entheseal surface is relatively large or small compared to other entheseal surfaces within the same individual. While bone surface area can correct for entheseal variation caused by bone size and differences in bone length ratios, it can itself be affected by systematic factors (Rauch, 2005). Therefore, our two-step adjustment procedure allows controlling for the influence of several different systematic factors.

Precision test

The delineation of the entheses of a small but representative proportion of the sample (n = 5) was repeated at least two months after the initial delineation by the same observer to test for intra-observer error. The subsample included one individual each of early and recent *H. sapiens*, *H. neanderthalensis*, *A. sediba,* and *A. africanus*. The deviation of the repetitions, obtained by calculating the percentage of the standard deviation divided by the mean, was consistently below 5% (mean = 2.45%, min = 0.09%, max = 4.8%), suggesting a high precision of the delineation procedure, as previously reported for the VERA measuring protocols (e.g., see Karakostis and Lorenzo, 2016; Castro et al., 2022; Kunze et al., 2022).

Statistical analysis

For the analyses, two subsamples were created. The first included all individuals but a reduced number of attachment sites (without FDS entheseal measurement). In order to include the FDS attachment site measurement in the second subsample, sample size had to be reduced. In particular, due to preservation or limited access, we could not measure the FDS enthesis in *Pongo abelii* 6286, *Gorilla gorilla* 6294, *Pan troglodytes* 10824 and 51376, Arene Candide 2, Shanidar 4, *A. afarensis*, and Grevenmacher individual 105. These individuals were therefore excluded from the second subsample.

Appendix C

Principal component analyses (PCA) based on a correlation matrix were performed on both subsamples. The australopiths were not included in the initial analyses but were later projected into the PC plot using the 'project' function in R-Studio (R v. 4.2.2; R Core Team, 2021). The absence of extreme outliers was confirmed using a z-score approach (Field, 2017). While there was one extreme value (>3.29) in both subsamples (after projection), the frequency percentages were as expected for a normal distribution (see Field, 2017). Moreover, the individual showing extreme z-scores (*A. sediba*) was not included in the actual calculation of the components, supporting the absence of influential outliers.

In addition to the PCAs, we applied two discriminant function analyses (DFA) using the adjusted measurements as variables. The sample was divided into two groups: the first comprised individuals of the genus *Homo*, whereas the second included all non-human great apes. The early fossil hominins were entered with unknown group membership. The aim of the DFA was to identify the variables that best distinguish between the two groups and classify the *Australopithecus* specimens based on these variables. The analyses were performed in SPSS v. 28.0.1.0 (IBM Corp., 2017). Since the Box's M test for the first dataset (without FDS) was non-significant, indicating equal covariance matrices, a within-groups covariance matrix was used for the analysis (Field, 2017). The Box's M test for the second dataset (with FDS) was statistically significant. To determine the cause and assess the effect on our analysis, we pursued different strategies: First, we ran the DFA using a separate-groups covariance matrix. Secondly, we transformed our data using log transformation and the z-score approach. Finally, we conducted Levene's test of homogeneity of variances and a test of multivariate normality. The test of multivariate normality was not statistically significant. In contrast, Levene's test produced significant results for the OP and ADM-FDM measurements, suggesting that variances were not homogenous among groups for those measurements. To assess the effect of these variables on the results, they were removed in the next step. However, none of the abovementioned adjustments appeared to have affected the analysis. In all cases, the Box's M test remained significant, and, more importantly, the comparative sample of later *Homo* and non-human primates showed the same classification rates (100%). This was also the case when a separate-groups covariance matrix was used, which is not affected by the violation of Box's M. Based on this finding and the common practice that Box's M can be disregarded when group sizes are equal (Field, 2017) (later *Homo* = 14, non-human primates = 15), we decided to use a within-groups covariance matrix for the analysis. The variables were entered stepwise, and the Leave-one-out classification method was chosen. In both analyses, the stepwise approach identified the adjusted measurements of the DI1, ECU and ADM-FDM attachment sites to provide the best separation between the groups, so these variables were retained in the analysis.

3. Results

3.1 Analyses excluding FDS

Based on the analyses of variance, the anatomical side had no significant effect on the analysis ($p > 0.05$).

In the first analysis without the FDS measurements (Figs. 2-4, Table 5), the variation in muscle attachment site proportions clearly distinguishes later *Homo* from non-human great apes. The two groups are separated on PC1 (explaining 35% of variance in the sample, Figure 2), with later *Homo* displaying negative PC1 values (with only one exception) and non-human primates showing positive values. The entheseal pattern shared by individuals with positive PC1 loadings includes proportionally large ADP, ABP-FPB, OP and APL entheses. In contrast, the pattern associated with PC1 negative combines a proportionally large DI1 with large ECU and ADM-FDM attachment sites. PC2 (21.09% of variance) does not contribute to the separation between later *Homo* and great apes as they overlap extensively on this axis. Generally, all groups overlap on this component, showing no genus-, species- or population-related distinction. The entheseal pattern on PC2 positive is characterized by proportionally large attachment sites of the ECU, ADM-FDM, ADP and ABP-FPB, whereas the pattern on PC2 negative entails relatively large DI1, OP and APL entheses. All australopiths show an entheseal pattern more similar to later *Homo* than non-human primates, although only *A. africanus* falls directly inside their convex hull in this plot. While *A. sediba* overlaps with recent modern humans on PC1, it considerably exceeds the range of variation of all later *Homo* groups and non-human great apes on PC2 due to its extreme positive value. *A. afarensis* plots closer to the center of PC1 while still overlapping with later *Homo* on this component and close to their convex hull on PC2.

Table 5. Eigenvalues and factor loadings of PC1-4 of the principal component analysis of entheseal proportions, not including FDS measurements.

Principal component[a]	**Eigenvalue**	**% of variance**	**Factor loadings**						
			OP	APL	DI1	ABP-FPB	ADP	ECU	ADM-FDM
PC1	2.45	35	0.42	0.32	-0.82	0.75	0.70	-0.40	-0.54
PC2	1.48	21.09	-0.40	-0.59	-0.37	0.22	0.50	0.60	0.40
PC3	1.11	15.79	-0.72	0.34	0.17	0.45	-0.01	-0.40	0.30
PC4	0.85	12.15	0.14	0.57	-0.38	-0.01	-0.26	0.37	0.40

[a] Only depicts PCs that are used for analysis.

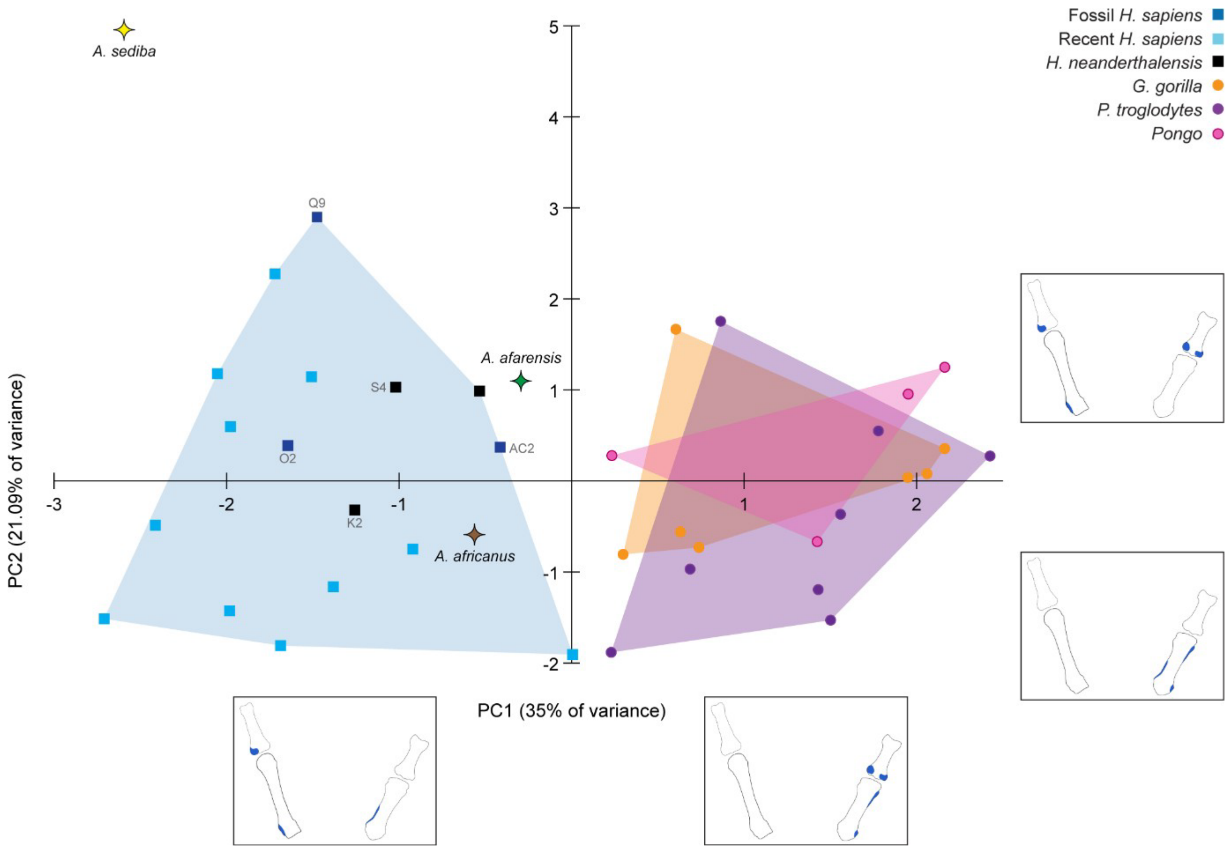

Figure 2. Principal component analysis on size-adjusted entheseal measurements without a priori group association. FDS attachment site measurements are not included. PC1 compared to PC2. Abbreviations: AC: Arene Candide; OH: Ohalo; Q: Qafzeh; KB: Kebara; LF: La Ferrassie; SH: Shanidar.

The entheseal pattern on PC3 (15.79% of variance, Figure 3) negative consists of proportionally large ECU, OP and ADP attachment sites, while individuals on PC3 positive show relatively large DI1, ADM-FDM, APL and ABP-FPB entheses. Plotting PC3 against PC1 shows the *Gorilla* group expanding further towards PC3 negative than the other great apes. However, this deviation from *Pan* and *Pongo* is mainly caused by one *Gorilla* individual showing unusually low values on this component. The remaining groups consistently overlap on PC3. While *A. sediba* still shows the highest positive value on this axis, it plots slightly closer to the range of variation of later *Homo* and non-human great ape genera on PC3. Additionally, *A. afarensis* plots inside the convex hull of later *Homo*, while *A. africanus* is positioned outside of it.

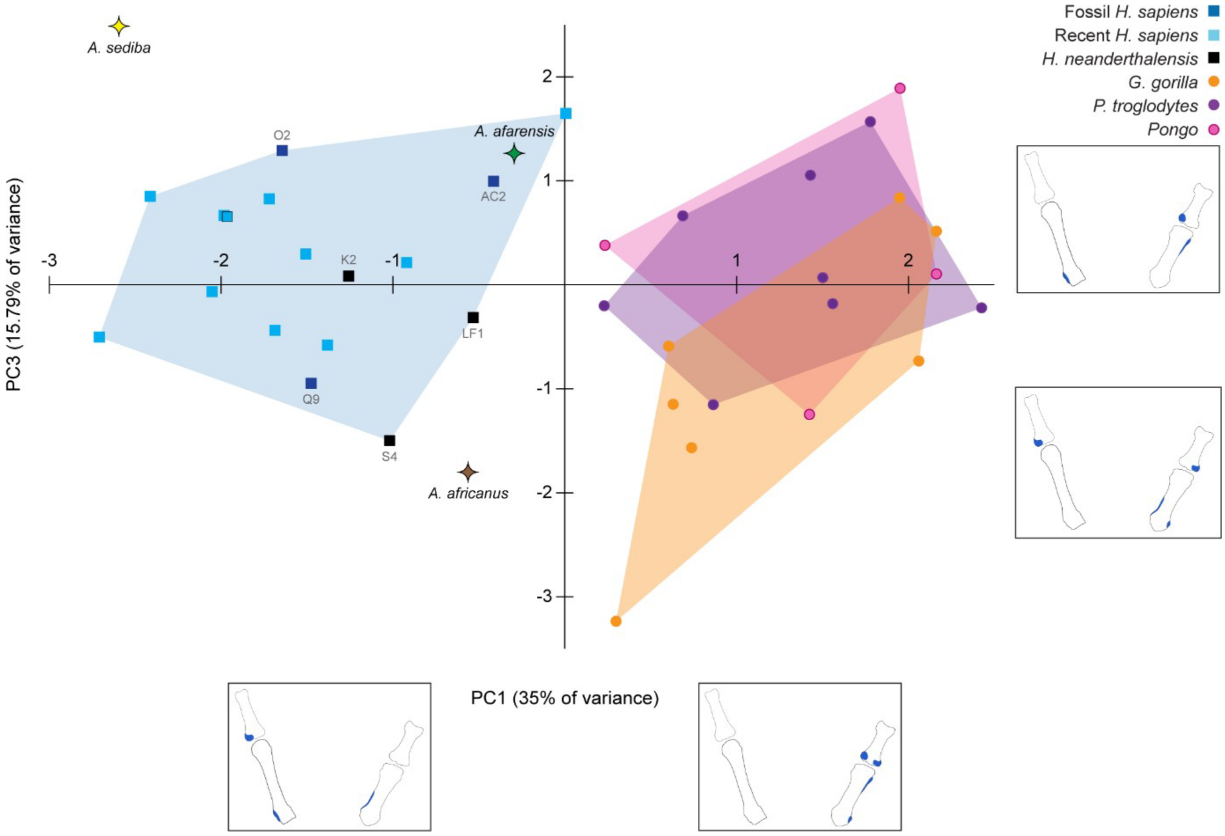

Figure 3. Principal component analysis on size-adjusted entheseal measurements without a priori group association. FDS attachment site measurements are not included. PC1 compared to PC3. Abbreviations: AC: Arene Candide; OH: Ohalo; Q: Qafzeh; KB: Kebara; LF: La Ferrassie; SH: Shanidar.

On PC4 (12.15% of variance, Figure 4), only proportionally large DI1 and ADP attachment sites are associated with negative loadings, while the remaining entheses (ABP-FPB, ADM-FDM, ECU, APL, OP) are correlated with positive values. This component does not contribute to the separation of later *Homo* and non-human primates, nor does it distinguish between the great apes. But, similar to PC3, it affects the position of the australopiths, which all have positive loadings on this axis. *A. sediba* is positioned closer to the group of later *Homo* than in previous plots, whereas *A. afarensis* and *A. africanus* plot outside their convex hull.

Supporting the results of the PCA, the DFA (Table 6) identified the proportionate surface area of the DI1, ADM-FDM and ECU entheses as the variables providing the best separation of the two groups (later *Homo* and non-human primates). Based on these variables,

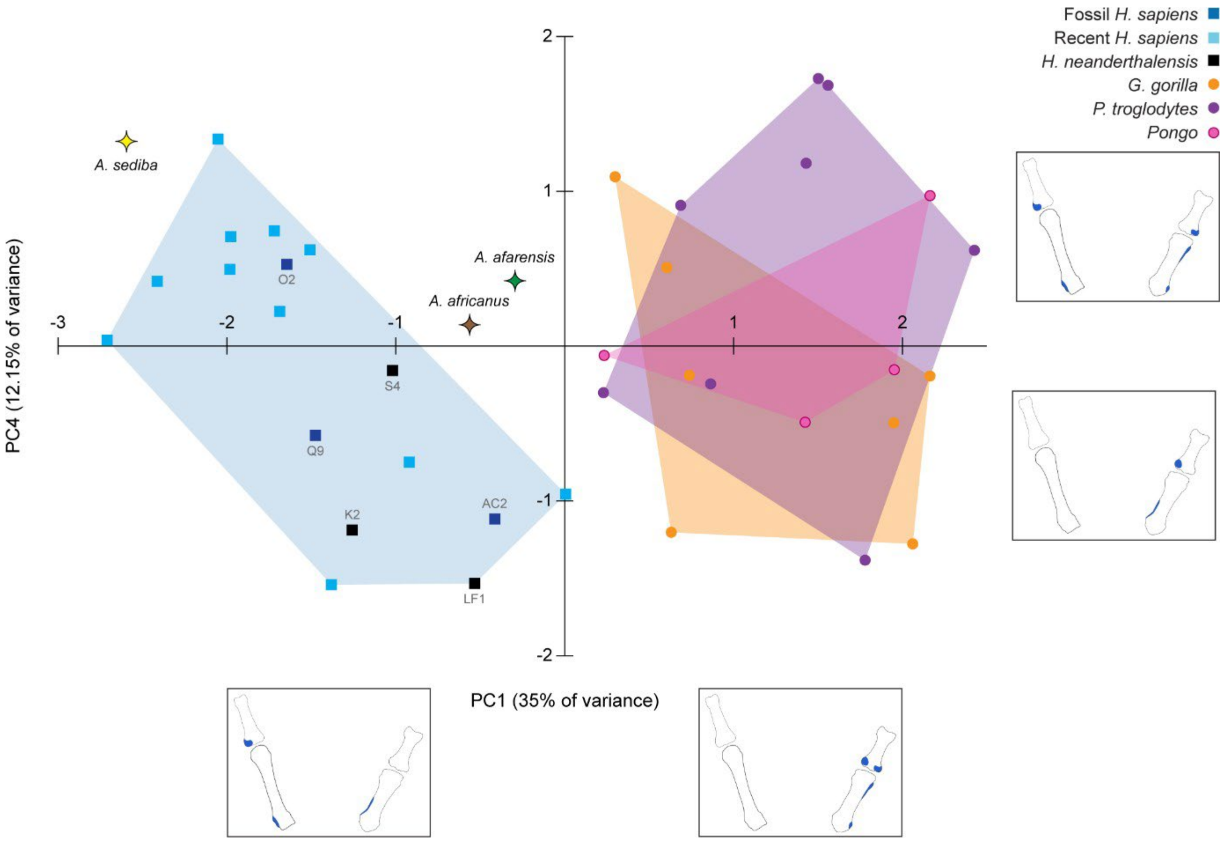

Figure 4. Principal component analysis on size-adjusted entheseal measurements without a priori group association. FDS attachment site measurements are not included. PC1 compared to PC4. Abbreviations: AC: Arene Candide; OH: Ohalo; Q: Qafzeh; KB: Kebara; LF: La Ferrassie; SH: Shanidar.

100% of the original grouped cases were correctly classified (Table 7). Among the australopiths, *A. afarensis* and *A. sediba* are classified as later *Homo* with a posterior probability of 79.6% and 100%, respectively (Table 8). In contrast, *A. africanus* is classified as a non-human primate with a posterior probability of 67.98%. These results were visualized in Figure 5, in which the discriminant scores are plotted for each group separately. Later *Homo* consistently shows positive scores while non-human primates display negative scores. *A. afarensis* and *A. africanus* plot between the two groups, with the latter closer to great apes and the former closer to later *Homo*. In contrast, *A. sediba* exhibits the highest discriminant scores in the sample, placing it above the later *Homo* group.

Table 6. Canonical discriminant function coefficient of the discriminant function analyses.

Analysis 1		**Analysis 2**	
DI1	5.05	DI1	5.57
ECU	2.62	ECU	3.94
ADM-FDM	5.36	ADM-FDM	5.65
Constant	-14.16	Constant	-14.84

Table 7. Statistics of the discriminant function analyses.

DFA	**Humans**[a]	**non-human primates**[a]	**Group centroid**[b]
Analysis 1	100/94.1	100/100	2.48/-2.22
Analysis 2	100/100	100/100	2.94/-2.74

[a] original / cross-validated
[b] humans / non-human primates

Table 8. Predicted group / posterior probability values of the discriminant function analysis[a].

	Analysis 1	**Analysis 2**	**Analysis 2 log**[b]
A. africanus	great ape / 0.68	great ape / 0.83	later *Homo* / 0.84
A. sediba	later *Homo* / 1	later *Homo* / 1	later *Homo* / 1
A. afarensis	later *Homo* / 0.8		

[a] Later *Homo* comprises *H. sapiens* and *H. neanderthalensis*.
[b] Results if size-adjusted entheseal measurements are log-transformed prior to the analysis (see Methods).

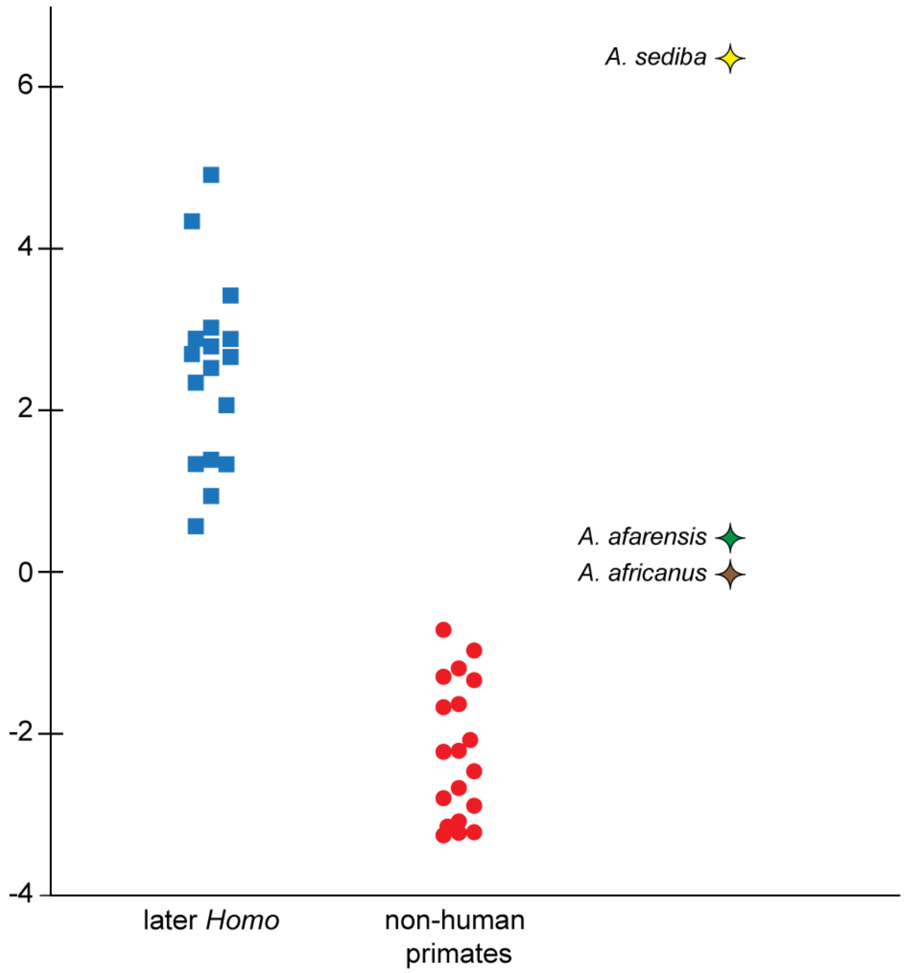

Figure 5. Results of the discriminant function analysis on size-adjusted entheseal measurements without the FDS entheseal measurements. Groups are depicted on the x-axis depicts, discriminant scores are depicted on the y-axis.

3.1 *Analyses including FDS*

In the next step, the FDS measurements were added to the analysis (Figs. 6, 7, Table 9). PC1 and PC2 are not significantly affected by anatomical side ($p > 0.05$), whereas anatomical side appears to influence PC3 ($p = 0.03$). The loadings on PC1 (36.37% of variance, Figure 6) are similar to the previous analysis. In addition, the FDS attachment site proportions highly correlate with the variation on PC1, with individuals plotting towards PC1 positive showing a proportionally large FDS enthesis. As in the previous PCA, non-human primates cluster on PC1 positive; all but one *Pongo* individual even present values above 1 on this axis. The later *Homo* group has negative PC1 values, leading to an increased separation between them and the great apes. The loadings on PC2 (19.67% of variance) are also similar to those of the first analysis, as the FDS surface area proportions are only slightly correlated with PC2 negative. However, including the FDS entheseal measurements separates the non-human primate genera on this component. While *Pan* and *Gorilla* show similar values, *Pongo* specimens exhibit higher positive PC2 values than most individuals from the other two genera. Among the australopiths, *A. sediba* shares the human-like configuration on PC1 but plots above later *Homo* on PC2. In contrast, *A. africanus* plots in between later *Homo* and the non-human primates on PC1, although slightly closer to the former. On PC2, it overlaps with recent modern humans as well as *Pan* and *Gorilla* specimens.

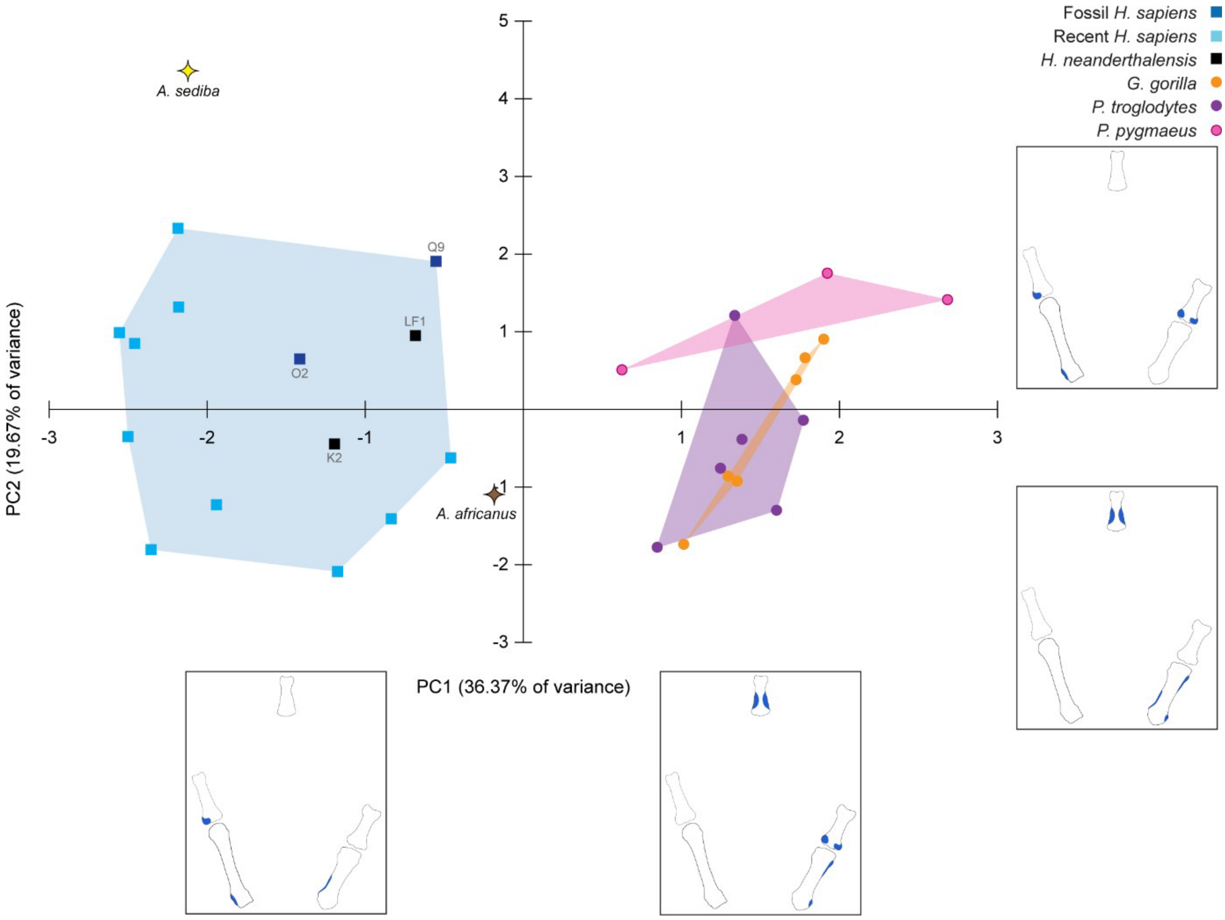

Figure 6. Principal component analysis on size-adjusted entheseal measurements without a priori group association. FDS attachment site measurements are included. PC1 compared to PC2. Abbreviations: OH: Ohalo; Q: Qafzeh; KB: Kebara; LF: La Ferrassie.

Table 9. Eigenvalues and factor loadings of PC1-3 of the principal component analysis of entheseal proportions, including FDS measurements.

Principal component[a]	Eigenvalue	% of variance	Factor loadings							
			OP	APL	DI1	ABP-FPB	ADP	ECU	ADM-FDM	FDS
PC1	2.91	36.37	0.44	0.21	-0.82	0.56	0.59	-0.52	-0.75	0.71
PC2	1.57	19.67	-0.62	-0.36	-0.38	0.49	0.58	0.46	0.38	-0.07
PC3	1.22	15.24	-0.25	0.72	-0.04	0.47	-0.13	-0.41	0.24	-0.41

[a]Only depicts PCs that are used for analysis.

PC3 (15.24% of variance, Figure 7) shows more overlap among the non-human primates. The entheseal pattern associated with PC3 negative includes proportionate entheses of DI1, ECU, FDS, OP and ADP, whereas PC3 positive exhibits a high correlation with the relative size of the APL attachment site and to a lesser degree with ADM-FDM and ABP-FPB attachment site proportions. *A. sediba* and *A. africanus* both show negative values on this component. As in the previous plot, *A. africanus* is positioned between later *Homo* and non-human primates, while it overlaps with all groups except *Pongo* on PC3. *A. sediba* has a similar PC3 value, placing it inside the convex hull of later *Homo*. Importantly, interpretations based on the variation displayed on this axis should be treated with caution due to the previously mentioned effect of anatomical side on PC3.

The discriminant function analysis, using the proportionate surface area of the DI1, ADM-FDM and ECU as variables, separates later *Homo* and non-human primates with an accuracy of 100% (original and cross-validation, Tables 6, 7). *A. sediba* is classified as later *Homo* with a posterior probability of 100% (Table 8). In contrast, the classification of *A. africanus* is less straightforward. As stated in the Methods section, the DFA including the FDS measurements was carried out multiple times using different matrices and transformed variables. While this procedure did not affect the overall accuracy of the analysis or the

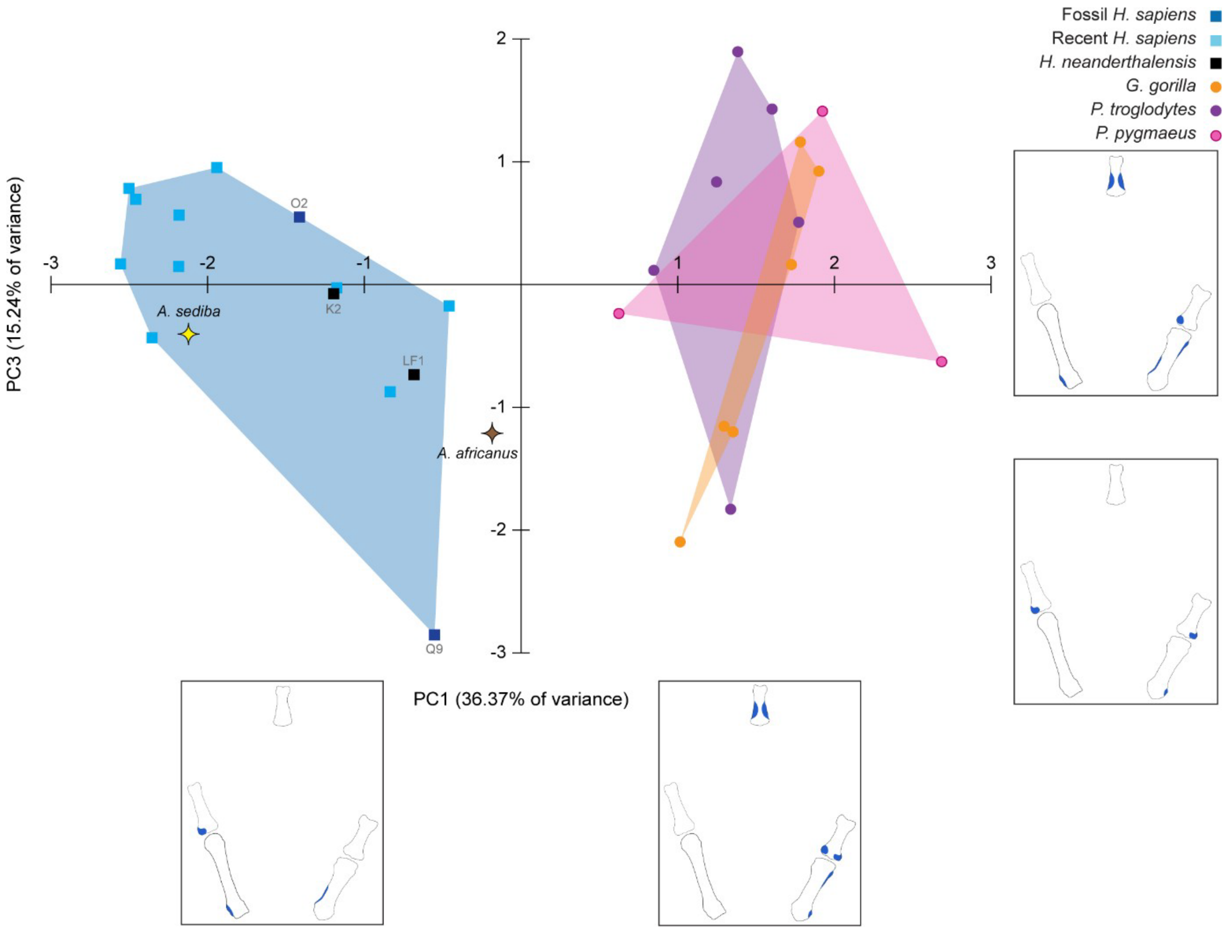

Figure 7. Principal component analysis on size-adjusted entheseal measurements without a priori group association. FDS attachment site measurements are included. PC1 compared to PC3. Abbreviations: OH: Ohalo; Q: Qafzeh; KB: Kebara; LF: La Ferrassie.

classification of *A. sediba*, it severely affected the classification of *A. africanus*. When using a within-groups covariance matrix or analyzing z-scores of the original measurements, *A. africanus* is classified as a non-human great ape (82.94% posterior probability). However, when the DFA is based on a separate-groups covariance matrix or when the variables are log-transformed, it is classified as later *Homo* (90.05% and 84.4% posterior probability, respectively). Plotting the discriminant scores sheds light on this issue. Figure 8 shows the discriminant scores when using a within-groups covariance matrix in the left panel, while the right panel depicts the scores when analyzing log-transformed variables. In both cases, *A. africanus* plots in between later *Homo* and non-human primates, shifting only slightly towards positive or negative discriminant scores. Therefore, we conclude that *A. africanus'* entheseal proportions are intermediate between those of later *Homo* and non-human primates, which causes slight changes to the analysis to impact its classification while all other individuals are unaffected.

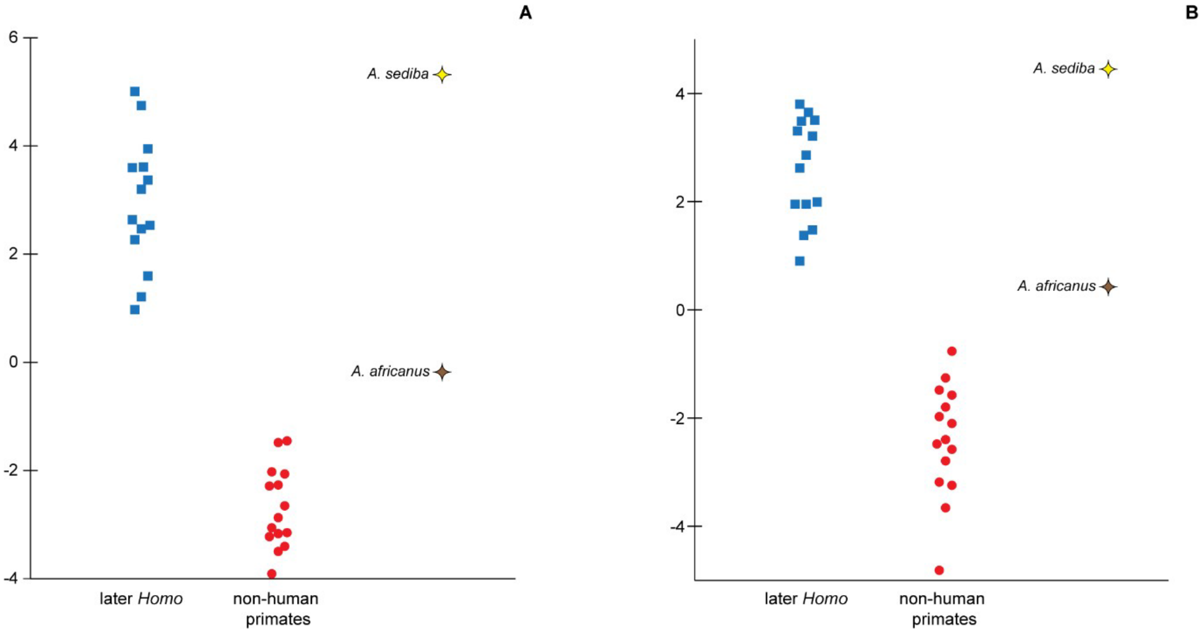

Figure 8. Results of the discriminant function analysis on size-adjusted entheseal measurements with the FDS measurements. Groups are depicted on the x-axis depicts, discriminant scores are depicted on the y-axis.

4. Discussion

The entheseal pattern characterizing the later *Homo* sample includes proportionally large DI1, ADM-FDM and ECU attachment sites. In a previous study focusing on the first metacarpal's entheseal patterns, the DI1 entheseal proportions clearly distinguished between later *Homo* and non-human great apes (Kunze et al., 2022). These results are confirmed here. The DI1 abducts the second digit (Netter et al., 2019) and stabilizes the thumb (Marzke et al., 1998). Electromyographic research has reported that the DI1 is highly activated during different types of tool use (Key et al., 2020) and hard hammer percussion manufacture of stone tools (Marzke et al., 1998). Here, a proportionally large attachment site of this muscle is associated with relatively large entheses of the fifth ray. This digit and the muscles attaching to it are known to play important roles in tool production and use (Marzke and Shackley, 1986; Marzke et al., 1998; Marzke, 2013; Kivell, 2015; Key et al., 2019; Fedato et al., 2020). During hard hammer percussion, the 5th digit of the non-dominant hand is mainly involved in handling, orienting and stabilizing the core against the impact force of the hammerstone. These activities involve high activation levels of the ADM and FDM, which abduct and flex the fifth digit, respectively, at the metacarpophalangeal joint (Marzke et al., 1998). The ADM additionally acts during tool use, mainly when tools of larger size, such as handaxes, are used (Key et al., 2020). The ECU, on the other hand, is one of the major extensor muscles of the wrist. Wrist extension in the dominant hand is crucial during knapping, as it stabilizes the wrist in the downswing phase and provides a mechanical advantage for the flexors (Williams et al., 2010, 2014).

However, the importance of the fifth digit and these three muscles is not limited to tool production and use. Previous research on entheseal patterns has shown that the ADM, FDM and ECU are frequently activated in individuals whose profession during life required a high amount of power grasping (Karakostis et al., 2017; also see Marzke et al., 1992; Goislard de Monsabert et al., 2012). The ECU coactivates with the *flexor carpi ulnaris* to deviate the wrist in the ulnar direction, which is essential in power grasping of and striking with cylindrical objects (Marzke et al., 1992). Moreover, wrist extension, as induced by the ECU, is needed when throwing an object (Young, 2003). Power grips have also been reported to involve activation of the DI1 (Long, II et al., 1970). In addition, the DI1, ADM and FDM appear to be essential for the stabilization and in-hand manipulation of objects, including but not limited to stone cores (Marzke et al., 1998; Marzke, 2013; Kivell, 2015; Key et al., 2019). Generally, in-hand manipulation and repositioning of objects are less frequent in great apes and are usually carried out by movements within the palm without engaging the fingertips (Christel, 1993; Bardo et al., 2017). As our later *Homo* sample spans a broad chronological and geographical range, we suggest that their entheseal pattern can likely be attributed to more general human-like hand use instead of being explicitly indicative of tool use. Individuals depicting these entheseal proportions would therefore have habitually engaged in activities involving power grasping and human-like in-hand manipulation, involving stabilization and control of objects with one hand.

In contrast, the pattern characterizing non-human primates consists of proportionally large attachment sites of OP, APL, ADP, ABP-FPB and, when included, FDS. Most of these muscles are involved in thumb ab- and adduction, among which the latter is an essential movement in great ape grasping techniques (Christel, 1993). Notably, the OP reportedly serves as a flexor and adductor in chimpanzees, contrasting its function as an abductor in humans (Marzke et al., 1999). While not occurring frequently, thumb abduction and opposition have been observed during vertical climbing in chimpanzees and mountain gorillas (Neufuss et al., 2017). The proportionally large FDS attachment site indicates habitual finger flexion, which was expected given that this movement plays a critical role in arboreal locomotion (Susman and Stern, 1979).

When including the FDS entheseal measurements, the principal component analysis shows a slight separation of the great ape taxa on the second PC (Figure 6). Compared to most *Gorilla gorilla* and *Pan troglodytes* specimens, *Pongo pygmaeus* individuals present larger entheseal proportions of ADP, ABP-FPB, ADM-FDM and ECU, whereas the other two primate species show relatively larger DI1, APL, OP and FDS attachment sites. While it was expected that entheseal patterns would generally differ among the great ape taxa as they engage in varying modes of locomotion and manipulation, it was surprising at first that a proportionally large FDS attachment site contributed to the entheseal patterns of *Gorilla* and *Pan*, but not to that of *Pongo* (Figure 6), whose locomotion is largely arboreal and thus likely involving increased finger flexion. However, it must be highlighted here that the PC2 loading of FDS is almost zero (-0.07), suggesting that the observed differences between non-human great ape species are almost exclusively driven by the relative recruitment of other muscles. In particular, the positive PC2 values of our *Pongo* specimens represent proportionally greater covariance among specific muscles of the first and fifth rays (Table 9). This could be related to that arboreal species show a high posture variability, leading to frequent readjustment of grips and high inter-variability in grasping techniques. Additionally, orangutans often use their mouth or foot to reposition tools, thereby freeing a hand to grasp branches (Bardo et al., 2017). Finally, great apes' hand and wrist morphology also shows notable differences among species. Compared to the African apes, *Pongo* is capable of greater wrist extension (85% compared to 42-76%; (Rose, 1988; Sarmiento, 1988; Orr, 2017), potentially enabling more frequent use of the ECU. *Pongo* also possesses the shortest thumb among great apes (Bardo et al., 2018), which likely affects their thumb involvement in grasping, particularly in techniques requiring thumb opposition (Almécija et al., 2015; Feix et al., 2015). However, these considerations should be treated with caution as they are based on general morphology and not necessarily habitual behavior. (e.g., Wallace et al., 2020). Unfortunately, interpreting the primate entheseal pattern on a more detailed level is difficult, as our knowledge of muscle activities and muscular coordination in non-human primate manipulatory behavior is limited (Bardo et al., 2017). Therefore, in order to substantiate a functional interpretation, further primatological research is required on the great ape's, and particularly *Pongo*'s, exact muscle coordination and grasping habits.

Among the australopiths, the entheseal pattern of *A. sediba* is most distinct from non-human primates. While it shows characteristics similar to later *Homo,* the pattern also includes distinctive proportions that separate *A. sediba* from all other individuals in the analysis: it combines a relatively large DI1 muscle attachment site with uniquely large entheseal proportions of the muscles attaching to the fifth ray and the first proximal phalanx. Despite these extreme proportions, the pattern suggests human-like hand use in *A. sediba*, including power grasping, in-hand manipulation and, potentially, tool use. Particularly the fifth digit in the form of the ADM, FDM and ECU muscles appears to play an essential role in *A. sediba*'s habitual manipulative behaviors. Previous work on *A. sediba*'s hand bones has pointed out its distinct morphology, including an unusually long thumb and a robust fifth metacarpal (Kivell et al., 2018). Because of these and other derived traits, researchers have suggested that *A. sediba* was capable of more human-like manipulative behavior (Kivell et al., 2018; Dunmore et al., 2020b). The analysis of muscle attachment sites of the first metacarpal has even suggested potential human-like tool use in this individual (Kunze et al., 2022). Our analysis, including a wider range of entheses, further supports habitual human-like hand use in *A. sediba*. While the entheseal pattern observed here should not be solely attributed to tool production and use, it shows an increased involvement of intrinsic musculature and the muscles of the fifth digit, which are known to be crucial for these activities.

The entheseal pattern of *A. africanus* is intermediate between later *Homo* and non-human great apes, but its position relative to these two groups varies depending on the analysis. Without the FDS entheseal measurement, the PCA positions it closer to later *Homo,* whereas the DFA classifies it as a non-human primate. When the FDS measurement is included, *A. africanus*' entheseal pattern is intermediate between both groups in both analyses. Particularly in the DFA, its classification changes when analysis parameters are altered (see Methods and Results), while the remaining sample, including *A. sediba*, provides the same results. Examinations of its hand morphology have led previous researchers to conclude that *A. africanus* was likely capable of performing precision and power squeeze grips (Ricklan, 1987; Marzke, 2013). Furthermore, although the trabecular bone fraction in its metacarpals indicates a high load on the hands, the trabecular bone distribution is more similar to the tool using species *H. sapiens* and *H. neanderthalensis* (Skinner et al., 2015). In contrast, the analysis of entheses of the first metacarpal has suggested a more ape-like thumb use in *A. africanus*, as its pattern is most similar to *G. gorilla* (Kunze et al., 2022; also see Green and Gordon, 2008;

Marchi et al., 2017; Galletta et al., 2019 for reports of more ape-like external morphology). While our study cannot fully support or refute these interpretations, the variability observed in our analyses indicates that *A. africanus* engaged in unique manipulative behaviors similar to neither later *Homo* nor non-human primates. It is important to keep in mind that the *A. africanus* hand is a composite. Consequently, the conflicting results could also be partly due to that the bones of this hand belonged to different individuals. Unfortunately, due to the fragmented nature of the fossil record, it is currently not possible to fully address this matter.

Finally, *A. afarensis* presents an entheseal pattern on the margin of variation seen in later *Homo*, suggesting habitual human-like hand use involving increased use of the fifth ray. Notably, the fifth digit of *A. afarensis* has been previously described as ape-like (Marzke et al., 1992). Its fifth metacarpal is less robust than in humans, where the robusticity of this bone is second only to the first metacarpal (Ricklan, 1987; Marzke et al., 1998). It has also been argued that the lack of a saddle joint between the hamate and the fifth metacarpal, which is a condition shared by all australopiths, limits abduction and flexion in this joint and does not allow opposing the fifth finger against the thumb (Marzke, 1983; Domalain et al., 2017). As a consequence, *A. afarensis* has been deemed unlikely to have produced the Lomekwian tools, as it was unable to "optimally orient the pulp of the 5th ray towards the hand-held object" (Domalain et al., 2017, p. 582) and therefore experienced limited grip force. This has been pointed out in particular by Domalain et al. (2017), who developed a sophisticated musculoskeletal model of *A. afarensis* to assess its ability to produce the Lomekwian stone tools. However, as was pointed out by the authors themselves, this model faces some limitations, among which are the inferred locations of muscle attachment sites. According to Domalain and colleagues, muscle attachment sites are the anatomical parameter leading to the most significant difference in outcome in the *A. afarensis* model. Yet, the exact location of its attachment sites is assumed based on a human and a chimpanzee model scaled to bone dimensions, without being identified on the bone surfaces directly. Furthermore, it is also worth emphasizing again the distinction between morphological evidence of habitual behavior *versus* biomechanical efficiency. Even though a biomechanical model might reflect whether *A. afarensis* was efficient (dextrous) in producing the Lomekwian tools (e.g., see Karakostis et al., 2021b), it cannot be used to infer its actual habitual behavior during life. In contrast, our analysis of habitual manual activity suggests that *A. afarensis* might have relied more on its fifth finger than previously suggested, regardless of how its dexterity may compare with other species. While these findings cannot provide definitive evidence that *A. afarensis* is the producer of Lomekwian tools, they still indicate that it habitually engaged in human-like hand use, involving frequent power grasping and in-hand manipulation, which would likely be necessary for manipulating such large stone industries (Harmand et al., 2015).

5. Conclusion

In this study, we investigated habitual hand use in *Australopithecus* based on a comparative analysis of their 3D entheseal patterns. Our results highlight the hypothesized importance of the fifth finger for human-like manipulation, as muscles attaching to this digit characterize habitual hand use in later *Homo*. Importantly, our study reports a high variation in muscle activation patterns among australopiths. Entheseal proportions in *A. sediba* and *A. afarensis* are more similar to later *Homo*, whereas *A. africanus* presents an entheseal pattern intermediate to humans and great apes, indicating unique hand use in this individual. Our results also suggest that *A. sediba* and *A. afarensis* habitually performed a suite of manual activities that were similar (yet not identical) to the power squeeze grasping and in-hand manipulation patterns seen in modern humans. The frequent activation of muscles needed to perform characteristic human-like grasping and manipulation in these early hominins lends further support to the notion that human-like hand use emerged prior to and likely influenced the evolutionary adaptation for higher manual dexterity in later hominins.

Acknowledgements

KH and FAK are supported by the German Research Foundation (DFG FOR 2237 awarded to K. Harvati & G. Jäger). KH is also supported by the European Research Council (CoG 724703, AdG 101019659). We are grateful to the following institutions and researchers for granting us access to fossil specimens and/or data: ARCHH (Ethiopia) and the Max Planck Society in Germany (W.H. Kimbel, Z. Alemseged, and F. Spoor), Evolutionary Studies Institute of the University of the Witwatersrand (B. Zipfel, S. Jirah, and T. Kivell), National Museum of Natural History in Paris (D. Grimaud-Hervé, F. Detroit, and M. Friess), Italian Ministry of Cultural Heritage and Activities (as well as the Museo Archeologico Del Finale and V. Sparacello). The 3D models of hand bone fossils from Israel are courtesy of the Dan David Center of Human Evolution and Biohistory Research, Shmunis Family Anthropological Institute, Sackler Faculty of Medicine, Tel Aviv University (H. May and I. Hershkovitz). We are grateful to the American Museum of Natural History (D. Boyer) for making the 3D models of great ape hand remains available online at Morphosource.org (Duke University), and the Digital Morphology Museum Kupri and the associated institutions and zoos (Kobe Oji Zoo, PRI Kyoto University, Tobe Zoological Park) for granting us access to the CT scans of primate hand remains. Finally, many thanks are due to Stefan Merker for providing us with access to and information on great ape hand remains from the State Museum of Natural History in Stuttgart and Loïc Costeur for access to and information on great ape hand remains from the Mammalian Collection of the Museum of Natural History in Basel.

References

Alba, D.M., Moyà-Solà, S., Köhler, M., 2003. Morphological affinities of the *Australopithecus afarensis* hand on the basis of manual proportions and relative thumb length. J. Hum. Evol. 44 (2), 225–254.

Almécija, S., Alba, D.M., 2014. On manual proportions and pad-to-pad precision grasping in *Australopithecus afarensis*. J. Hum. Evol. 73, 88–92.

Almécija, S., Moyà-Solà, S., Alba, D.M., 2010. Early Origin for Human-Like Precision Grasping: A Comparative Study of Pollical Distal Phalanges in Fossil Hominins. PLOS ONE 5 (7), e11727.

Almécija, S., Smaers, J.B., Jungers, W.L., 2015. The evolution of human and ape hand proportions. Nature Communications 6, 7717.

Archer, W., Aldeias, V., McPherron, S.P., 2020. What is 'in situ'? A reply to Harmand et al. (2015). J. Hum. Evol. 142, 102740.

Baksa, G., Mandl, P., Benis, S., Patonay, L., Balint, G.P., Balint, P.V., 2018. Gross Anatomy of the Human Hand, In: Balint, P.V., Mandl, P. (Eds.), Ultrasonography of the hand in rheumatology. Springer, Cham, Switzerland, pp. 15–41.

Bardo, A., Cornette, R., Borel, A., Pouydebat, E., 2017. Manual function and performance in humans, gorillas, and orangutans during the same tool use task. Am. J. Phys. Anthropol. 164 (4), 821–836.

Bardo, A., Dunmore, C.J., Cornette, R., Kivell, T.L., 2023. Morphological integration and shape covariation between the trapezium and first metacarpal among extant hominids. American Journal of Biological Anthropology, https://doi.org/10.1002/ajpa.24800.

Bardo, A., Vigouroux, L., Kivell, T.L., Pouydebat, E., 2018. The impact of hand proportions on tool grip abilities in humans, great apes and fossil hominins: A biomechanical analysis using musculoskeletal simulation. J. Hum. Evol. 125, 106–121.

Benjamin, M., Kumai, T., Milz, S., Boszczyk, B.M., Boszczyk, A.A., Ralphs, J.R., 2002. The skeletal attachment of tendons—tendon 'entheses'. Comparative Biochemistry and Physiology Part A: Molecular & Integrative Physiology 133 (4), 931–945.

Biewener, A.A., Fazzalari, N.L., Konieczynski, D.D., Baudinette, R.V., 1996. Adaptive changes in trabecular architecture in relation to functional strain patterns and disuse. Bone 19 (1), 1–8.

Boesch-Achermann, H., Boesch, C., 1993. Tool Use in Wild Chimpanzees: New Light From Dark Forests. Curr Dir Psychol Sci 2 (1), 18–21.

Bousquié, L., Karakostis, F.A., Crevecoeur, I., Villotte, S., 2022. Technical note: investigating activity-induced 3d hand entheseal variation in a documented South African sample. Archaeol. Anthropol. Sci. 14 (11).

Bowland, L.A., Scott, J.E., Kivell, T.L., Patel, B.A., Tocheri, M.W., Orr, C.M., 2021. Homo naledi pollical metacarpal shaft morphology is distinctive and intermediate between that of australopiths and other members of the genus Homo. Journal of human evolution 158, 103048.

Byrne, R.W., Corp, N., Byrne, J.M., 2001. Manual dexterity in the gorilla: bimanual and digit role differentiation in a natural task. Animal cognition 4 (3-4), 347–361.

Cashmore, L.A., Zakrzewski, S.R., 2013. Assessment of Musculoskeletal Stress Marker Development in the Hand. Int. J. Osteoarchaeol. 23 (3), 334–347.

Castro, A.A., Karakostis, F.A., Copes, L.E., McClendon, H.E., Trivedi, A.P., Schwartz, N.E., Garland, T., 2022. Effects of selective breeding for voluntary exercise, chronic exercise, and their interaction on muscle attachment site morphology in house mice. J. Anat. 240, 279-295.

Christel, M., 1993. Grasping techniques and hand preferences in Hominoidea, In: Preuschoft, H., Chivers, D.J. (Eds.), Hands of primates. Springer-Verlag, Wien, pp. 91–108.

Cignoni, P., Callieri, M., Corsini, M., Dellepiane, M., Ganovelli, F., Ranzuglia, G., 2008. MeshLab: an Open-Source Mesh Processing Tool, In: Sixth Eurographics Italian Chapter conference. Eurographics Italian Chapter Conference, Salerno, Italy. July 2nd - 4th, 2008. The Eurographics Association, Aire-la-Ville, pp. 129–136.

Corp, N., Byrne, R.W., 2002. Leaf Processing by Wild Chimpanzees: Physically Defended Leaves Reveal Complex Manual Skills. Ethology 108 (8), 673–696.

Currey, J.D., 2002. Bones: Structure and Mechanics. Princeton University Press, Princeton, NJ, Oxfordshire, 436 pp.

Deymier, A.C., Schwartz, A.G., Cai, Z., Daulton, T.L., Pasteris, J.D., Genin, G.M., Thomopoulos, S., 2019. The Multiscale Structural and Mechanical Effects of Mouse Supraspinatus Muscle Unloading on the Mature Enthesis. Acta Biomaterialia 83, 302–313.

Deymier-Black, A.C., Pasteris, J.D., Genin, G.M., Thomopoulos, S., 2015. Allometry of the Tendon Enthesis: Mechanisms of Load Transfer Between Tendon and Bone. Journal of Biomechanical Engineering 137 (11), 111005.

Diogo, R., Potau, J.M., Pastor, J.F., Paz, F.J. de, Ferrero, E.M., Bello, G., Barbosa, M., Aziz, M.A., Burrows, A.M., Arias-Martorell, J., Wood, B.A., 2013. Photographic and Descriptive Musculoskeletal Atlas of Chimpanzees: With Notes on the Attachments, Variations, Innervation, Function and Synonomy and Weight of the Muscles. CRC Press, Boca Raton.

Diogo, R., Richmond, B.G., Wood, B.A., 2012. Evolution and homologies of primate and modern human hand and forearm muscles, with notes on thumb movements and tool use. J. Hum. Evol. 63 (1), 64–78.

Domalain, M., Bertin, A., Daver, G., 2017. Was Australopithecus afarensis able to make the Lomekwian stone tools? Towards a realistic biomechanical simulation of hand force capability in fossil hominins and new insights on the role of the fifth digit. Comptes Rendus Palevol 16 (5-6), 572–584.

Domínguez-Rodrigo, M., Alcalá, L., 2016. 3.3-Million-Year-Old Stone Tools and Butchery Traces? More Evidence Needed. PaleoAnthropol. 2016, 46–53.

Domínguez-Rodrigo, M., Pickering, T.R., Bunn, H.T., 2012. Experimental study of cut marks made with rocks unmodified by human flaking and its bearing on claims of ~3.4-million-year-old butchery evidence from Dikika, Ethiopia. Journal of Archaeological Science 39 (2), 205–214.

Doran, D.M., 1996. Comparative positional behavior of the African apes, In: McGrew, W.C., Marchant, L.F., Nishida, T. (Eds.), Great ape societies. Cambridge University Press, Cambridge, pp. 213–224.

Dunmore, C.J., Bardo, A., Skinner, M.M., Kivell, T.L., 2020a. Trabecular variation in the first metacarpal and manipulation in hominids. Am. J. Phys. Anthropol. 171 (2), 219–241.

Dunmore, C.J., Skinner, M.M., Bardo, A., Berger, L.R., Hublin, J.-J., Pahr, D.H., Rosas, A., Stephens, N.B., Kivell, T.L., 2020b. The position of *Australopithecus sediba* within fossil hominin hand use diversity. Nat. Ecol. Evol. 4 (7), 911–918.

Falótico, T., Coutinho, P.H.M., Bueno, C.Q., Rufo, H.P., Ottoni, E.B., 2018. Stone tool use by wild capuchin monkeys (Sapajus libidinosus) at Serra das Confusões National Park, Brazil. Primates; journal of primatology 59 (4), 385–394.

Fedato, A., Silva-Gago, M., Terradillos-Bernal, M., Alonso-Alcalde, R., Bruner, E., 2020. Hand grasping and finger flexion during Lower Paleolithic stone tool ergonomic exploration. Archaeol. Anthropol. Sci. 12 (11).

Feix, T., Kivell, T.L., Pouydebat, E., Dollar, A.M., 2015. Estimating thumb-index finger precision grip and manipulation potential in extant and fossil primates. J. R. Soc. Interface 12 (106).

Feix, T., Romero, J., Schmiedmayer, H.-B., Dollar, A.M., Kragic, D., 2016. The GRASP Taxonomy of Human Grasp Types. IEEE Trans. Human-Mach. Syst. 46 (1), 66–77.

Field, A., 2017. Discovering Statistics Using IBM SPSS Statistics, 5th ed. Sage Publications, Thousand Oaks CA.

Fleagle, J.G., 2013. Apes and Humans, In: Fleagle, J.G. (Ed.), Primate adaptation and evolution, 3. ed. ed. Elsevier Acad. Press, Amsterdam, pp. 151–168.

Foster, A., Buckley, H., Tayles, N., 2014. Using Enthesis Robusticity to Infer Activity in the Past: A Review. J. Archaeol. Method. Theory 21 (3), 511–533.

Fragaszy, D.M., Crast, J., 2016. Functions of the Hand in Primates, In: Kivell, T.L., Lemelin, P., Richmond, B.G., Schmitt, D. (Eds.), The Evolution of the Primate Hand. Anatomical, Developmental, Functional, and Paleontological Evidence. Developments in Primatology: Progress and Prospects. Springer, New York, pp. 313–344.

Galletta, L., Stephens, N.B., Bardo, A., Kivell, T.L., Marchi, D., 2019. Three-dimensional geometric morphometric analysis of the first metacarpal distal articular surface in humans, great apes and fossil hominins. J. Hum. Evol. 132, 119–136.

Goislard de Monsabert, B., Rossi, J., Berton, E., Vigouroux, L., 2012. Quantification of hand and forearm muscle forces during a maximal power grip task. Med. Sci. Sports Exerc. 44 (10), 1906–1916.

Granger, D.E., Stratford, D., Bruxelles, L., Gibbon, R.J., Clarke, R.J., Kuman, K., 2022. Cosmogenic nuclide dating of Australopithecus at Sterkfontein, South Africa. PNAS 119 (27), e2123516119.

Green, D.J., Gordon, A.D., 2008. Metacarpal proportions in *Australopithecus africanus*. J. Hum. Evol. 54 (5), 705–719.

Guérin, G., Frouin, M., Talamo, S., Aldeias, V., Bruxelles, L., Chiotti, L., Dibble, H.L., Goldberg, P., Hublin, J.-J., Jain, M., Lahaye, C., Madelaine, S., Maureille, B., McPherron, S.J.P., Mercier, N., Murray, A.S., Sandgathe, D., Steele, T.E., Thomsen, K.J., Turq, A., 2015. A multi-method luminescence dating of the Palaeolithic sequence of La Ferrassie based on new excavations adjacent to the La Ferrassie 1 and 2 skeletons. Journal of Archaeological Science 58, 147–166.

Gumert, M.D., Malaivijitnond, S., 2013. Long-tailed macaques select mass of stone tools according to food type. Philosophical transactions of the Royal Society of London. Series B, Biological sciences 368 (1630), 20120413.

Harmand, S., Arroyo, A., 2023. Linking primatology and archaeology: The transversality of stone percussive behaviors. Journal of human evolution 181, 103398.

Harmand, S., Lewis, J.E., Feibel, C.S., Lepre, C.J., Prat, S., Lenoble, A., Boës, X., Quinn, R.L., Brenet, M., Arroyo, A., Taylor, N., Clément, S., Daver, G., Brugal, J.-P., Leakey, L., Mortlock, R.A., Wright, J.D., Lokorodi, S., Kirwa, C., Kent, D.V., Roche, H., 2015. 3.3-million-year-old stone tools from Lomekwi 3, West Turkana, Kenya. Nature 521 (7552), 310–315.

Hawkey, D.E., Merbs, C.F., 1995. Activity-induced Musculoskeletal Stress Markers (MSM) and Subsistence Strategy Changes Among Ancient Hudson Bay Eskimos. Int. J. Osteoarchaeol. 5 (4), 324–338.

Hershkovitz, I., Speirs, M.S., Frayer, D.W., Nadel, D., Wish-Baratz, S., Arensburg, B., 1995. Ohalo II H2: A 19,000-year-old skeleton from a water-logged site at the Sea of Galilee, Israel. Am. J. Phys. Anthropol. 96 (3), 215–234.

Hotz, G., Steinke, H., 2012. Knochen, Skelette, Krankengeschichten. Spitalfriedhof und Spitalarchiv – zwei sich ergänzenden Quellen. Basler Zeitschrift für Geschichte und Altertumskunde 112, 105–138.

IBM Corp., 2017. IBM SPSS Statistics for Windows. IBM Corp., Armonk, NY.

Jones, L.A., Lederman, S.J., 2006. Human Hand Function. Oxford University Press, New York.

Jurmain, R., Cardoso, F.A., Henderson, C.Y., Villotte, S., 2012. Bioarchaeology's Holy Grail: The Reconstruction of Activity, In: Grauer, A.L. (Ed.), A Companion to Paleopathology. Blackwell companions to anthropology. Wiley-Blackwell, Chichester, West Sussex, Malden, MA, pp. 531–552.

Karakostis, F.A., 2023. Statistical protocol for analyzing 3D muscle attachment sites based on the "Validated Entheses-based Reconstruction of Activity" (VERA) approach. Int. J. Osteoarchaeol. 33, 461–474.

Karakostis, F.A., Buikstra, J.E., Prevedorou, E., Hannigan, E.M., Hotaling, J., Hotz, G., Liedl, H., Moraitis, K., Siek, T.J., Waltenberger, L., Widrick, K.J., Harvati, K., 2021a. New insights into the manual activities of individuals from the Phaleron cemetery (Archaic Athens, Greece). Journal of Archaeological Science 131, 105415.

Karakostis, F.A., Haeufle, D., Anastopoulou, I., Moraitis, K., Hotz, G., Tourloukis, V., Harvati, K., 2021b. Biomechanics of the human thumb and the evolution of dexterity. Current Biology 31 (6), 1317–1325.e8.

Karakostis, F.A., Harvati, K., 2021. New horizons in reconstructing past human behavior: Introducing the "Tübingen University Validated Entheses-based Reconstruction of Activity" method. Evol. Anthropol. 30 (3), 185–198.

Karakostis, F.A., Hotz, G., 2022. Reflections of manual labor in the hand entheses of early industrial women workers with extensively documented life histories. American Journal of Biological Anthropology https://doi.org/10.1002/ajpa.24636.

Karakostis, F.A., Hotz, G., Scherf, H., Wahl, J., Harvati, K., 2017. Occupational manual activity is reflected on the patterns among hand entheses. Am. J. Phys. Anthropol. 164 (1), 30–40.

Karakostis, F.A., Hotz, G., Tourloukis, V., Harvati, K., 2018. Evidence for precision grasping in Neandertal daily activities. Science Advances 4 (9), eaat2369.

Karakostis, F.A., Jeffery, N., Harvati, K., 2019a. Experimental proof that multivariate patterns among muscle attachments (entheses) can reflect repetitive muscle use. Sci. Rep. 9, 16577.

Karakostis, F.A., Lorenzo, C., 2016. Morphometric patterns among the 3D surface areas of human hand entheses. Am. J. Phys. Anthropol. 160 (4), 694–707.

Karakostis, F.A., Reyes-Centeno, H., Franken, M., Hotz, G., Rademaker, K., Harvati, K., 2020. Biocultural evidence of precise manual activities in an Early Holocene individual of the high-altitude Peruvian Andes. Am. J. Phys. Anthropol. 174 (1), 35–48.

Karakostis, F.A., Wallace, I.J., 2023. Climbing influences entheseal morphology in the humerus of mice: An experimental application of the VERA methodology. American Journal of Biological Anthropology 181, 130–139.

Karakostis, F.A., Wallace, I.J., Konow, N., Harvati, K., 2019b. Experimental evidence that physical activity affects the multivariate associations among muscle attachments (entheses). The Journal of Experimental Biology 222 (23), jeb213058.

Key, A.J.M., Dunmore, C.J., Marzke, M.W., 2019. The unexpected importance of the fifth digit during stone tool production. Sci. Rep. 9 (1), 16724.

Key, A.J.M., Farr, I., Hunter, R., Winter, S.L., 2020. Muscle recruitment and stone tool use ergonomics across three million years of Palaeolithic technological transitions. J. Hum. Evol. 144, 102796.

Kivell, T.L., 2015. Evidence in hand: recent discoveries and the early evolution of human manual manipulation. Phil. Trans. R. Soc. B 370 (1682), 20150105.

Kivell, T.L., 2016a. A review of trabecular bone functional adaptation: what have we learned from trabecular analyses in extant hominoids and what can we apply to fossils? Journal of anatomy 228 (4), 569–594.

Kivell, T.L., 2016b. The Primate Wrist, In: Kivell, T.L., Lemelin, P., Richmond, B.G., Schmitt, D. (Eds.), The Evolution of the Primate Hand. Anatomical, Developmental, Functional, and Paleontological Evidence. Developments in Primatology: Progress and Prospects. Springer, New York, pp. 17–54.

Kivell, T.L., Churchill, S.E., Kibii, J.M., Schmid, P., Berger, L.R., 2018. The hand of *Australopithecus sediba*. PaleoAnthropol. 2018, 282–333.

Kivell, T.L., Ostrofsky, K.R., Richmond, B.G., Drapeau, M.S.M., 2020. Metacarpals and manual phalanges, In: Zipfel, B., Richmond, B., Ward, C.V. (Eds.), Hominin postcranial remains from Sterkfontein, South Africa, 1936-1995. Human evolution series. Oxford University Press, New York, NY, pp. 106–143.

Kunze, J., Karakostis, F.A., Merker, S., Peresani, M., Hotz, G., Tourloukis, V., Harvati, K., 2022. Entheseal Patterns Suggest Habitual Tool Use in Early Hominins. PaleoAnthropology 2022 (2), 195–210.

Landsmeer, J.M.F., 1962. Power grip and precision handling. Annals of the rheumatic diseases 21, 164–170.

Larson, S.G., 2018. Nonhuman Primate Locomotion. American journal of physical anthropology 165 (4), 705–725.

Leijnse, J.N., Spoor, C.W., Pullens, P., Vereecke, E.E., 2021. Kinematic and dynamic aspects of chimpanzee knuckle walking: finger flexors likely do not buffer ground impact forces. The Journal of Experimental Biology 224 (19).

Lemelin, P., Diogo, R., 2016. Anatomy, Function, and Evolution of the Primate Hand Musculature, In: Kivell, T.L., Lemelin, P., Richmond, B.G., Schmitt, D. (Eds.), The Evolution of the Primate Hand. Anatomical, Developmental, Functional, and Paleontological Evidence. Developments in Primatology: Progress and Prospects. Springer, New York, pp. 155–193.

Long, C., II, Conrad, P.W., Hall, E.A., Furler, S.L., 1970. Intrinsic-Extrinsic Muscle Control of the Hand in Power Grip and Precision Handling: An Electromyographic Study. JBJS 52 (5), 853–867.

Maier, M.A., Hepp-Reymond, M.-C., 1995. EMG Activation Patterns During Force Production in Precision Grip: I. Contribution of 15 Finger Muscles to Isometric Force. Exp. Brain Res. 103, 108–122.

Marchi, D., Proctor, D.J., Huston, E., Nicholas, C.L., Fischer, F., 2017. Morphological correlates of the first metacarpal proximal articular surface with manipulative capabilities in apes, humans and South African early hominins. Comptes Rendus Palevol 16 (5-6), 645–654.

Marzke, M.W., 1983. Joint functions and grips of the *Australopithecus afarensis* hand, with special reference to the region of the capitate. J. Hum. Evol. 12 (2), 197–211.

Marzke, M.W., 1997. Precision grips, hand morphology, and tools. Am. J. Phys. Anthropol. 102 (1), 91–110.

Marzke, M.W., 2013. Tool making, hand morphology and fossil hominins. Phil. Trans. R. Soc. B 368 (1630), 20120414.

Marzke, M.W., Marchant, L.F., McGrew, W.C., Reece, S.P., 2015. Grips and hand movements of chimpanzees during feeding in Mahale Mountains National Park, Tanzania. American journal of physical anthropology 156 (3), 317–326.

Marzke, M.W., Marzke, R.F., Linscheid, R.L., Smutz, P., Steinberg, B., Reece, S., An, K.N., 1999. Chimpanzee thumb muscle cross sections, moment arms and potential torques, and comparisons with humans. Am. J. Phys. Anthropol. 110 (2), 163–178.

Marzke, M.W., Shackley, M.S., 1986. Hominid hand use in the pliocene and pleistocene: Evidence from experimental archaeology and comparative morphology. J. Hum. Evol. 15 (6), 439–460.

Marzke, M.W., Tocheri, M.W., Steinberg, B., Femiani, J.D., Reece, S.P., Linscheid, R.L., Orr, C.M., Marzke, R.F., 2010. Comparative 3D quantitative analyses of trapeziometacarpal joint surface curvatures among living catarrhines and fossil hominins. Am. J. Phys. Anthropol. 141 (1), 38–51.

Marzke, M.W., Toth, N., Schick, K., Reece, S., Steinberg, B., Hunt, K., Linscheid, R.L., An, K.-N., 1998. EMG Study of Hand Muscle Recruitment During Hard Hammer Percussion Manufacture of Oldowan Tools. Am. J. Phys. Anthropol. 105 (3), 315–332.

Marzke, M.W., Wullstein, K.L., Viegas, S.F., 1992. Evolution of the power ("squeeze") grip and its morphological correlates in hominids. Am. J. Phys. Anthropol. 89 (3), 283–298.

Matarazzo, S., 2008. Knuckle walking signal in the manual digits of Pan and Gorilla. American journal of physical anthropology 135 (1), 27–33.

Milella, M., Belcastro, M.G., Zollikofer, C.P.E., Mariotti, V., 2012. The Effect of Age, Sex, and Physical Activity on Entheseal Morphology in a Contemporary Italian Skeletal Collection. Am. J. Phys. Anthropol. 148 (3), 379–388.

Morley, J., Bucchi, A., Lorenzo, C., Püschel, T.A., 2022. Characterizing the body morphology of the first metacarpal in the Homininae using 3D geometric morphometrics. American Journal of Biological Anthropology 177 (4), 748–759.

Napier, J.R., 1956. The Prehensile Movements of the Human Hand. The Journal of Bone and Joint Surgery. British volume 38 (4), 902–913.

Netter, F.H., 2017. Atlas of Human Anatomy E-Book, 7th ed. ed. Netter Basic Science Ser. Elsevier, Philadelphia, 928 pp.

Netter, F.H., Machado, C.A.G., Hansen, J.T., Benninger, B., Brueckner, J.K., 2019. Atlas of Human Anatomy, 7th ed. Netter basic science. Elsevier, Philadelphia, PA.

Neufuss, J., Robbins, M.M., Baeumer, J., Humle, T., Kivell, T.L., 2017. Comparison of hand use and forelimb posture during vertical climbing in mountain gorillas (Gorilla beringei beringei) and chimpanzees (Pan troglodytes). Am. J. Phys. Anthropol. 164 (4), 651–664.

Neufuss, J., Robbins, M.M., Baeumer, J., Humle, T., Kivell, T.L., 2019. Manual skills for food processing by mountain gorillas (Gorilla beringei beringei) in Bwindi Impenetrable National Park, Uganda. Biological Journal of the Linnean Society 127, 543–562.

Noldner, L.K., Edgar, H.J.H., 2013. Technical Note: 3D Representation and Analysis of Enthesis Morphology. Am. J. Phys. Anthropol. 152 (3), 417–424.

Orr, C.M., 2016. Functional Morphology of the Primate Hand: Recent Approaches Using Biomedical Imaging, Computer Modeling, and Engineering Methods, In: Kivell, T.L., Lemelin, P., Richmond, B.G., Schmitt, D. (Eds.), The Evolution of the Primate Hand. Anatomical, Developmental, Functional, and Paleontological Evidence. Developments in Primatology: Progress and Prospects. Springer, New York, pp. 227–257.

Orr, C.M., 2017. Locomotor Hand Postures, Carpal Kinematics During Wrist Extension, and Associated Morphology in Anthropoid Primates. Anatomical record (Hoboken, N.J. : 2007) 300 (2), 382–401.

Parfitt, A.M., Travers, R., Rauch, F., Glorieux, F.H., 2000. Structural and Cellular Changes During Bone Growth in Healthy Children. Bone 27 (4), 487–494.

Pickering, R., Kramers, J.D., Hancox, P.J., Ruiter, D.J. de, Woodhead, J.D., 2011. Contemporary flowstone development links early hominin bearing cave deposits in South Africa. Earth and Planetary Science Letters 306 (1-2), 23–32.

R Core Team, 2021. R: A language and environment for statistical computing. R Foundation for Statistical Computing, Vienna.

Rabey, K.N., Green, D.J., Taylor, A.B., Begun, D.R., Richmond, B.G., McFarlin, S.C., 2015. Locomotor Activity Influences Muscle Architecture and Bone Growth but Not Muscle Attachment Site Morphology. J. Hum. Evol. 78, 91–102.

Rauch, F., 2005. Bone growth in length and width: the Yin and Yang of bone stability. Journal of musculoskeletal & neuronal interactions 5 (3), 194–201.

Richmond, B.G., Roach, N.T., Ostrofsky, K.R., 2016. Evolution of the Early Hominin Hand, In: Kivell, T.L., Lemelin, P., Richmond, B.G., Schmitt, D. (Eds.), The Evolution of the Primate Hand. Anatomical, Developmental, Functional, and Paleontological Evidence. Developments in Primatology: Progress and Prospects. Springer, New York, pp. 515–543.

Ricklan, D.E., 1987. Functional anatomy of the hand of *Australopithecus africanus*. J. Hum. Evol. 16 (7-8), 643–664.

Rose, M.D., 1988. Functional anatomy of the cheiridia, In: Schwartz, J.H. (Ed.), Orangutan Biology. Oxford University Press, New York, pp. 299–310.

Ruff, C., Holt, B., Trinkaus, E., 2006. Who's Afraid of the Big Bad Wolff?: "Wolff's law" and Bone Functional Adaptation. Am. J. Phys. Anthropol. 129 (4), 484–498.

Samuel, D.S., Nauwelaerts, S., Stevens, J.M.G., Kivell, T.L., 2018. Hand pressures during arboreal locomotion in captive bonobos (Pan paniscus). The Journal of Experimental Biology 221 (Pt 8).

Sarmiento, E.E., 1988. Anatomy of the hominoid wrist joint: Its evolutionary and functional implications. Int J Primatol 9 (4), 281–345.

Scherf, H., Harvati, K., Hublin, J.-J., 2013. A comparison of proximal humeral cancellous bone of great apes and humans. J. Hum. Evol. 65 (1), 29–38.

Scherf, H., Wahl, J., Hublin, J.-J., Harvati, K., 2016. Patterns of activity adaptation in humeral trabecular bone in Neolithic humans and present-day people. Am. J. Phys. Anthropol. 159 (1), 106–115.

Schlecht, S.H., 2012. Understanding Entheses: Bridging the Gap Between Clinical and Anthropological Perspectives. The Anatomical Record 295, 1239–1251.

Schlecht, S.H., Martin, C.T., Ochocki, D.N., Nolan, B.T., Wojtys, E.M., Ashton-Miller, J.A., 2019. Morphology of Mouse Anterior Cruciate Ligament-Complex Changes Following Exercise During Pubertal Growth. Journal of Orthopaedic Research 37 (9), 1910–1919.

Schmitt, D., Zeininger, A., Granatosky, M.C., 2016. Patterns, Variability, and Flexibility of Hand Posture During Locomotion in Primates, In: Kivell, T.L., Lemelin, P., Richmond, B.G., Schmitt, D. (Eds.), The Evolution of the Primate Hand. Anatomical, Developmental, Functional, and Paleontological Evidence. Developments in Primatology: Progress and Prospects. Springer, New York, pp. 345–369.

Schwarcz, H.P., Buhay, W.M., Grün, R., Valladas, H., Tchernov, E., Bar-Yosef, O., Vandermeersch, B., 1989. ESR Dating of the Neanderthal Site, Kebara Cave, Israel. Journal of Archaeological Science 16 (6), 653–659. Skinner, M.M., Stephens, N.B., Tsegai, Z.J., Foote, A.C., Nguyen, N.H., Gross, T., Pahr, D.H., Hublin, J.-J.,

Kivell, T.L., 2015. Human-like hand use in *Australopithecus africanus*. Science 347 (6220), 395–399.

Sparacello, V.S., Rossi, S., Pettitt, P., Roberts, C., Riel-Salvatore, J., Formicola, V., 2018. New insights on Final Epigravettian funerary behavior at Arene Candide Cave (Western Liguria, Italy). J. Anthropol. Sci. 96, 161–184.

Stephens, N.B., Kivell, T.L., Pahr, D.H., Hublin, J.-J., Skinner, M.M., 2018. Trabecular bone patterning across the human hand. Journal of human evolution 123, 1–23.

Susman, R.L., Stern, J.T., 1979. Telemetered electromyography of flexor digitorum profundus and flexor digitorum superficialis in Pan troglodytes and implications for interpretation of the O. H. 7 hand. Am. J. Phys. Anthropol. 50 (4), 565–574.

Syeda, S.M., Tsegai, Z.J., Cazenave, M., Skinner, M.M., Kivell, T.L., 2023. Cortical bone distribution of the proximal phalanges in great apes: implications for reconstructing manual behaviours. Journal of anatomy 243, 707–728.

Taylor, C.L., Schwarz, R.J., 1955. The anatomy and mechanics of the human hand. Artificial limbs 2 (2), 22–35.

Thompson, N.E., 2020. The biomechanics of knuckle-walking: 3-D kinematics of the chimpanzee and macaque wrist, hand and fingers. The Journal of Experimental Biology 223 (Pt 14).

Thompson, N.E., Patel, B.A., Stern, J.T., JR., Larson, S.G., 2019. 3-D kinematics, kinetics, and EMG of knuckle-walking in chimpanzees. Am. J. Phys. Anthropol. 168 (S68), 246–247.

Trautmann, B., 2012. Luxembourg in the Middle Ages - An Anthropological Study of the Living Conditions of the Rural Society of Grevenmacher. Doctoral dissertation, Eberhard Karls Universität Tübingen.

Trinkaus, E., 1983. The Shanidar Neandertals. Academic Press, New York.

Tsegai, Z.J., Kivell, T.L., Gross, T., Nguyen, N.H., Pahr, D.H., Smaers, J.B., Skinner, M.M., 2013. Trabecular bone structure correlates with hand posture and use in hominoids. PLOS ONE 8 (11), e78781.

Turcotte, C.M., Green, D.J., Kupczik, K., McFarlin, S., Schulz-Kornas, E., 2020. Elevated activity levels do not influence extrinsic fiber attachment morphology on the surface of muscle-attachment sites. Journal of anatomy 236 (5), 827–839.

Turcotte, C.M., Rabey, K.N., Green, D.J., McFarlin, S.C., 2022. Muscle attachment sites and behavioral reconstruction: An experimental test of muscle-bone structural response to habitual activity. American Journal of Biological Anthropology 177 (1), 63–82.

Tuttle, R., Basmajian, J.V., Regenos, E., Shine, G., 1972. Electromyography of knuckle-walking: results of four experiments on the forearm of Pan gorilla. American journal of physical anthropology 37 (2), 255–265.

Valladas, H., Reyss, J.L., Joron, J.L., Valladas, G., Bar Yosef, O., Vandermeersch, B., 1988. Thermoluminescence dating of Mousterian 'Proto-Cro-Magnon' remains from Israel and the origin of modern man. Nature 331, 614–616.

van Leeuwen, T., Vanhoof, M.J.M., Kerkhof, F.D., Stevens, J.M.G., Vereecke, E.E., 2018. Insights into the musculature of the bonobo hand. Journal of anatomy 233, 328–340.

Vercellotti, G., Alciati, G., Richards, M.P., Formicola, V., 2008. The Late Upper Paleolithic skeleton Villabruna 1 (Italy): a source of data on biology and behavior of a 14,000 year-old hunter. J. Anthropol. Sci. 86, 143–163.

Vereecke, E.E., Wunderlich, R.E., 2016. Experimental Research on Hand Use and Function in Primates, In: Kivell, T.L., Lemelin, P., Richmond, B.G., Schmitt, D. (Eds.), The Evolution of the Primate Hand. Anatomical, Developmental, Functional, and Paleontological Evidence. Developments in Primatology: Progress and Prospects. Springer, New York, pp. 259–284.

Visalberghi, E., Sirianni, G., Fragaszy, D., Boesch, C., 2015. Percussive tool use by Taï Western chimpanzees and Fazenda Boa Vista bearded capuchin monkeys: a comparison. Philosophical transactions of the Royal Society of London. Series B, Biological sciences 370 (1682).

Wallace, I.J., Burgess, M.L., Patel, B.A., 2020. Phalangeal curvature in a chimpanzee raised like a human: Implications for inferring arboreality in fossil hominins. PNAS 117 (21), 11223–11225.

Wallace, I.J., Winchester, J.M., Su, A., Boyer, D.M., Konow, N., 2017. Physical Activity Alters Limb Bone Structure but Not Entheseal Morphology. J. Hum. Evol. 107, 14–18.

Walter, R.C., 1994. Age of Lucy and the First Family: Single-crystal ^{40}Ar/^{39}Ar dating of the Denen Dora and lower Kada Hadar members of the Hadar Formation, Ethiopia. Geol. 22 (1), 6–10.

Wilczak, C., Mariotti, V., Pany-Kucera, D., Villotte, S., Henderson, C.Y., 2017. Training and Interobserver Reliability in Qualitative Scoring of Skeletal Samples. Journal of Archaeological Science: Reports 11, 69–79.

Williams, E.M., Gordon, A.D., Richmond, B.G., 2010. Upper limb kinematics and the role of the wrist during stone tool production. Am. J. Phys. Anthropol. 143 (1), 134–145.

Williams, E.M., Gordon, A.D., Richmond, B.G., 2014. Biomechanical strategies for accuracy and force generation during stone tool production. J. Hum. Evol. 72, 52–63.

Williams-Hatala, E.M., Hatala, K.G., Hiles, S., Rabey, K.N., 2016. Morphology of Muscle Attachment Sites in the Modern Human Hand Does Not Reflect Muscle Architecture. Sci. Rep. 6, 28353.

Young, R.W., 2003. Evolution of the human hand: the role of throwing and clubbing. J. Anat. 202 (1), 165–174.

Zumwalt, A., 2006. The Effect of Endurance Exercise on the Morphology of Muscle Attachment Sites. The Journal of Experimental Biology 209 (3), 444–454.